Fibre-imprint Technology Development

Zhi (Nick) Wang, BE (Hons)

A thesis submitted in partial fulfilment
of the requirements for the degree of
Master of Engineering
in
Electrical and Computer Engineering
at the
University of Canterbury,
Christchurch, New Zealand.

4 November 2011

ABSTRACT

Nanoimprint lithography (NIL) has become a promising technology for high-resolution nano-scale patterning, numerous applications have been exploited by using NIL. However, the need for fast, high-throughput process is required in the production of large-area patterns. In particular, the reel-to-reel nanoimprint lithography has been proven to yield large areas of continuous, high-resolution patterns in the micro- and nano-scale range.

In this work, self-aligning fibre imprinting process is developed by using continuous reel-to-reel roller embosser, which can be potentially applied to a range of different fibre materials. This work contains a complete and thorough demonstration including the process of stamp fabrication, fibre imprinting process and full characterization of the imprinted fibre. The proposed techniques involved in this work are described, and the results are analyzed. These techniques include fabricating fibre guide structure, fine feature writing and nickel stamp replication.

1mm-diameter Teflon monofilament is chosen for this fibre imprinting work, the characterization results confirmed that replicated structures are transfered from the electroplated nickel stamp onto the Teflon fibre. The factors which impact the imprinted results are studied, such as roller gap width and rolling speed. It is also shown that more than 50 imprints have been performed using the same stamp without significant degradation.

ACKNOWLEDGEMENTS

First and foremost I would like to thank my supervisor Professor Richard Blaikie, for his guidance, encouragement, and support throughout my study. He is always there to give me useful advices. I would like to thank Helen Devereux for training me so many machines and experimental processes; I appreciate your advice and patience for answering me many questions during my stay in the laboratory. Thank you Gary Turner for training me the use of electron beam lithography system, and help me to find the suitable fibre material for this project. I would also like to thank David Healy in the Mechanical Workshop to make the roller embosser and titanium electroplating baskets for this work.

I am so grateful to Dr. Volker Nock for providing the step-by-step training of SU-8 lithography process, mask writer and teaching me using Tanner tool software to design the mask. I will also thank Dr. Xianming Liu for his assistance with electroplating bath setup and related troubleshooting. For other technical help or advice I would like to thank the following staff or students: Dr. Andrew Clow, Dr. Jessica Chai, Dr. Lakshman Silva, Prateek Mehrotra, Mohammad Bari, Senthuran Sivasubramaniam, David Kim, and Jonathan Tse.

Finally, I would like to thank my parents for the support, optimism and love. I would not have been able to do this without you. Thanks, Mum and Dad.

CONTENTS

LIST OF FIGURES

LIST OF TABLES

Chapter 1

INTRODUCTION

1.1 GENERAL BACKGROUND

In recent years, the demand for micro- and nano-scale patterning has increased dramatically. This has enabled many new applications in the areas of electronics and biotechnology which include biological sensors, actuators, micro-fluidic devices, photovoltaic cell and many others [Ahn and Guo 2009]. High resolution of the patterned structures is essential for many of these applications. Moreover, a reliable, fast, and high-throughput process is particularly required to achieve success in these industries. Nanoimprint lithography (NIL) clearly shows as a promising technology for high-resolution nanometer-scale patterning. However, conventional NIL is not a continuous process. Thus, low-throughput becomes a major roadblock which limits the use of conventional NIL for patterning large-area products.

Compared to the conventional NIL processes, roll-to-roll nanoimprint lithography (R2RNIL) has become a reliable method in the production of large-area of micro and nano-scale patterns with low cost [Ahn and Guo 2008]. This process runs a polymer film through a set of rollers, usually one roll with patterned stamp and one or more pressure rolls. Two common methods for patterning using R2RNIL include thermal embossing and UV curing. In thermal roll-to-roll embossing, a heat source is applied to raise the temperature of a polymer above the glass transition temperature, and pressing the mold onto polymer at certain pressure. The mold is then cooled and the substrate with patterned structures is released from the roller [FaGan 2008]. UV R2R embossing is a low pressure, room temperature process. It is a new technique used for high volume manufacturing of micro-scale structures such as micro optical devices or holograms [Chang et al 2006]. In UV R2R embossing, a polymer film is coated with a liquid phase UV curable resin and placed in contact with an imprinting roller while simultaneously exposing the contact region to high intensity UV light source to cure and harden the resin. The polymer film is then released from the roller with patterned microstructures [Ahmed 2010].

1.2 PROJECT MOTIVATIONS

In this thesis techniques for roll-to-roll imprinting onto polymer fibres are described. Fibre-imprint technology was developed and demonstrated by Professor Richard Blaikie and research engineer Gary Turner in 2008. The names of all 1073 past and present All Blacks were imprinted onto a single Teflon string and stitched into the silver fern [Blaikie and Turner 2008]. However, it is a discontinuous imprinting process which does not allow the production for high-throughput patterning. In addition, the use of silicon as the imprinting mold is very brittle under pressure, which also affects the quantity of fibre-imprint process.

The motivation of this work is to enable continuous reel-to-reel imprinting process with patterned micro and nano-scale structures onto flexible fibre materials with increased throughput. The reel-to-reel imprinting technology presented in this work inherits its high-resolution features from conventional NIL because it is based on a mechanical embossing approach, but with an increased imprinting speed. The reel-to-reel imprinting process primarily targets large-area patterning of micro- and nano-scale structures. In the conventional approach, embossing a large area requires a very large force. Large contact areas between the mold surface and the imprinted substrate also produce significant adhesion force, which makes the demolding process extremely difficult without damaging the imprinted substrate [Ahn and Guo 2008]. Reel-to-reel imprinting process solves these issues encountered in the conventional NIL process, because the imprinting process proceeds in a narrow region transverse to the fibre materials moving direction, thus requiring a much smaller force to replicate the patterns. Also, the molds used in reel-to-reel process are electroplated nickel stamps, therefore the demolding process requires much less force and reduces probability of mold damage.

1.3 THESIS OBJECTIVES

The main aim of this thesis is to develop the processes of imprinting micro and nano-scale patterns onto a range of different fibre materials by means of reel-to-reel roller embossing, and characterize the imprinted fibres. The experimental work for this thesis is divided into two sections: stamp manufacture and fibre-imprinting process. The step-by-step goals to fulfill the thesis objectives are shown in Table 1.1.

Firstly, the stamp with fine features is fabricated by combining optical/e-beam lithography with nickel electroplating technique. A mask with designed micro-scale patterns is required for optical lithography process, whereas e-beam lithography is employed for direct writing of nano-scale patterns. Secondly, the fibre guide structures can be fabricated by two alternative methods, SU-8 lithography and KOH silicon etching. Next, optical/e-beam lithography is used for patterning on top of the guide structures, and the nickel seed layer is then deposited on guide structures by evaporation. Nickel

Goal	**Process and Technique**
Fabricating the stamp with fine features	Optical/e-beam lithography combined with nickel electroplating technique
Fabricating fibre guide structures	SU-8 lithography/KOH silicon etching
Stamp patterning on guide structures	Optical/e-beam lithography
Fabricating stamp with guide structures	E-beam evaporation and nickel electroplating technique
Characterize fabricated stamp	Profilometry/SEM/AFM
Imprint patterned structures onto fibres	Roller embosser and fibre monofilament
Characterize imprinted results	SEM sputter coater and SEM/AFM

Table 1.1 Thesis objectives.

electroplating is the final step to fabricate the stamp with guide structures. There are some practical issues to SU-8 lithography method, such as edge-bead effect, seed layer deposition and stamp separation. Thus, KOH silicon etching method is preferred to fabricate the guide structures. Electroplated nickel has been widely used as the nanoimprint stamp because of its reasonable hardness, tensile strength, ductility and good corrosion resistance [Dennis and Such 1993]. Scanning electron microscope (SEM) and atomic force microscope are applied to characterize the electroplated nickel stamp. Fibre imprinting process is carried out by roller embosser; the imprinted fibre monofilament is then coated with a thin layer of gold-palladium (AuPd) by SEM sputter coater. Characterization of imprinted fibres by SEM and AFM is the last step.

1.4 THESIS OUTLINE

Chapter 2 provides an extensive background and contains four main sections. The first section provides the literature review of previous related work; nanoimprint lithography (NIL) and other imprinting techniques are introduced. The second main section describes the prior work of fibre imprinting and Adidas thread developed in 2008. The last two sections present the prototype of roller embosser and proposed techniques for this thesis.

Chapter 3 contains the detailed fabrication procedures and techniques. This chapter begins with the processes of fabricating fibre guide structures using two different methods, SU-8 lithography and KOH silicon etching. The processes of stamp patterning on guide structures are also presented by using optical and e-beam lithography. Nickel electroplating is the last main section which includes the electroplating background, as well as the plating bath used for this thesis.

Chapter 4 describes the stamp manufacture with fine features and fibre guide structures. This involves the stamp design, step-by-step results and characterization of final fabricated stamp using SEM and AFM. The issues of using SU-8 guide structures are discussed, the process and improved results of using KOH-etched guide structures are also presented. Edge-bead effect and pH drop of plating bath are explained at the end of this chapter.

Chapter 5 begins with the material choice for this fibre imprinting process. The imprinting procedures using roller embosser are demonstrated in the second section. This involves calibration of roller embosser, determining the roller gap width by using feeler gauge during the imprinting process. The stamp lifetime and the effect of roller gap width are discussed in details. Finally, the imprinted results by utilizing SEM and AFM measurements are presented, and issues that occurred in the imprinting process are studied.

Chapter 6 reviews and summarizes the main achievements of this work. The resolved issues and remaining issues are discussed. It also outlines some possible future work based on the findings of this thesis.

Chapter 2

BACKGROUND

2.1 INTRODUCTION

This chapter describes some general applications of imprinting technique, previous related work on fibre imprinting as well as an introduction to the reel-to-reel imprinting process which is used for this work. At the end of this chapter, the proposed techniques involved in this work are briefly introduced.

Imprinting is a process of transferring writing from a master copy to another form; imprinting can be observed in daily life, such as imprinting a footprint into snow, making waffle in a pressure process with waffle iron, or replicating a seal into wax. Imprinting techniques have also been widely used in various industries, such as chip manufacturing by employing nanoimprint lithography (NIL) or polymer banknote printing process etc.

Fibre imprinting has been developed in 2008. A jersey was presented with the names of all 1073 past and present All Blacks imprinted onto a fibre that was stitched into the silver fern. It is this work that is built on this thesis. Furthermore, "on-fiber-devices" have been fabricated by thermal nanoimprint technology combined with Ni electroplating technology in 2009 [Mekaru et al 2009]. Flexibility and large-area patterning with greatly improved throughput were demonstrated by Fibre imprinting process. The process of previous fibre imprinting work will be reviewed in this chapter, the results and issues will also be discussed. In this work, the continuous imprinting of micro or nano sized patterns by using a new apparatus of reel-to-reel imprinting onto polymer fibres is demonstrated.

2.2 PREVIOUS RELATED WORK OF IMPRINTING

2.2.1 Applications of Nanoimprint Lithography

Nanoimprint lithography (NIL) is a high-throughput pattering technique that allows the fabrication of nanostructures with great precision. Thermal NIL and UV NIL are two main NIL methods as outlined in Figure 2.1 [Bhushan 2010]. NIL was first reported as thermoplastic molding, and is therefore often referred as thermal NIL [Chou et al 1995]. In a standard thermal NIL process, a thermoplastic polymer is deformed by pressing the stamp into the polymer at a temperature above the glass transition temperature of the polymer. Afterwards, the polymer is cooled down to below the glass transition temperature and the stamp is removed. In UV NIL, transparent stamps, often referred to as templates, are imprinted into UV curable polymer at room temperature. The polymer is exposed to UV radiation through the stamp which cures the polymer. Subsequently, the stamp is removed. The advantages of hot embossing process includes low-cost and high fidelity of reproduction. However, the most severe disadvantage of hot embossing is the long process time due to repeated heating and cooling cycles. Another drawback is the limited area, which can be embossed per cycle. Compared to the hot embossing process, UV NIL is a low pressure, low viscosity process which is operated at room temperature. The main drawback of UV NIL process is the necessary UV-transparent stamps. They have to be highly stable and highly UV transparent.

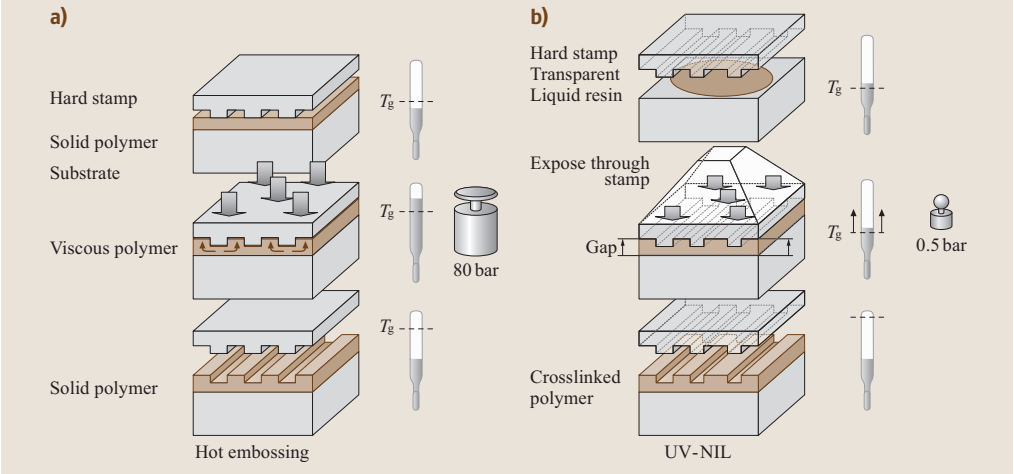

Figure 2.1 Schematic of NIL process: (a) thermal NIL (hot embossing) and (b) UV-NIL [Bhushan 2010].

NIL has been considered to be one of the most promising candidates for large-scale production of nanometer-sized structures. Many applications in microelectronics, photonics, magnetic devices and the biological field have been developed using this simple, low cost and high resolution technique. Within the rapidly growing field of lab-on-a-chip applications, NIL provides an attractive, low cost method for molding of

complex structures, integrating micro and nanofluidic, optics, mechanics and electronics on a single chip. For example, a 60 nm channel metal oxide semiconductor field-effect transistor (MOSFET) on 4 inch wafer was successfully fabricated by using NIL process at the nanostructure laboratory of Princeton University [Chou and Zhang 2003]. The nanotransistors were designed to have four lithographical layers to form the active area, gate, via and metal contact as shown in Figure 2.2 [Chou 2004]. All lithography levels were performed by NIL.

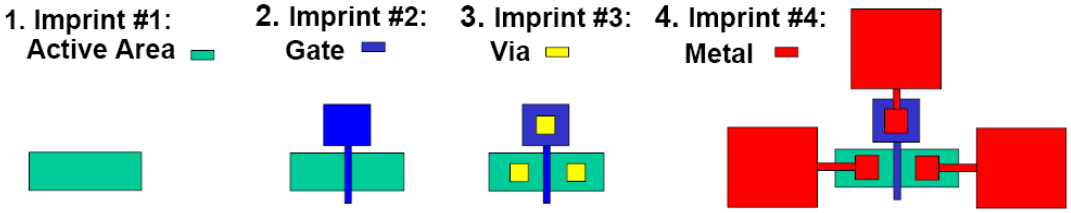

Figure 2.2 The top view of the four-level patterns. Imprint#1: active area; Imprint#2: gate; Imprint#3: via; Imprint#4: metal contact [Chou 2004].

Figure 2.3(a) [Chou 2004] shows the SEM image of fabricated 60 nm channel length MOSFET, and the current-voltage (I-V) measurement of the nano-MOSFETs over whole 4 inch wafer shown in Figure 2.3(b) [Chou 2004] demonstrate that the devices operate properly.

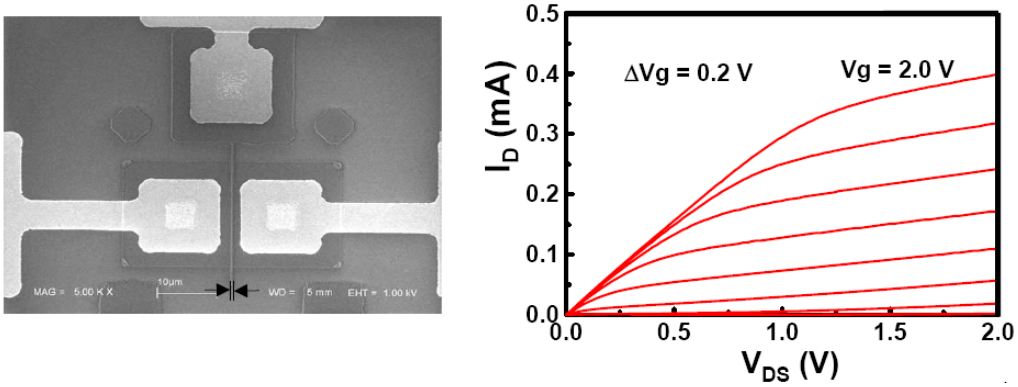

(a) (b)

Figure 2.3 (a) The SEM image of fabricated 60 nm channel length MOSFET; (b) The I-V measurement of the MOSFETs fabricated using NIL at four lithographic levels [Chou 2004].

NIL is an also advantageous method to fabricate the nanofluidic channels used for applications such as DNA stretching experiments. The nanofluidic channels with well-controlled dimensions has fabricated at Solid-State Electronics Lab of University of Michigan. A schematic of the NIL process is shown in Figure 2.4 [Guo et al 2004], the sealed nanofluidic channels can be fabricated by using a template mold to imprint into a thin polymer layer to leave unfilled and self-enclosed channels.

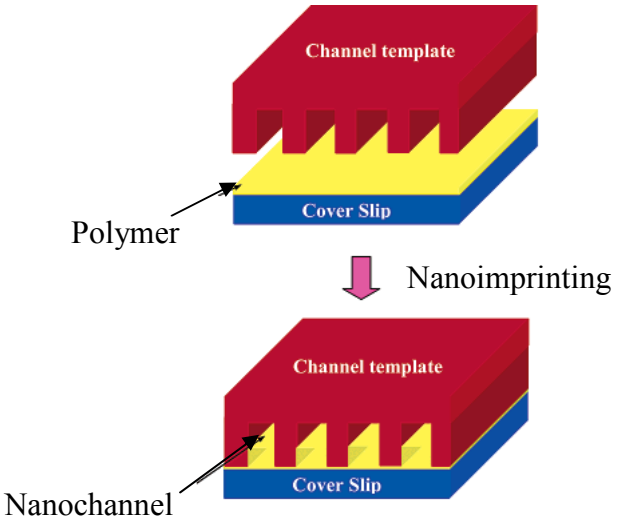

Figure 2.4 Schematic of the nanofluidic channel fabricated by using NIL process [Guo et al 2004].

Figure 2.5 shows the SEM images of imprinted nanofluidic channels of various cross sections [Guo et al 2004]. The nanofluidic channels are fabricated by simply imprinting a channel template into a thin polymer layer on a substrate in a single step. The size of the fluidic channels can be easily controlled by the width and the depth of the channels on the template, and by the initial polymer thickness on the substrate.

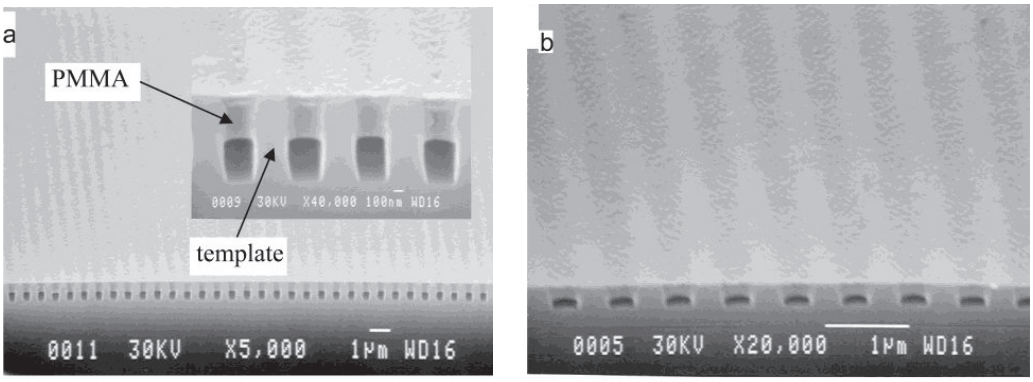

(a) (b)

Figure 2.5 SEM images of imprinted nanofluidic channels of various cross sections. (a)300(width) × 500(height) channels;inset shows a close-up view. (b) 300 × 140 nm channels [Guo et al 2004].

2.2.2 Imprinting into flexible products

Imprinting has been widely used in the banknote printing process, for example there are three printing processes used in the printing of banknotes at the Bank of England [of England].

- Offset Litho - the printing plates transfer the ink to the paper via an intermediate offset roller.
- Intaglio - this process is used to add the portrait of Majesty the Queen and the raised print on the front of the note.
- Letterpress - this process is used for the cypher and serial numbers on the front of the note.

Furthermore, imprinting is also extensively used in printing security features on banknotes and credit cards, because securing the note against forgery is a primary requirement. For example, the Reserve Bank of New Zealand offers a range of new and sophisticated security features on its polymer banknotes. Figure 2.6 shows the imprinted security features on a 20 dollar banknote [of New Zealand]. People are able to verify whether the banknote is genuine by examining those security features.

Figure 2.6 Imprinted security features on 20 dollar banknote [of New Zealand].

Imprinted holograms, three-dimensional images formed by the interference of light beams from a laser or other coherent light source, are security features that are also generally used for valuable documents and products, such as banknote, credit card, identification card (ID), promotional book and software cover [Fournier 2000]. The exelgram is a kind of hologram, a picture made by mixing images created with laser

beams, and printed on metal foil. An exelgram image printed on a banknote changes color, or shows a different picture as it is moved in the light [Fournier 2000]. Exelgrams are almost impossible to fake and are now used on banknotes in many countries. Figure 2.7 presents the imprinted exelgram on an Australian 100 dollar banknote [Lee 1992].

Figure 2.7 Printed exelgram on Australian 100 dollar banknote [Lee 1992].

Fabric laser etching is another imprinting method which uses a laser to burn the design into the top layer of fleece, polyester or microfiber products. It leaves the burned area with a darker tone of the products original color creating a three dimensional tone-on-tone effect. For instance, the stunning design was engraved onto the micro-fiber throw pillows as shown in Figure 2.8 [Laser 2009]. Other imprinting methods such as debossing, foil stamping, etching and embroidery are also used at different areas such as production of leather goods, gift cards, book cover and handicraft; manufacturing of printed circuit board (PCB), semiconductor devices and many others.

(a) (b)

Figure 2.8 (a) micro-fiber throw pillow with engraved design (b) close up of engraving [Laser 2009].

2.3 FIBRE IMPRINTING

Fibre imprinting technology was firstly developed by Professor Richard Blaikie and research engineer Gary Turner at the MacDiarmid Institute of Advanced Materials and Nanotechnology at University of Canterbury in 2008. Using fibre imprinting technology to imprint All Blacks (New Zealand's national rugby team) names into a thread, and this has been commercialized by UC's technology transfer company, Canterprise Limited. The procedure and results of this Adidas campaign are illustrated in Section 2.3.2, after first describing other work on fibre imprinting.

2.3.1 Other Work on Fibre Imprinting

"On-fibre-device" are becoming a reality as the next generation of micro electro mechanical systems (MEMS) requires flexibility and large size. An on-the-fibre device is fabricated by thin-film-coating, patterning and etching on the surface of a thin fibre to make MEMS such as sensors and actuators. Harutaka Mekaru and his team [Mekaru et al 2009] have developed a thermal nanoimprint technology to fabricate weaving guide structures supporting electric contact points on the surface of a thin fibre. A mold with arrays of cylindrical poles of 5, 10 and 20 μm in diameters for electrical contact structures were fabricated by combining MEMS processing with Ni-electroplating technology as shown in Figure 2.9 [Mekaru et al 2009].

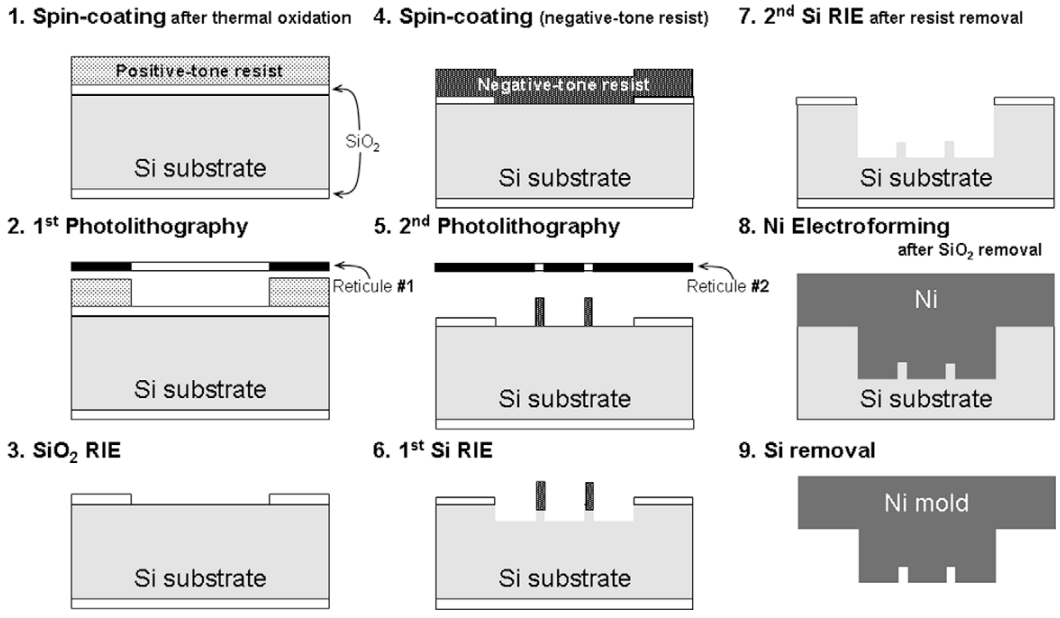

Figure 2.9 Schematic diagrams of fabricating Ni mold for electrical contact structures [Mekaru et al 2009].

Figure 2.10 [Mekaru et al 2009] shows the SEM images of Ni mold for subsequent fibre imprinting process which includes arrays of cylindrical holes of 5, 10 and 20 μm in diameter, four kinds of guide structures with depths of 20, 30, 40 and 50 μm were achieved by the Si etching process.

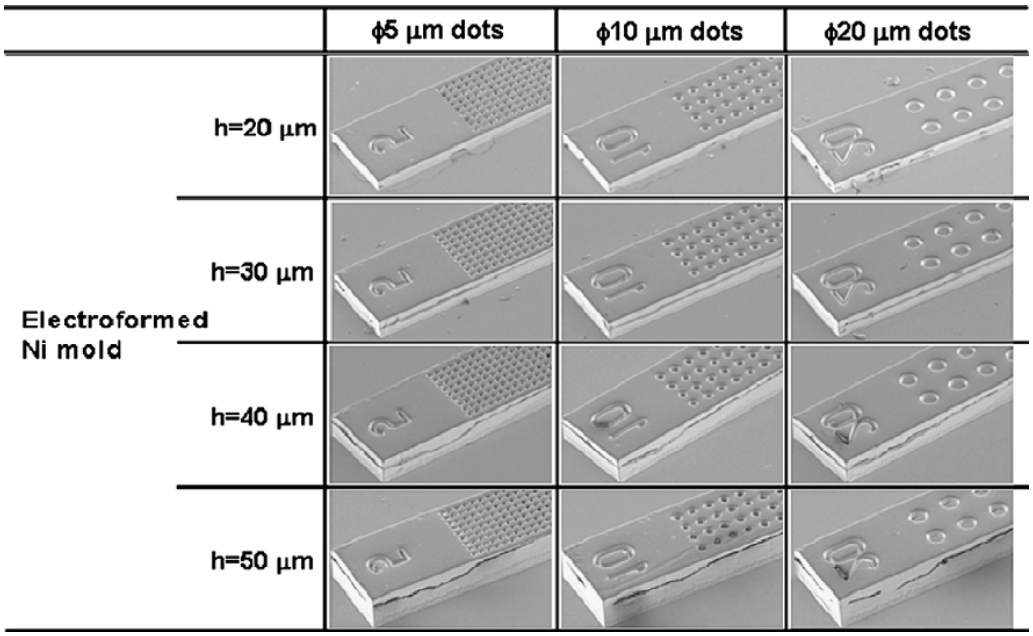

Figure 2.10 SEM images of electroplated-Ni molds with cylindrical patterns [Mekaru et al 2009].

The weaving guide structures in the electroplated-Ni mold were then imprinted onto the surface of the nylon fibres by the thermal nanoimprint system, and the depths of imprinted structures were measured to be 4.5-15 μm. Figure 2.11 shows the top-view of the imprinted nylon fibres using an optical microscope [Mekaru et al 2009].

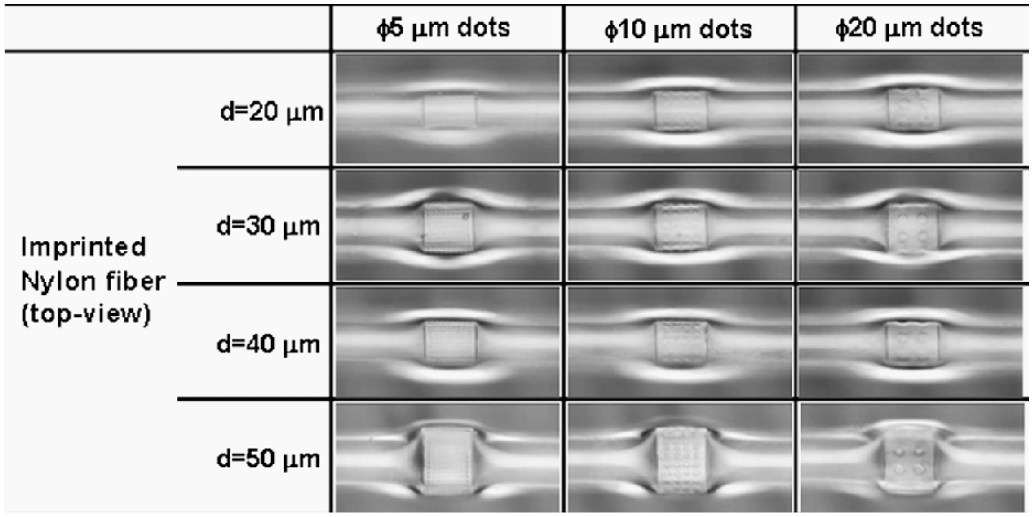

Figure 2.11 Top-view of imprinted guide structures on nylon fibres, "d" means depth [Mekaru et al 2009].

2.3.2 Adidas Campaign 2008

As mentioned at the beginning of this section, the names of 1073 past and present All Blacks were imprinted onto a single thread using a basic fibre imprinting process. The next step would be to imprint the names of as many as 100,000 fans on to a single thread for a special edition jersey in a campaign organized by All Blacks sponsor Adidas. Figure 2.12 (a) shows the single thread in comparison with a New Zealand 20 cent coin, and Figure 2.12 (b) shows the single thread which has been stitched into the silver fern of an All Blacks jersey [Blaikie 2008].

(a) (b)

Figure 2.12 (a) a single thread with imprinted All Blacks names (b) the thread sewn into the silver fern of All Blacks jersey [Blaikie 2008].

The method developed for Adidas thread is a form of embossing, similar to techniques used for CD replication. Electron-beam lithography (EBL) was used to write patterns onto a sacrificial resist layer on a flat silicon substrate, and then reactive-ion etching (RIE) was used to transfer this into a hard relief pattern in the underlying silicon. This then acts as the stamp for subsequently embossing the writing into fibres, using pressure to imprint the patterns onto the fibre materials. The schematic diagram of this process is illustrated in Figure 2.13.

The key factor of this technique required the use of non-stick fibre material to prevent the fibre sticking to the mold during the embossing process. Teflon fibre was used for this work, any other polymer fibres can also be used. Examples images of a silicon mold and embossed patterns are included in Figure 2.14 [Blaikie 2008] below.

The process of fibre imprinting used for Adidas campaign demonstrated the high resolution of imprinted patterns. However there are some issues for this process which should be taken into consideration. For instance, the silicon mold is extremely fragile and can be easily broken under pressure during the imprinting process. As a result, the problem of material and time wasting can occur if the silicon mold needs to be used frequently. As this imprinting process is performed by a press, the imprinting capacity is significantly limited. A faster and more economical imprinting method is the continuous reel-to-reel process, which provides a practical solution for large-

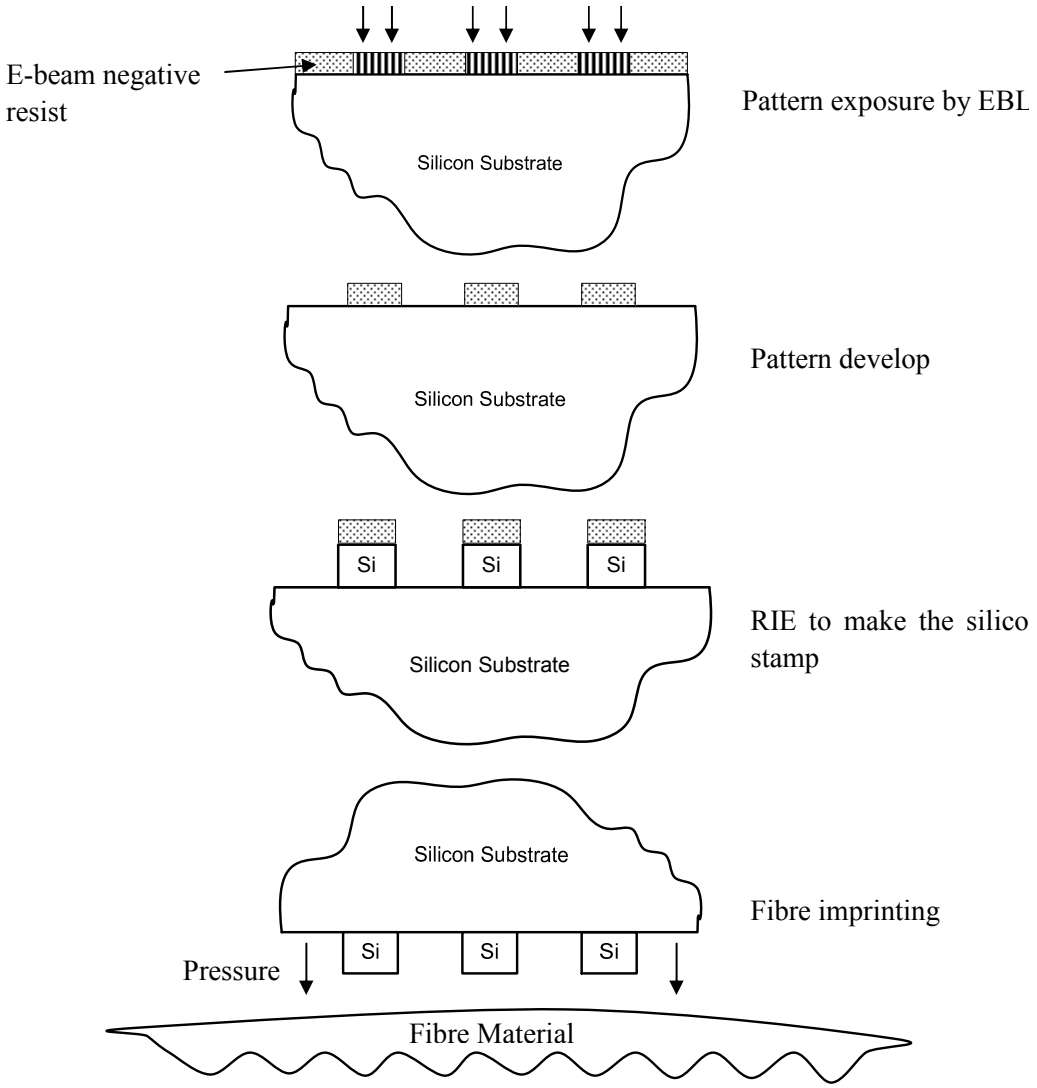

Figure 2.13 Fibre imprinting process used for 2008 Adidas campaign.

area micro- or nano-scale patterning. Reel-to-reel processes offer greatly improved throughput by overcoming the challenges faced by conventional imprinting methods in maintaining pressure uniformity and successful large-area imprinting and demolding. In the conventional approach, embossing a large area requires a very large force. The reel-to-reel system runs the fibres through a set of rollers, usually one patterned roll and one pressure roll. Three distinct advantages in using this process are the following: rollers create very high pressures at the contact areas with a low applied force; it allows the use of a small stamp to imprint significantly large areas; and transitioning from a discontinuous to a continuous process.

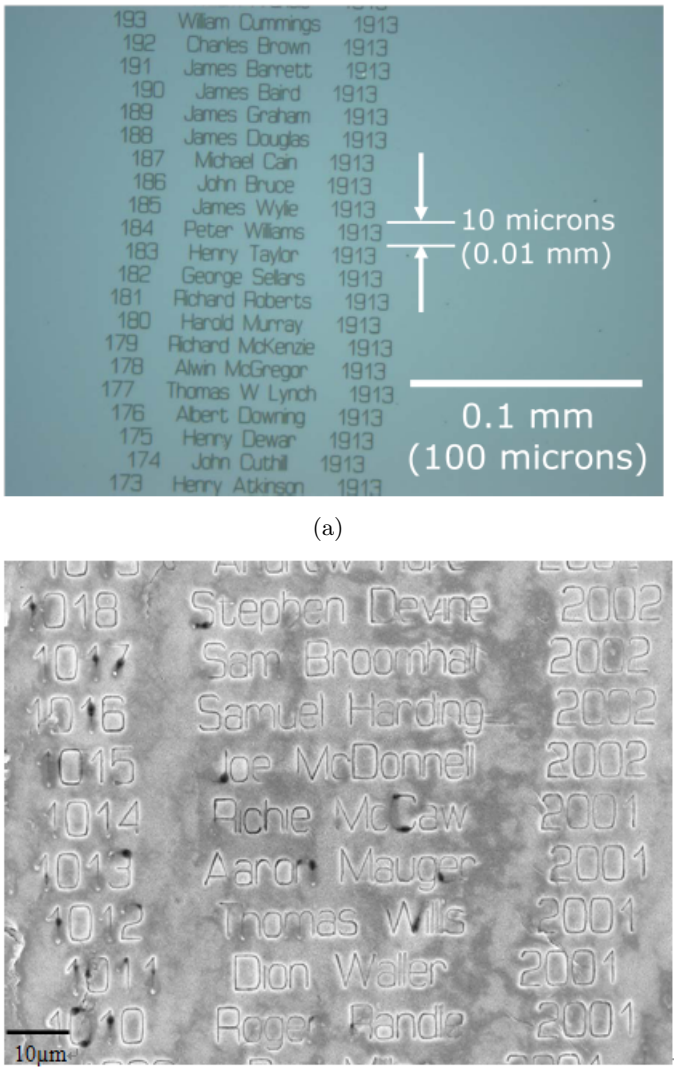

(a)

(b)

Figure 2.14 (a) Silicon mold (b) Imprinted patterns on Teflon fibre [Blaikie 2008].

2.4 ROLLER EMBOSSER PROTOTYPE

Two common methods for creating patterns using reel-to-reel process include thermal nanoimprint system and roller embosser. The thermal nanoimprint system uses a heat source to raise the temperature of a polymer above the glass transition temperature of the substrate to be patterned and applying the contact force at a very short interval. The mold is then cooled and demolded from the patterned substrate. For this work, non-thermal roller embosser was designed and made by the mechanical workshop at University of Canterbury. The prototype of roller embosser used for this work is shown in Figure 2.15. Future modification of the system for thermal nanoimprint is possible by including heater elements onto the rollers.

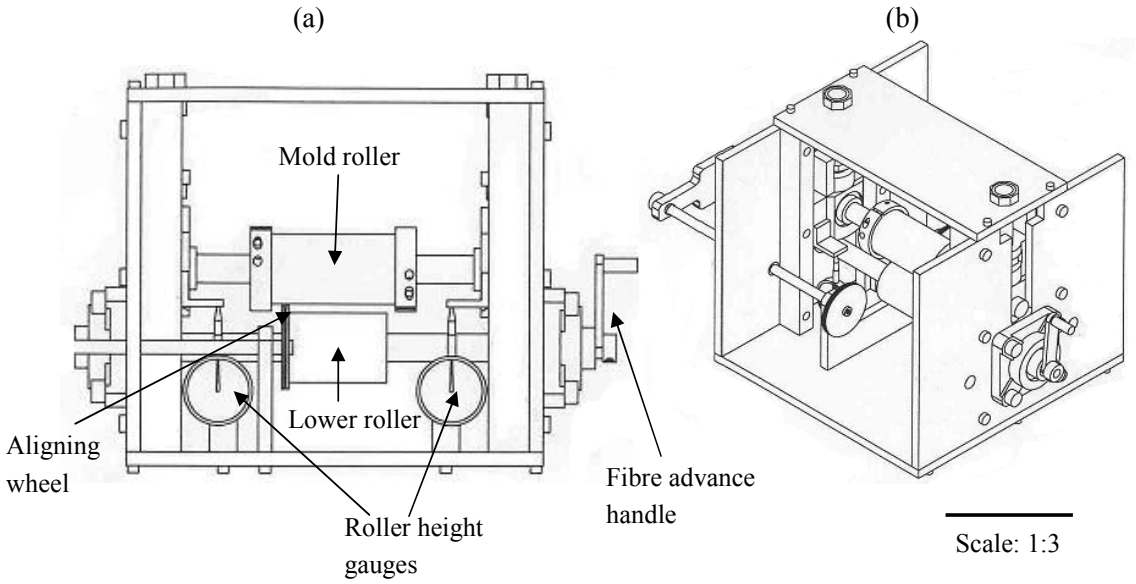

Figure 2.15 (a)Front view(b)Isometric view of roller embosser prototype.

The roller embosser prototype is mainly consisted of top roller, bottom roller, handle, aligning wheel, two gauges and two bolts sitting on the top plate. The dimension of top roller is 5 cm (diameter) × 10 cm (length), and the dimension of bottom roller is 5 cm (diameter) × 7.5 cm (length). Both rollers have sufficient areas for imprinting since the Ni mold size is limited by the lithography as well as the electroplating process. The roller gap between top and bottom rollers are adjusted by screwing two bolts on the top plate, and the gap width can be read from two front gauges. The reading of two front depth gauges indicate the gap width between upper and lower rollers. Each division of the gauge is 1/100 of the circle (1 mm); in other words, each division represents 10 μm, and the graduation of the small circle is 1 mm/div. Ideally, the Ni mold is wrapped around the top roller, the fibre string is then continuously fed through the aligning wheel and imprinted by the roller embosser as slowly winding the handle on right side of the roller embosser. The detailed instruction of using this roller embosser is described in Section 5.3.

2.5 OVERVIEW OF PROPOSED TECHNIQUES

Fibre guide structure, fine features writing and stamp replication are three major techniques involved for this work. The use of large-scale guide structure is proposed to self-align the fibres with the patterned stamp during the imprinting process. SU-8 lithography and KOH silicon etching are two proposed methods to create guide structures. Micro- or nano-scale fine features are exposed on the ridges of fabricated guide structures, optical or e-beam lithography is applied for this process. Electroplating technique is used to manufacture the stamp which is the last step before imprinting

the fibres using roller embosser.

2.5.1 Fibre Guide Structure

Fibre guide structures are designed for self-aligning process, which means the fibres will be automatically aligned to the fine features on the stamp during the imprinting process. In comparison with those fine features (∼100 nm thickness) on the Ni stamp, some large grooves with 1 mm wide (∼100 μm thickness) are produced so that fibre string will be easily aligned to these grooves during the imprinting process. Micromachining is the basic idea to build up the alignment grooves and two alternative methods were considered. The first method is to apply SU-8 lithography as illustrated in Figure 2.16(a). SU-8 is a high contrast, epoxy based negative photoresist designed for micromachining. The SU-8 film thickness ranges from 1 μm up to hundreds of micrometers by controlling the spinning speed. It is commonly used to pattern high aspect ratio structures with vertical side walls. The groove structures will be exposed by mask aligner. After developing, the groove structures are highly cross-linked which brings the high stability to chemicals such as electroplating solution while fabricating the nickel stamp.

The second method is to use potassium hydroxide (KOH) silicon etch to create those large grooves. KOH is a commonly used silicon etch chemistry for micromachining silicon wafers. KOH is a wet etch which attacks silicon preferentially in the <100> plane, producing a characteristic anisotropic V-etch, with sidewalls that form a 54.7° angle with the surface. Photolithography and reactive ion etch are required for this process. A diagram of KOH-etched guide structure is shown in Figure 2.16(b). The processes of fabricating fibre guide structures using both methods will be explained in Section 3.2.

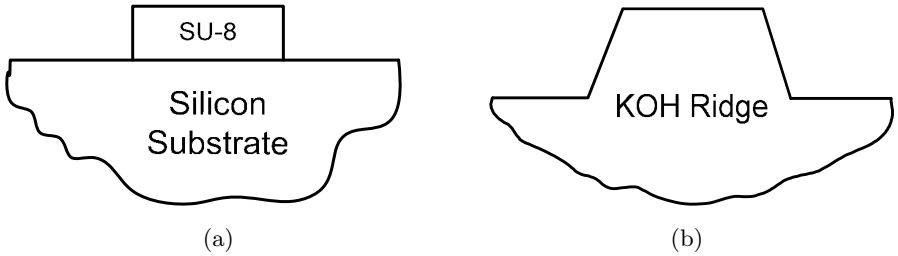

Figure 2.16 Schematic diagrams of fibre guide structures fabricated by two methods (a) SU-8 lithography (b) KOH silicon etching.

2.5.2 Fine Feature Writing

After the fibre guide structures are fabricated by either method, a layer of resist is spin-coated on top of the guide structures as shown in Figure 2.17. Optical or e-beam

lithography is then applied to write the micro- or nano-scale features on the ridges of fibre guide structures. A mask with designed features and alignment windows is required for optical lithography process, whereas e-beam lithography is a direct writing tool which can import the design from the system. The features after development are presented in Figure 2.18(a).

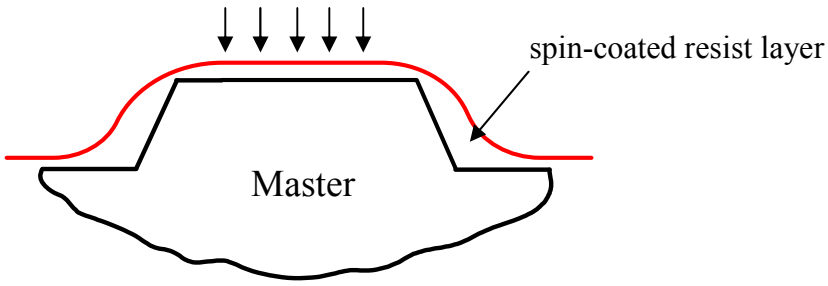

Figure 2.17 Fine feature writing by optical/e-beam lithography.

2.5.3 Nickel Stamp Replication

Prior to performing the fibre imprinting process, stamps with patterned features have to be fabricated by lithography techniques coupled with nickel electroplating. Both techniques have been widely used for replicating nickel nanoimprint stamps [Ansari et al 2005, J. et al 2006, Dutta et al 2007]. Electroplating is the process of producing a coating, usually metallic, on a surface by the action of electric current. Nickel is the most commonly used electroplated deposit because of its reasonable hardness, tensile strength and good corrosion resistance [Dennis and Such 1993]. The electroplated stamp thickness mainly depends on the plating time, cathode current density, plating bath temperature and some other parameters. In general, low current density is applied initially in order to achieve high resolution of replicated fine features; high current density is then applied to replicate the large-scale guide structures. Figure 2.18 shows the schematic diagram of the master pattern and the replicated nickel stamp. The electroplated nickel stamp after separation from the master is shown in Figure 2.18(b). The fine features on the ridges from the master are replicated into the groove structures of the nickel stamp which is opposite polarity. The electroplating bath and detailed process applied for this work will be described in Section 3.5.

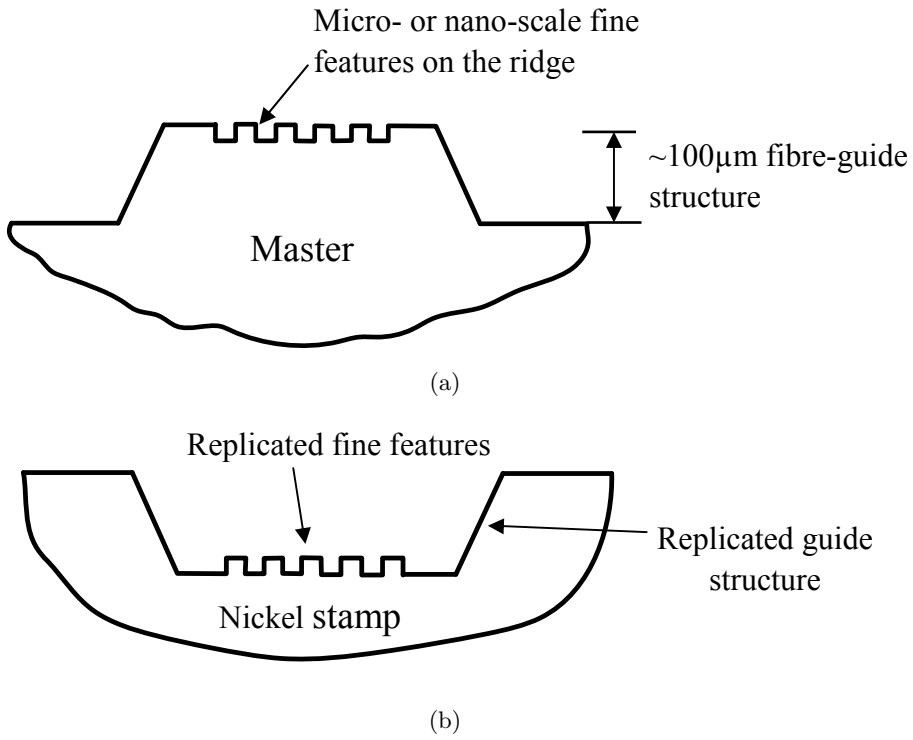

Figure 2.18 Large-scale fibre guide structure with fine features writings on the ridges. (a)master and (b)nickel daughter replica.

2.6 SUMMARY

In this chapter, the various applications of imprinting work are discussed. The previous work related to fibre imprinting is also reviewed which includes the Adidas thread developed in 2008, the results and issues are presented in Section 2.3.2. The roller embosser used for this thesis is introduced in Section 2.4, and the proposed techniques of this thesis are presented in Section 2.5 which include fabricating fibre guide structures, fine feature writing and nickel stamp replication.

In the next chapter, the detailed fabrication procedures and techniques involved for this work are demonstrated. The methods and processes of producing fibre guide structures are presented. Fine features writings on the ridges of guide structures are described in Section 3.3, the electroplating background and step-by-step electroplating process are presented in Section 3.5.

Chapter 3

FABRICATION PROCEDURES AND TECHNIQUES

3.1 INTRODUCTION

This chapter outlines the fabrication procedures and the techniques used to develop the fibre-imprint technology. It begins with the fabrication procedures for making the self-aligning guide structures by two different micromachining techniques, followed by patterning and the process of nickel stamp fabrication. The last section describes the details of fibre-imprint process.

3.2 FABRICATING FIBRE GUIDE STRUCTURES

Guide structures are required in order to automatically align the fibres to the micro- and nano-scale features on the stamp when using a continuous roller-imprint process. The guide structures used here are constructed using 1 mm wide (∼100 μm thickness) grooves for self-aligning 1 mm diameter fibres. The micromachining techniques involved in this process are SU-8 lithography and potassium hydroxide (KOH) silicon etching, and the challenges are that these structures are much larger (by a factor of 10-1,000) than the nano-scale features that are patterned on the stamp in a later process.

3.2.1 SU-8 Lithography

SU-8 2000 is a high contrast, epoxy based negative photoresist designed for micromachining and other microelectronic applications. SU-8 2000 is capable of producing very high aspect ratio structures with vertical sidewalls. Film thickness up to 250 μm can be achieved with a single coat process for SU-8 2100 which is used in this experiment. A normal process of SU-8 lithography is: spin coat, soft bake, expose, post exposure bake, followed by develop as shown in Figure 3.1 [MicroChem 2011].

Step 1: Substrate Pretreatment

To obtain maximum process reliability, the substrate should be clean and dry prior to applying SU-8 2100 resist. Firstly, a dehydration bake for at least 12 hours is performed in a 185°C oven, followed by plasma ashing in oxygen at 100 W for 20 minutes. Any

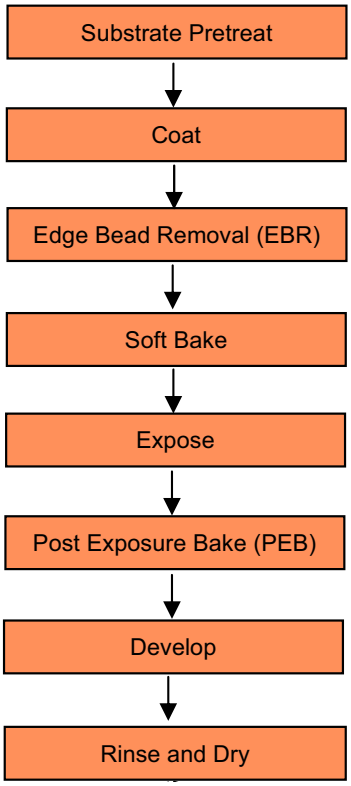

Figure 3.1 Process flow of SU-8 lithography [MicroChem 2011].

organic substances are removed from the exposed silicon surfaces in this oxygen plasma ashing stage.

Step 2: Spin-Coating and Edge Bead Removal (EBR)

From SU-8 2000 datasheet, Figure 3.2 provides the information required to select the appropriate SU-8 2000 resist and spin conditions to achieve the desired film thickness.

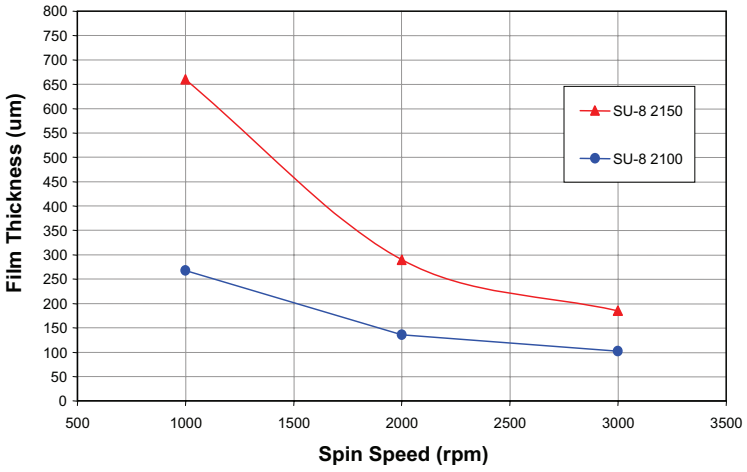

Figure 3.2 SU-8 2000 spin speed versus thickness [MicroChem 2011].

In order to achieve the desired 100 μm film thickness, the recommended spin speed, ramp and time are set into the spinner according to the figure above. A Headway PWM32 spinner is used, and the spinning parameters used in this experiment are shown in Table 3.1.

	Ramp [rpm/s]	**Speed [rpm]**	**Time [s]**
Stage1	85	500	10
Stage2	10030	3000	30

Table 3.1 Spinning parameters.

During the spin coating process step, a buildup of photoresist may occur on the edge of the substrate. To minimize the contamination of the hotplate, this thick bead should be removed. This can be accomplished by using a small amount of acetone applied at the edge of the wafer either at the top or from the bottom. Figure 3.3 shows spin-coated SU-8 2100 film thickness measured by profilometry over exposed step edge which is 98 μm$\pm$2 μm, close to the target value of 100 μm and in agreement with the data sheet value for 3000 rpm spin speed.

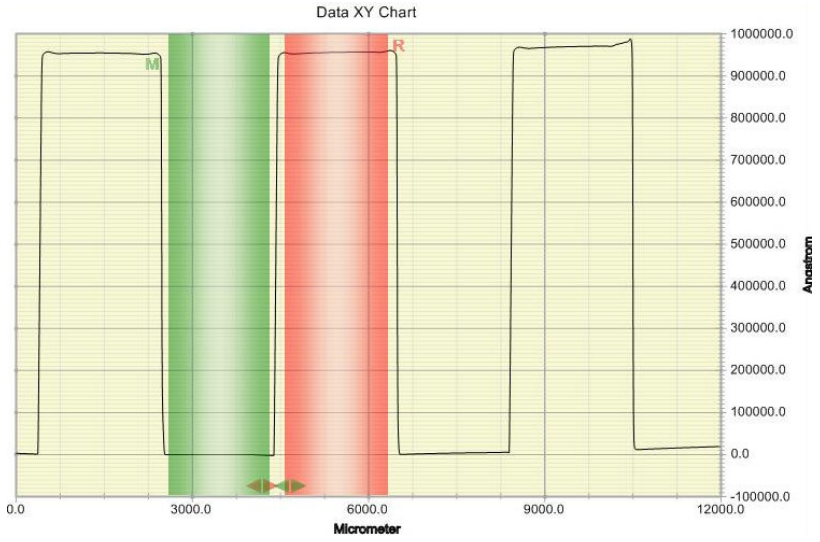

Figure 3.3 SU-8 film thickness (Angstrom).

Step 3: Soft Bake

After coating, the resist film contains remaining solvent; the substrate must then be soft baked to evaporate the solvent, so as to avoid mask contamination as well as improve resist adhesion to the substrate. A Stuart SH1D hot plate is used for this step. Table 3.2 shows the soft bake temperatures and times for SU-8 2100 at 100 μm film thickness. The temperature ramping stages (stage 1 & stage 3) are required to minimize effects of differential thermal expansion of the substrate and SU-8, which can lead to cracking or delaminating of the SU-8.

	T [°C]	**Time [min]**
Stage1	65	5
Stage2	95	45
Stage3	RT	Cool down to RT for at least half an hour on hotplate

Table 3.2 Soft bake times.

Step 4: Photolithography of SU-8 Photoresist

Photolithography is the most common technique to transfer the micro-sized patterns from a mask onto a layer of thin film. The thin film layer is light sensitive and called photoresist. This section outlines the photolithography procedure of contact masking with SU-8 2100 photoresist. The photolithography process is employed with a Karl Suss MA6 mask aligner (Figure 3.4). A mask with patterns and alignment marks is required for photolithography. The mask data is designed by L-Edit Tanner Tools, although many other design tools are available, and exposed by Heidelberg Instrument's μPG 101 mask writer. The μPG 101 can expose DXF and CIF formats data exported from L-Edit. After the mask is exposed by the mask writer, development, chrome etching, resist striping and cleaning are the rest of procedures for mask making. Figure 3.5 shows the designed mask for fibre guide structures as well as defined alignment marks.

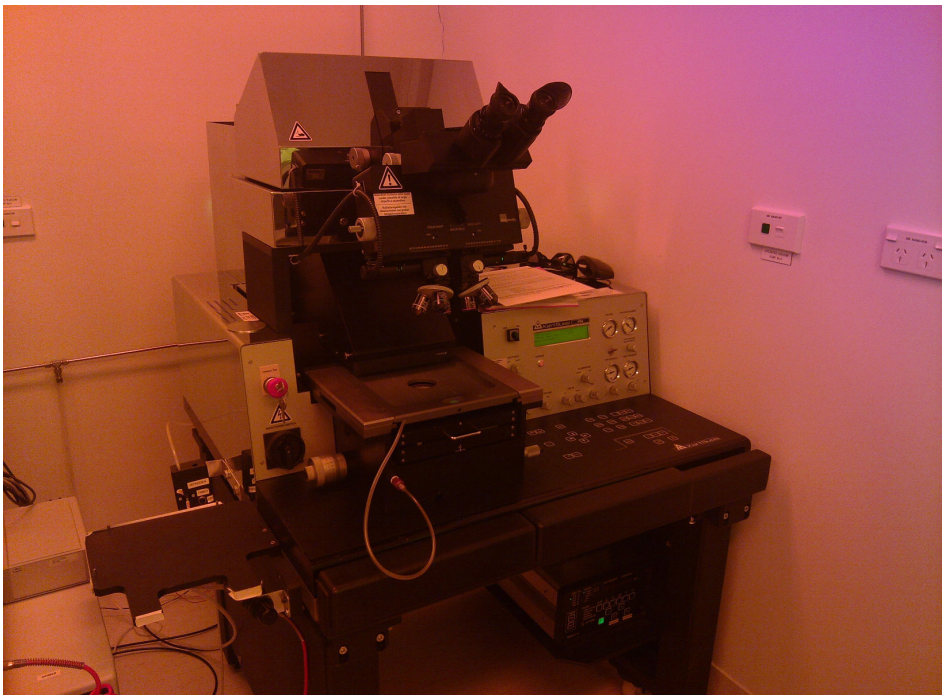

Figure 3.4 Karl Suss MA6 mask aligner in the yellow room.

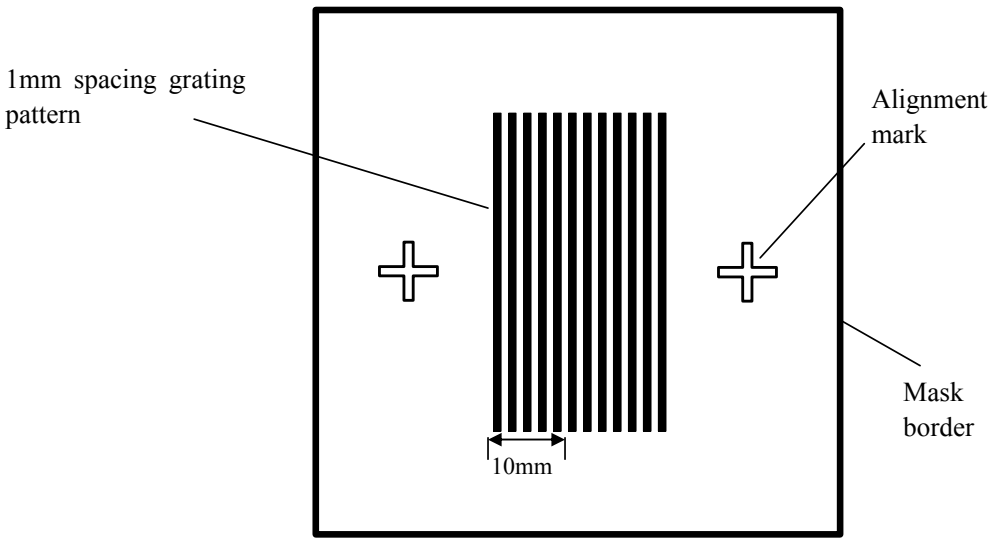

Figure 3.5 Designed mask for fibre guide structures.

For exposure a long pass filter is used to eliminate UV radiation below 350 nm. To determine the optimum exposure time, the intensity (mW/cm^2) of the mask aligner is measured using a UV intensity meter, and the exposure energy (mJ/cm^2) required for the selected photoresist thickness can be found from Table 3.3.

Thickness(μm)	**Exposure dose(mJ/cm^2)**
100 – 150	240 – 260
160 – 225	260 – 350
230 – 270	350 – 370
280 – 550	370 – 600

Table 3.3 Exposure dose required for various SU-8 thicknesses [MicroChem 2011].

Multiple exposure mode is applied since the exposure time is too long to do at once, and multiple exposures prevent the resist from overheating during exposure. The intensity of UV light at 365 nm wavelength is measured by Suss MicroTec UV intensity meter (Model 1000), which is 3.1 mW/cm^2. The resultant exposure time can be calculated by dividing the corresponding exposure energy into the measured UV intensity as shown in Formula 3.1. Karl Suss MA6 mask aligner has a multiple exposure mode allowing the user to expose resists multiple times without changing the alignment. This is particularly useful for thick resists (e.g. SU-8) where the exposure time can be long and heating of the resist can be an issue. Therefore, a long exposure could break into several short exposures which allows the sample to cool down between exposure steps. To use this feature, the user has to specify individual exposure length, the time delay between exposures, and the number of cycles of exposure to be completed. In this work, to ensure a 100 μm thickness of SU-8 resist is fully exposed, 10 exposure cycles

are applied. Each exposure lasts 10 seconds, and the time delay between exposure steps is set to 10 seconds as well.

$$T = \frac{E}{P} = \frac{240mJ}{3.1mW} = 78s \tag{3.1}$$

Step 5: Photolithography of SU-8 Photoresist

Following exposure, a post exposure bake (PEB) must be performed to selectively cross-link the exposed portions of the films. This bake is performed on programmable ECHOTHERM^{TM} HP30 hot plate manufactured by Torrey Pines Scientific. To minimize stress and resist cracking during PEB process, a slow ramp is recommended. Rapid cooling after PEB must be avoided. Table 3.4 shows the recommended times and temperatures for PEB step. The visible latent pattern image should be seen during or after PEB, otherwise it is an indication of insufficient exposure.

	T [°C]	**Time [min]**
Stage1	65	10
Stage2	95	15
Stage3	RT	Cool down to RT for at least half an hour on hotplate

Table 3.4 Post exposure bake times.

Step 6: Development and Rinse

PGMEA (1-methoxy-2-propyl-acetate) solvent is the developer for SU-8 2100 photoresist, immersing the substrate into the developer for 10-15 minutes; the use of an ultrasonic bath is helpful when developing thick film structures. After the development, the substrate is rinsed with Isopropyl Alcohol (IPA), and any white film produced during the IPA rinse is an indication of underdevelopment of the unexposed photoresist. Simply immersing or spraying the substrate with additional SU-8 developer will remove the white film. Finally, the substrate is blown dry with nitrogen. An example of a completed SU-8 guide structure is shown in Figure 3.6.

3.2.2 Potassium Hydroxide (KOH) Silicon Etching

The vertical sidewalls of the guide structures produced in SU-8 caused some problems in later electroplating processes so an alternative method for fabricating the guide structures was also developed. This uses anisotropic etching of silicon in potassium hydroxide (KOH) and the experimental procedures of this orientation-dependent etching are demonstrated and described in this section.

The etching of silicon with KOH solution is highly anisotropic, which attacks silicon preferentially in the <100> plane, producing a characteristic V-etch, with sidewalls that form a 54.7° angle with the surface [Bean 1978]. More discussion on KOH etching method will be explained in Section 4.3.2. Si wafers with 200 nm thick LPCVD (low

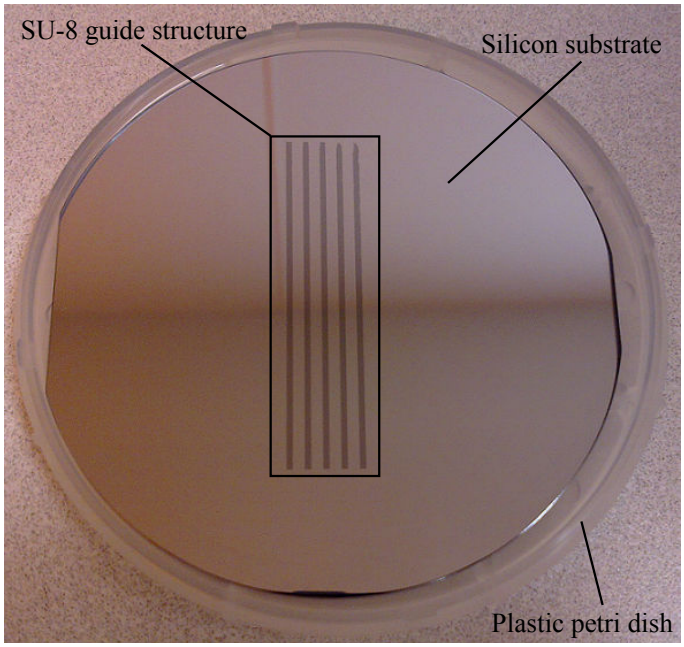

Figure 3.6 Completed SU-8 guide structure.

pressure chemical vapour deposition) silicon nitride (Si_3N_4) on both sides are used, and Si_3N_4 is acting as a mask in this work. The steps of KOH etching are illustrated in Figure 3.7, and the steps are fully explained as follows.

Step 1: Photoresist Processing

As mentioned in the previous section, a mask with patterns and alignment marks in chromium are required. The mask designed for the SU-8 lithography process can be reused for KOH etching as both masks have the same grating patterns. AZ1518 photoresist is spin-coated onto the silicon nitride substrate at 4000 rpm for 60 seconds, and the resultant thickness is 1.8 μm (Figure 3.8). This is then soft baked at 100°C for 90 seconds on a hotplate. The exposure time is 20-25 seconds by using Kaul Suss MA-6, followed by 60 seconds development in AZMIF300 with 2.38% of TMAH (Tetramethyl ammonium hydroxide), and then the substrate is rinsed in DI water. If a feature appears rounded and enlarged, it is considered overexposed. If features are missing, it is considered underexposed.

In fact, the develop time varies with the exposure time, for example, under-exposure causes longer developing time. The color change on the surface of the substrate is a good indication of whether the development has been completed, as the SU-8 features are large enough to see by eye. The substrate is then hard baked at 100°C for 120 seconds, the oxygen plasma ashing for 15 seconds is performed to remove any exposed photoresist residue.

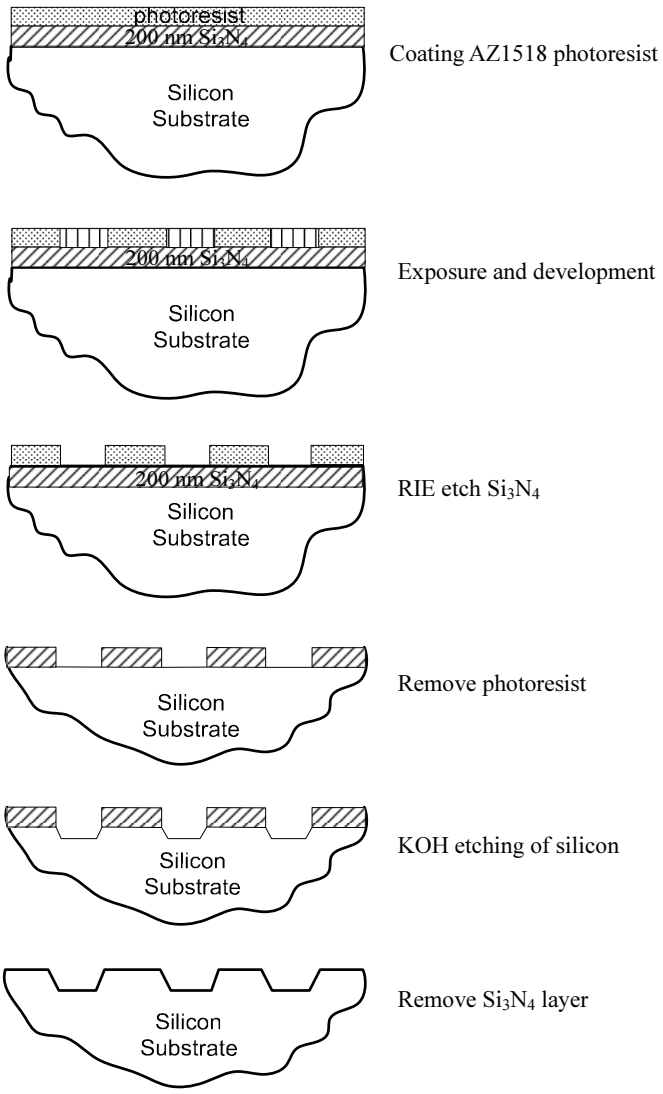

Figure 3.7 Steps of potassium hydroxide etching.

Step 2: Silicon Nitride Mask Making

After the desired pattern is transferred by photolithography, the Si_3N_4 on the silicon substrate is etched by using reactive ion etching (RIE) with the photoresists as the mask. This process is carried out in an Oxford Plasmalab 80 Plus system with CHF_3 and Ar gas (Figure 3.9). Dry etching is a safer and convenient process from the operator's point of view than the alternative technique of wet etching with hydrofluoric acid (HF). The etching process is carried out at low temperature using liquid nitrogen to cool the substrate. The etch conditions used are shown in Table 3.5.

Gases	**Electrode**	**Flow rate(sccm)**	**RF Power(W)**	**Temperature(K)**
CHF_3/Ar	NiCr	60/50	200	253

Table 3.5 RIE etch parameters.

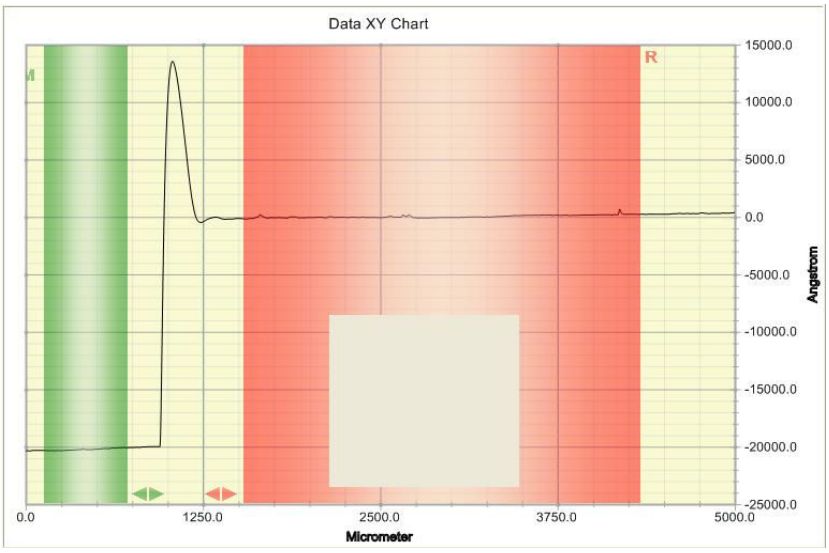

Figure 3.8 AZ1518 photoresist thickness measured using profilometry across a surface scratch (which is responsible for the peak to the right of the step edge).

An approximate etch rate of 5 nm/min can be achieved with the parameters used in the table above. As the Si_3N_4 layer depth is 200 nm, the etching time is about 40 minutes. However, it is important to be aware of any Si_3N_4 residue on the substrate surface as this will affect the following KOH etching process, therefore a longer etching time should be considered. Until now, the "hard mask" of Si_3N_4 is made. Following RIE the wafer is rinsed with acetone to remove the remaining photoresist, and then rinsed with deionised (DI) water and blown dry.

Step 3: Potassium Hydroxide Etching

The materials needed for potassium hydroxide (KOH) etching are:

- KOH pellets
- Glass container
- Water bath with stirrer motor

The KOH etching apparatus is shown in Figure 3.10 [Drysdale 2003]. The flask is immersed in the water bath that maintained the temperature at 87°C. The polypropylene balls are floated on the water bath surface to reduce evaporation during long etches. The evaporation of the water causes the water level to drop, as a result the etching temperature will reduce. The etch solution is stirred by a magnetic stirring bar in the flask, which is actuated by a water-controlled magnetic stirrer motor placed underneath the flask.

The recipe of etchant is a 30% KOH solution which mixes 100 g of KOH pellets with 200 ml of DI water. The average etch rate is 66 μm/hour. The last step is to remove any front side Si_3N_4 protection by using RIE and rinse with DI water. Figure

Figure 3.9 Oxford Plasmalab 80 plus RIE chamber with liquid nitrogen tank.

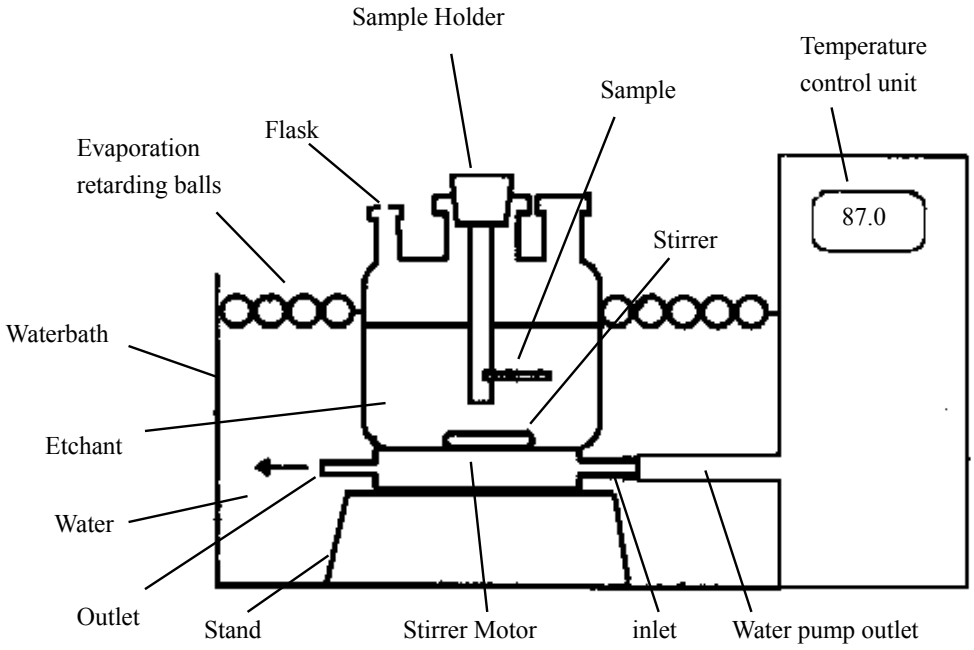

Figure 3.10 KOH etching experiment setup [Drysdale 2003].

3.11 shows a photograph of a completed KOH etched guide structure and the etched silicon depth measured by profilometry which is around 130 μm (Figure 3.12); the etch rate of 80 μm/hour is close to the expected value.

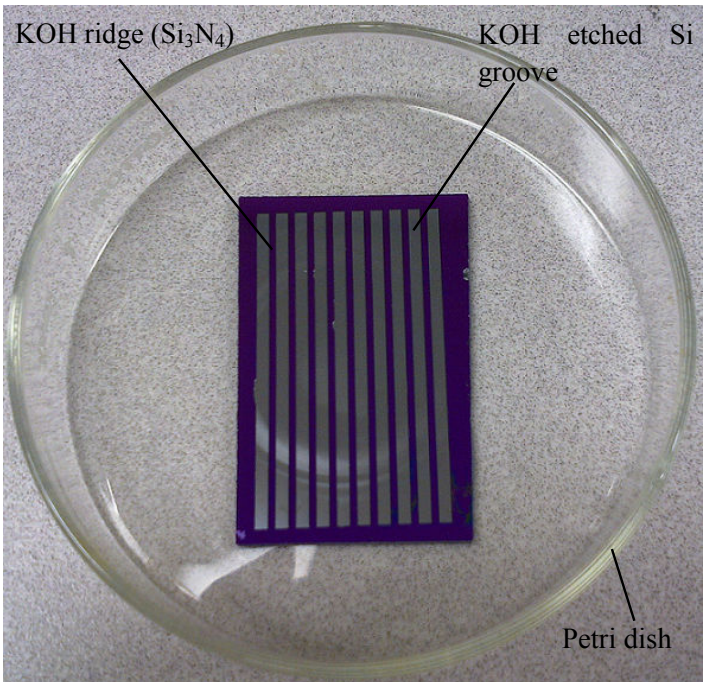

Figure 3.11 Completed KOH etched guide structure.

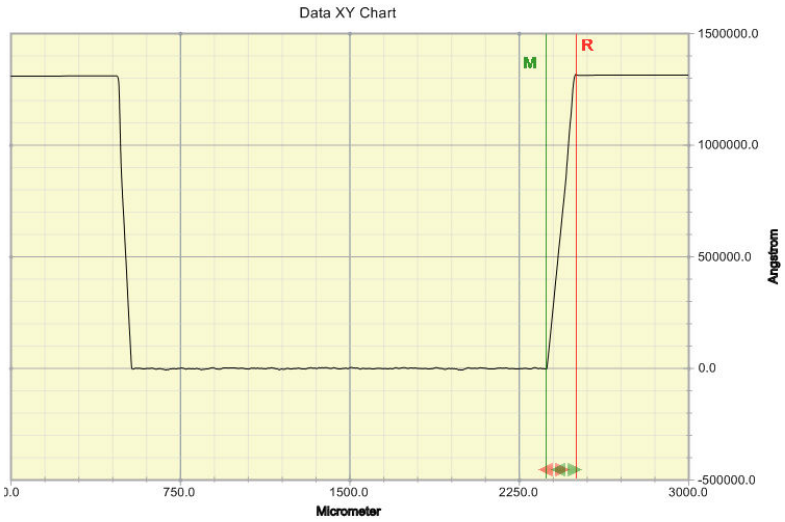

Figure 3.12 KOH etched silicon depth.

3.3 STAMP PATTERNING

After the guide structures are created by one of the two alternative techniques which have been described in Section 3.2, patterning on top of those groove structures is the next process. Two different lithography techniques are used: photolithography and e-beam lithography. In this section, the procedures of pattern exposure and development of both techniques are introduced.

3.3.1 Photolithography

This section outlines the fine feature writings onto the guide structures by using photolithography technique. Photolithography is the process of transferring geometric shapes from a mask to the surface of a silicon wafer. The steps involved in the photolithography process are: wafer cleaning, spin-coating photoresist, soft baking, exposure and development. There are two types of photoresist: positive and negative as illustrated in Figure 3.13. For positive resist, the resist is exposed with UV light wherever the underneath materials are to be removed. For example, AZ1518 photoresist is used for stamp patterning. In these resists, exposure to the UV light changes the chemical structure of the resist so that it becomes more soluble in the developer. The exposed resist is then removed by the developer. Negative resists behave in just the opposite manner. Exposure to the UV light causes the negative resist to become polymerized, and more difficult to dissolve. Therefore, the negative resists remain on the substrate wherever it is exposed, the developer only wash away the unexposed areas. One very common negative photoresist is SU-8 photoresist which is used for creating guide structure as introduced in Section 3.2.1.

An important parameter for exposure is the contact method between mask and wafer. There are six types of exposure program for Karl Suss MA6 mask aligner used for this experiment. Vacuum contact exposure is adopted because it is the normal photolithographic procedure in the UoC laboratory, and this mode performs the highest resolution levels as the best contact between mask and wafer is achieved.

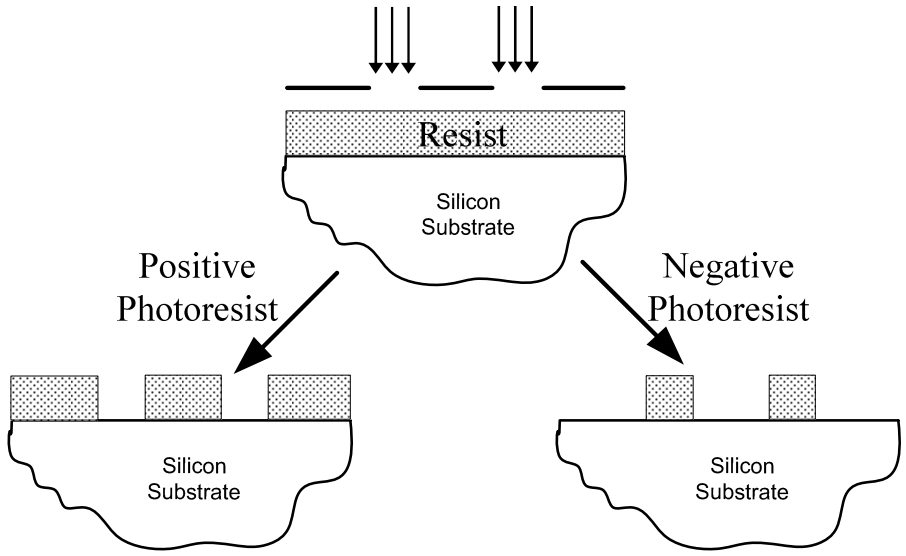

Figure 3.13 Positive photoresist, developer removes exposed material & Negative photoresist, developer removes unexposed material.

Step 1: Mask Making

Figure 3.14 shows the designed mask which is used for the following photolithography. The use of alignment windows allow the patterns to be superimposed onto the top of the corresponded guide structures.

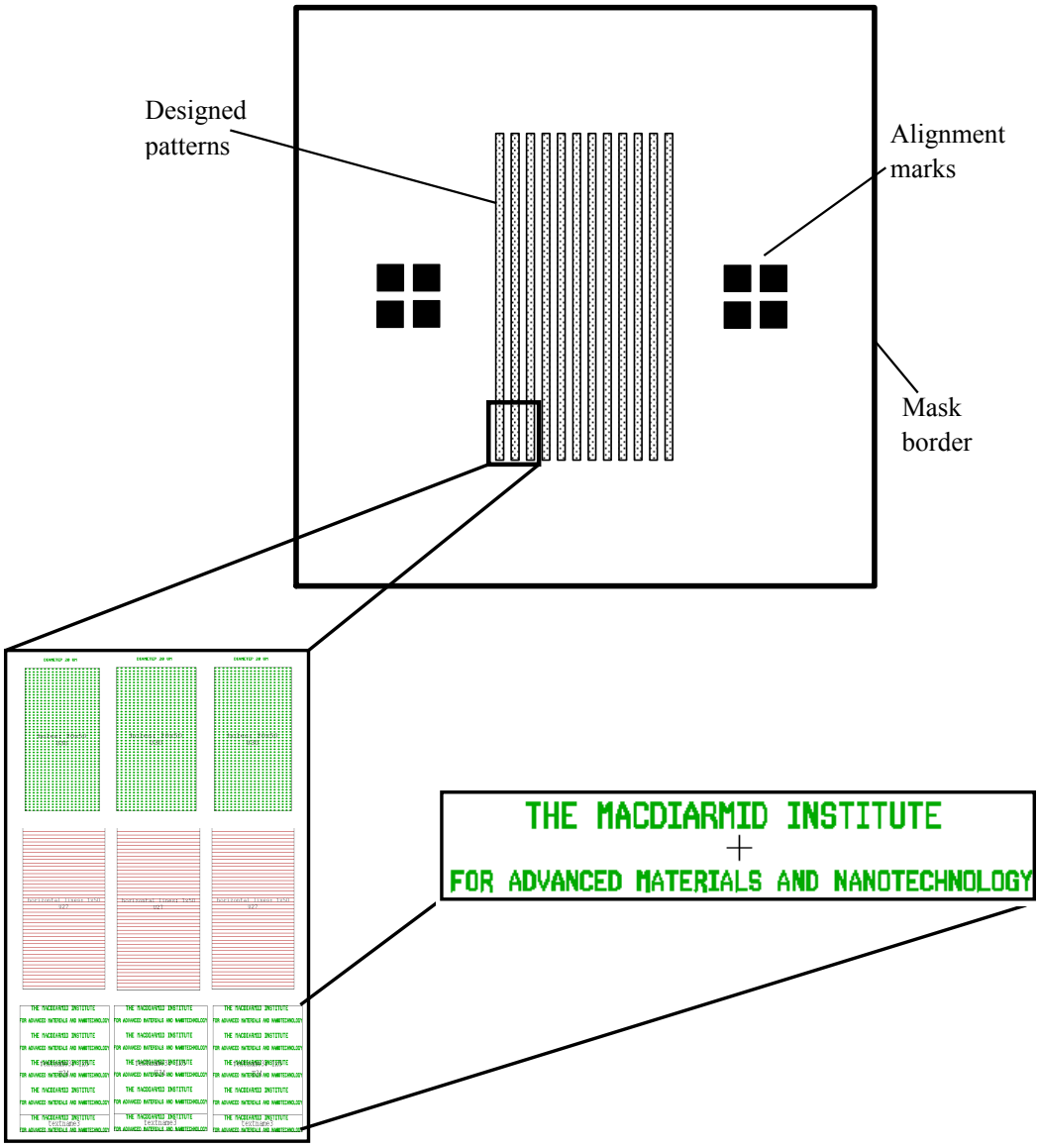

Figure 3.14 Designed mask for photolithography patterning.

Step 2: Photoresist Processing

AZ1518 resist is used for patterning fine features on top of the guide structures, the procedures of patterning AZ1518 resist on SU-8 structures are the same as for the Si_3N_4 mask patterning excluding the hard bake step. However, with SU-8 lithography process, developed AZ1518 fine features are very likely to be destroyed as the transparent SU-8 photoresist is highly reflective. In order to reduce reflections from the bottom silicon substrate, bottom antireflective coating (BARC) AZ-BARLi-II is introduced. Before spin-coating AZ1518 photoresist, a layer of BARC is spin-coated at 3000 rpm for 60 seconds. Then, the BARC layer is baked on a hot plate at 200°C for 60 seconds, and the thickness is measured to be approximately 180 nm using the profilometry.

3.3.2 E-beam lithography

E-beam lithography (EBL) is the specialized technique for creating the extremely fine patterns, the feature size of EBL is able to achieve nanometer regime. The advantage of using EBL is that complex and submicron patterns can be easily generated without the use of a mask. However, as a pattern is generated in beam size increments, the main drawback of EBL is the long exposure time for large-scale pattern. In this work, EBL is used to produce the submicron features for the stamp, so as to demonstrate the capability of fibre-imprint technology.

The Raith 150 EBL in the University of Canterbury nanofabrication laboratory (UCNFL) is a fully integrated system that consists mainly of a LEO 1500 series electron microscope with added laser-interferometer stage, robotic chamber loading, pattern generator hardware to control the beam and the Raith software package (Figure 3.15). There are two computer screens, the left is connected to the computer running the Raith150 software. The right-hand screen is connected to the LEO computer, all operation of SEM can be done here, such as focusing, adjusting alignment of the optics, scanning of images, etc.

Figure 3.15 Raith 150 electron beam lithography system.

Step 1: Electron-beam Resist Processing

First, 4% High Molecular Weight (HMW) PMMA resist is spin-coated onto the silicon substrate at 4000 rpm for 60 seconds, the resultant thickness is about 120 nm. It is then baked at 185°C oven for 30 minutes.

Step 2: Pattern Exposure and Development

Single pixel line writing mode is employed to obtain high resolution, and a line dose test was carried out in order to determine the minimum line does which is 1400 pAs/cm (Figure 3.16). Methyl Isobutyl Ketone (MIBK) solvent is used as the developer to remove the exposed PMMA resist. The substrate is immersed into MIBK solvent for 30 seconds, then rinse with IPA solvent.

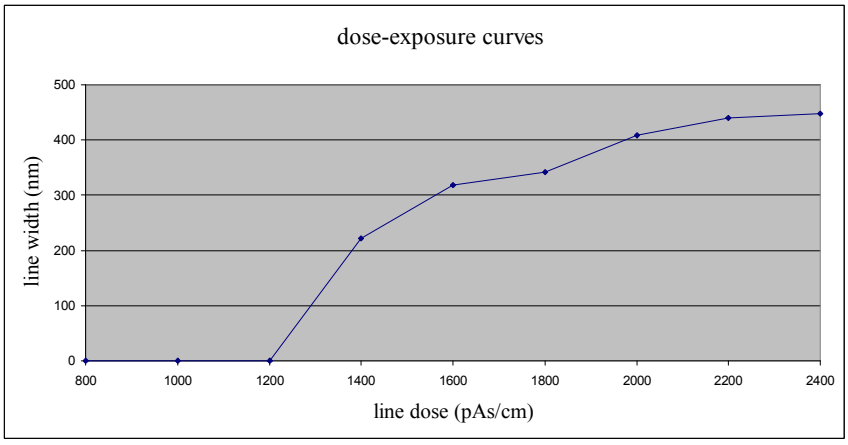

Figure 3.16 Line dose test for PMMA exposed in Raith 150 system.

3.4 E-BEAM EVAPORATION

After developing the optical or e-beam defined pattern, a thin conductive layer of nickel is deposited on top of the photoresist or e-beam resist which acts as a cathode base for the following electroplating process. The conventional DC sputtering is not suited for nickel coating, because in magnetron sputtering of ferromagnetic materials such as Ni, the magnetic field is shunted through the target and it is very difficult to form a closed-loop of magnetic flux on the target surface. Hence, E-beam evaporation is applied in this process. The equipment used in this process is the Edwards Auto-500 magnetron sputterer which is presented in Figure 3.17. For evaporating nickel pellet in a graphite crucible, the e-beam source is usually set at 85 mA, at typical process pressures of around 10^{-5} mbar.

Figure 3.17 Edwards Auto-500 magnetron sputterer.

However, the electrical connection of nickel seed layer for SU-8 guide structure is an issue as the SU-8 lithography produces high aspect ratio vertical sidewalls, e-beam evaporation only provides directional deposition which means the sidewalls of SU-8 structures cannot be covered with nickel. Only top and bottom regions of SU-8 structures are covered with nickel after e-beam evaporation as seen in Figure 3.18(b). Hence, KOH etching process is more feasible due to its sloped sidewalls as shown in Figure 3.19, The KOH etched sidewalls are uniformly covered with nickel seed layer.

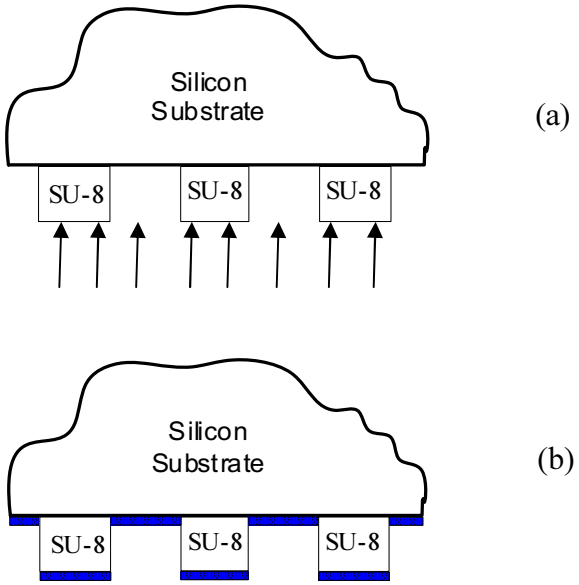

Figure 3.18 (a) e-beam evaporation of nickel onto SU-8 guide structure (b) deposited nickel seed layer on SU-8 guide structure.

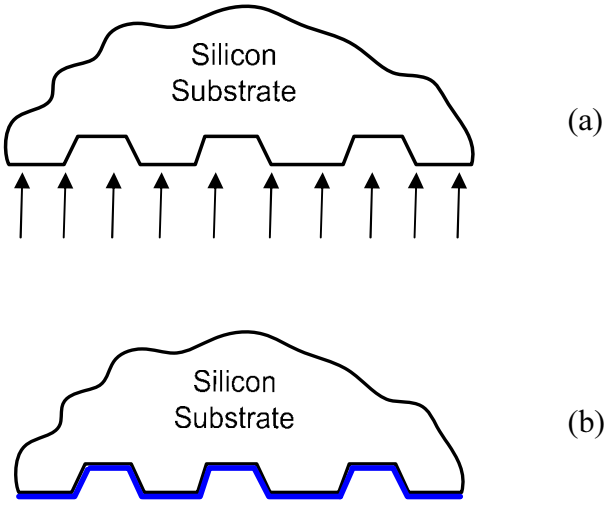

Figure 3.19 (a) e-beam evaporation of nickel onto KOH etched guide structure (b) deposited nickel seed layer on KOH etched guide structure.

3.5 NICKEL ELECTROPLATING

Nickel electroplating coupled with optical or e-beam lithography has been widely used for fabricating nickel nanoimprint stamps. Electroplating is the process of producing a coating, usually metallic, on a surface by the action of electric current.

3.5.1 Electroplating Background

Electroplating is often used for its excellent surface finishes and ability to create uniform parts of varying thickness, electroplating has more recently been incorporated into the nanofabrication industry. Electroplating is performed by running a current through a positive anode "target" and a negative cathode, or substrate, in an aqueous ionic solution. The target is composed of the pure metal, and the substrate is which the metal is deposited. Many different pure metals and alloys can be electroplated. Nickel is the most widely used electroplated deposit because of its reasonable hardness, tensile strength, ductility and good corrosion resistance [Dennis and Such 1993]. Nickel also produces a fine-grained electrodeposit which copies the surface profiles precisely and has a limiting surface roughness determined by surface oxidation [Sexton and Marnock 2000].

Nickel electroplating requires the passage of direct current between two electrodes that are immersed in a conductive, aqueous solution of nickel salts as shown in Figure 3.20 [Pai 2001]. The flow of direct current causes the anode to dissolve and the cathode to become covered with nickel. The nickel in solution is present in the form of divalent positively charged ions (Ni^{2+}). When current flows, the positive ions react with two electrons and are converted to metallic nickel (Ni^0) at the cathode surface. The reverse occurs at the anode which metallic nickel is dissolved to form divalent positively charged ions which enter the solution. The nickel ions discharged at the cathode are replenished by those formed at the anode [PLC 1978].

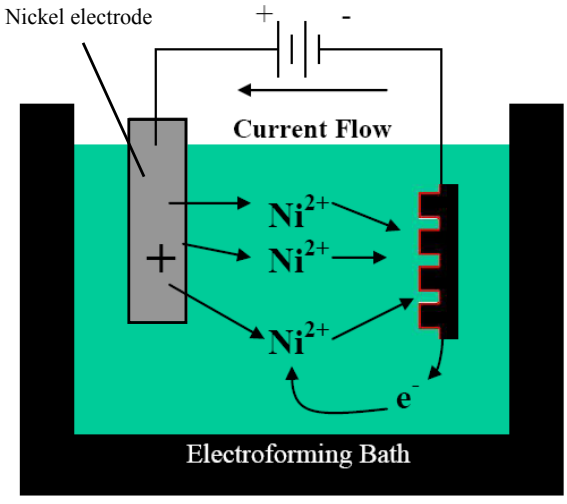

Figure 3.20 Schema of nickel electroplating [Pai 2001].

A schematic of the nickel electroplating process is shown in Figure 3.21. In this figure, the patterned substrate (a) is coated with a thin conductive 'seed layer' (b) by e-beam evaporation. (c) The substrate, along with the nickel target, is then placed into the plating solution. The target is attached to the positive end of a current source and the substrate is connected to the negative terminal of the current source. (d) Delamination, to remove the nickel stamp from the patterned substrate.

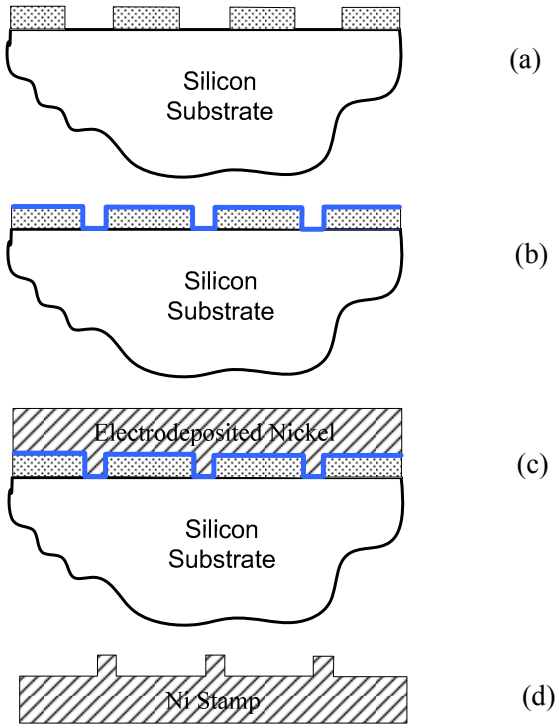

Figure 3.21 Nickel electroplating process.

3.5.2 Electroplating Bath

The common types of solution used for nickel electroplating are shown as follows:

- Watt nickel plating solution
- Nickel sulphamate solution
- All-chloride solution
- Sulphate-chloride solution
- All-sulphate solution
- Hard nickel solution

Nickel sulphamate bath is chosen for this project. Compared to the other types of baths, nickel sulphamate bath generally produces deposits with the lowest internal stress, and it provides high rates of deposition by applying high current density. The solution compositions of nickel sulphamate bath are shown in Table 3.6 [PLC 1978].

Solution Composition	**g/l**	**Functions**
Nickel Sulphamate concentrate, $Ni(NH_2SO_3)_2$	400 – 500	Source of nickel serving as well as conductive electrolyte
Boric Acid, H_3BO_3	30 – 40	pH buffer and stabilizer
Nickel Chloride, $NiCl_2$	5 – 15	Improve conductivity

Table 3.6 Basic nickel sulphamate bath composition and their functions.

In order to minimize the internal stress of the plating bath, and to achieve the uniform electrodeposited thickness, the temperature and pH value should be precisely controlled. The details of operating conditions of nickel sulphamate bath are as follows:

- Cathode current density: 0.02 to 0.16 A/cm^2, 0.03 A/cm^2 is used in this experiment, since low current density will result relatively uniform thickness distribution.
- pH value: 3.9 – 4.5, sulphamic acid is used to lower the pH value of electrolyte solution if necessary. pH test paper will be used to determine the pH value.
- Temperature: 40°C – 60°C, the optimum temperature is 48°C. Water bath is used to well maintain the temperature.
- Agitation: magnetic stirrer would be sufficient for agitation of the solution in 1L beaker setup.

The plating bath setup in the laboratory is shown in Figure 3.22 below, high purity (99.99%) nickel pellets are placed into the anode titanium made basket which is corrosion resistant.

3.5.3 Delamination and Cleaning

When electroplating has finished, the nickel stamp is peeled off from the substrate physically with a scalpel. Figure 3.23 shows the electroplated Ni stamp with Si substrate at bottom before delamination. The plating stress generated with KOH etching process is much less than SU-8 lithography process, therefore the nickel stamp can be easily separated from the substrate. Any residual resist is washed from the stamp by soaking in acetone and further cleaning with DI water. Figure 3.24(a) shows the fabricated Ni stamp after delamination, the fine features have been well replicated on the shiny nickel surface as presented on Figure 3.24(b).

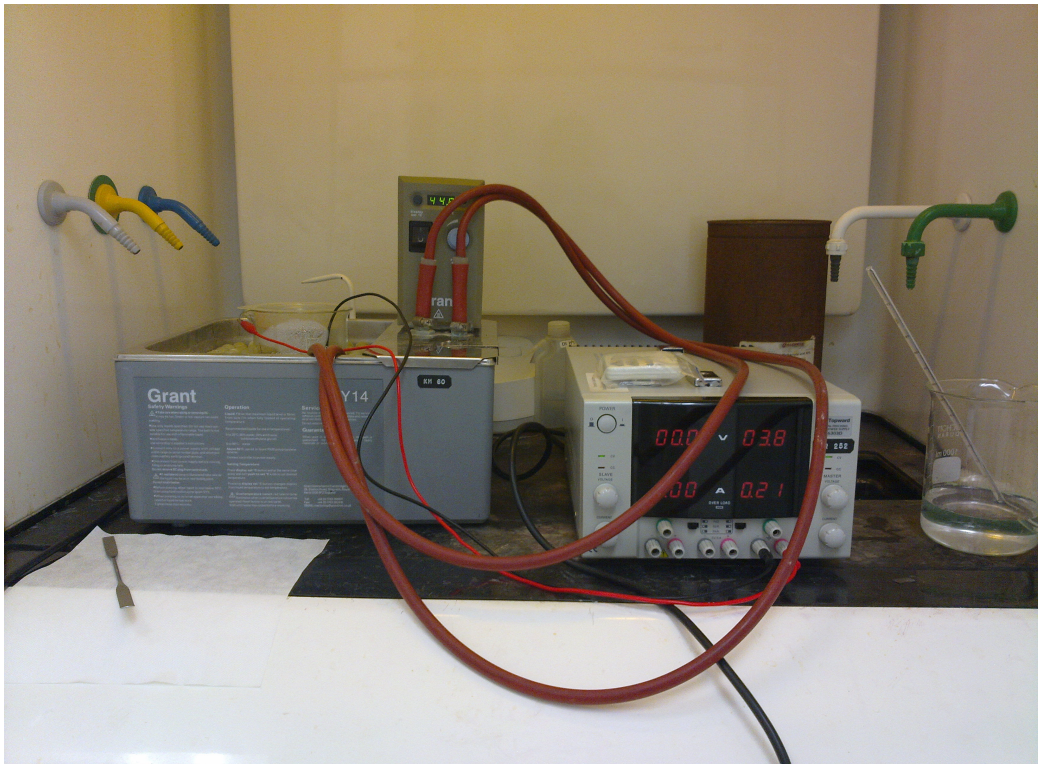

Figure 3.22 Plating setup in the laboratory.

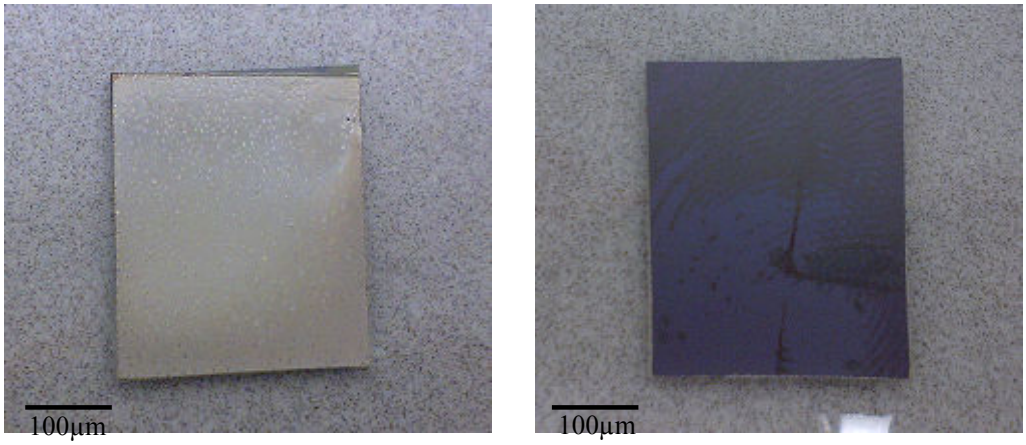

(a) (b)

Figure 3.23 Electroplated Ni stamp before delamination (a) front side with electroplated nickel (b) back side with Si substrate.

3.6 SUMMARY

The full fabrication procedures to develop the fibre-imprint technology are described in the chapter. SU-8 lithography and KOH silicon etching methods are utilized to fabricate the fibre guide structures, which have been explained in Section 3.2.1 and

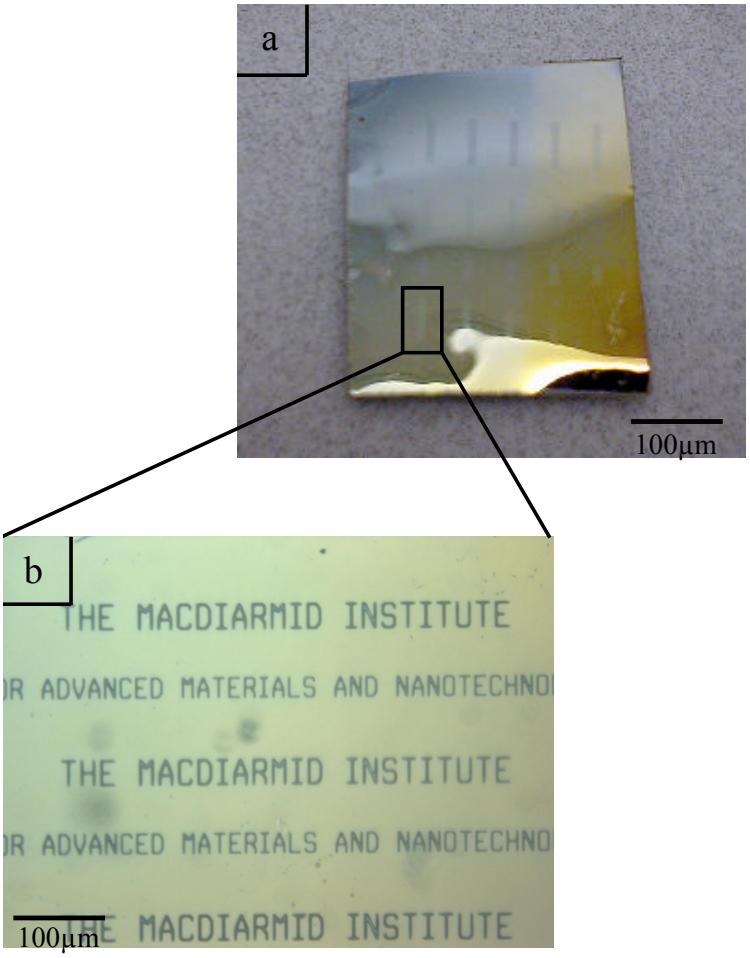

Figure 3.24 (a) Fabricated Ni stamp after delamination (b) replicated fine features on Ni stamp.

Section 3.2.2 respectively. Section 3.3 introduces two techniques for fine feature writings onto the guide structures, and the following section describes the method of depositing conductive seed layer for the subsequent electroplating process. Section 3.5 gives a brief overview of electroplating technique and the typical electroplating solutions, the electroplating setup for this work and some fabricated nickel stamps are shown at the end of this section.

Chapter 4

STAMP MANUFACTURE

4.1 INTRODUCTION

In this chapter the detailed processes of manufacturing stamps with fine features as well as fiber guide structures by using different methods are described, using the techniques described in Chapter 3. The first section introduces the methods of making stamps with fine features; this involves the use of photolithography and electron beam lithography combined with nickel electroplating technique. The next section presents the techniques and process recipes of fabricating stamps with guide structures. There are two alternative methods of creating grooves as guide structure, SU-8 lithography is the first option, although several issues were raised with the use of SU-8 grooves, especially the sidewall coverage during the e-beam evaporation process as discussed in the previous chapter. To avoid or minimize the issues appeared in the SU-8 process, KOH etched Si grooves were also used; the process and improved results are presented in this section. In the final section, the edge-bead effects as well as some other problems will be discussed.

4.2 FINE FEATURES

The stamp with fine features (micro- and nano-scale patterns) are designed by photo lithography and electron beam lithography processes, followed by nickel replication. A mask with micro scale patterns in chromium was required for the photolithography process, whereas e-beam lithography uses direct writing of nano-scale patterns onto the substrates.

4.2.1 Photolithography for Fine Features

The first step to manufacture the stamp using photolithography process is to design the mask as briefly mentioned in Section 3.3.1, using software L-Edit from Tanner Tools in this case. The designed mask for this stamp consists of three basic patterns which are arrays of 20 $\times$ 50 pillar structures with the radius of 10 μm (Figure 4.1(a)), a series

of 50 horizontal/vertical lines with the height/width of 3 μm (Figure 4.1(b)), and text features with 50 μm size of each character (Figure 4.1(c)).

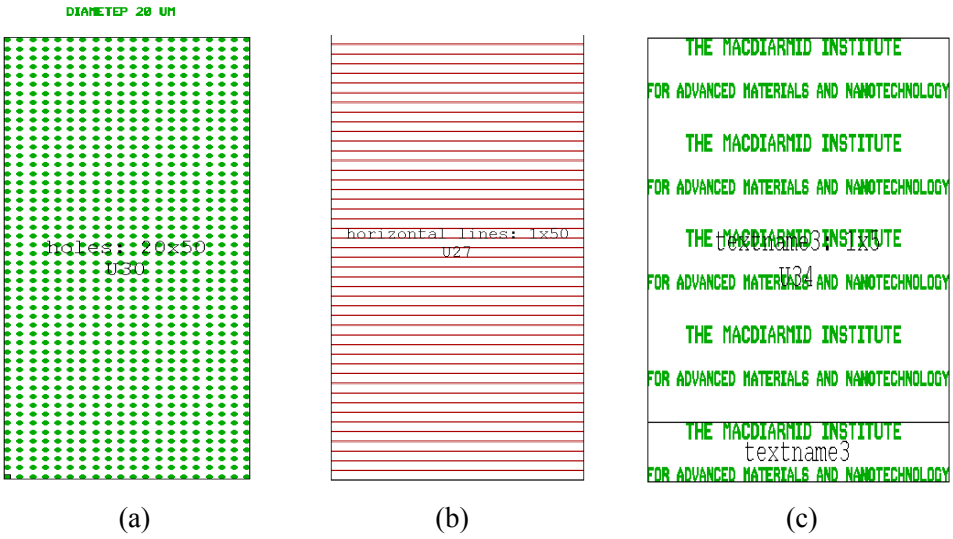

Figure 4.1 (a) Pillar features (b) Horizontal line features (c) Text features.

The procedure for photolithography with AZ1518 positive photoresist, on 25 mm by 25 mm samples of silicon wafer, was as follows. Initially, each sample was cleaned by immersion and rinse in acetone, isopropyl alcohol and then methanol, and then they were blown dry with nitrogen, and dehydrated in a hotplate at 100°C for 60 seconds. A Headway PWM32 spinner was used, one sample at a time was placed on the photoresist spinner's chuck with vacuum turned on. The sample was spin-coated at 4000 rpm for 60 seconds, two or three drops of photoresist were expelled from a 1ml pipette onto the centre of the sample. After spinning, the sample was soft baked at 100°C for 90 seconds on a hotplate. If the sample was baked at a higher temperature or a longer time, it would be difficult to dissolve the exposed photoresist during the development. The sample was exposed for 20 seconds by Karl Suss MA6 mask aligner, then developed by immersion in AZMIF300 solution for 17 seconds, followed by a rinse in DI water. The features after development were captured by Olympus optical microscope BX30, see Figure 4.2.

The substrate is then coated with a thin layer of nickel by e-beam evaporation or thermal evaporator. The final step to fabricate the stamp is nickel electroplating; the fine features are first electroplated from the Ni seed layer through the patterned structures in the photoresist, followed by overplating across the whole sample since the electroplating process is isotropic. The details of electroplating procedures were discussed in Section 3.5. The features on the nickel stamp were observed using SEM, the top view of the stamps after peel-off is shown in Figure 4.3.

To demonstrate the features on the silicon substrate are well replicated onto the

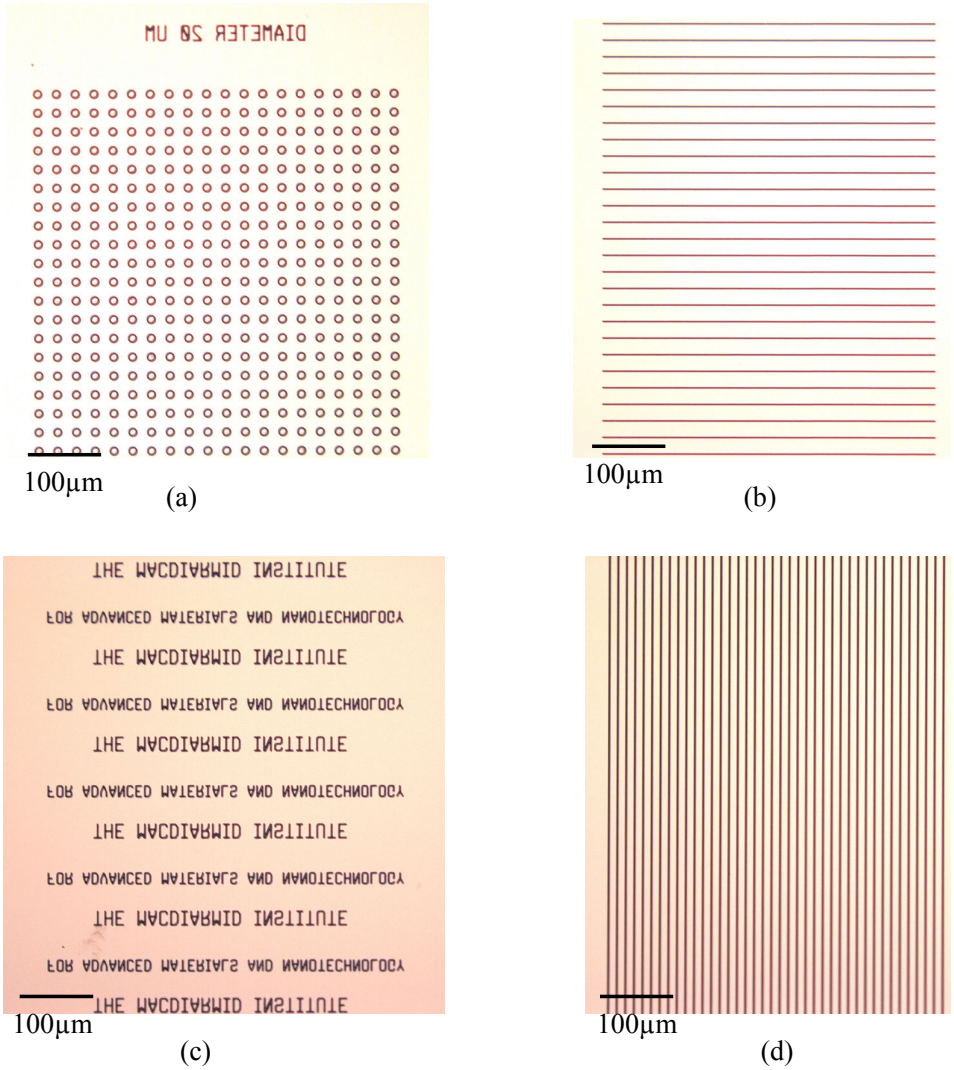

Figure 4.2 Fine features after development (a) Pillar features (b) Horizontal lines features (c) Text features (d) Vertical lines features.

fabricated Ni stamp from electroplating process, the diameter of the pillar features and the width of the vertical line features on the Ni stamp are measured by the SEM tools which are shown in Figure 4.4. The measured results on the Ni stamp are closed to the designed feature size (see Figure 4.1).

The 3D SEM images of fabricated nickel stamp show the better vision than the top view images. The cut piece of nickel stamp is mounted onto the angled sample holder inside the chamber, the tilt angle can be adjusted from the toolbar. Figure 4.5 shows the 3D SEM images of pillar and text features on the nickel stamp. The pillar structures on nickel stamp (Figure 4.5(a)) are not perfectly cylindrical, this could be caused by the underexposure or underdevelopment. In the first circumstance, insufficient light energy reaching the photoresist, the chemical reaction will be incomplete, as the result the photoresist will not become fully soluble, so the pattern will only be partially

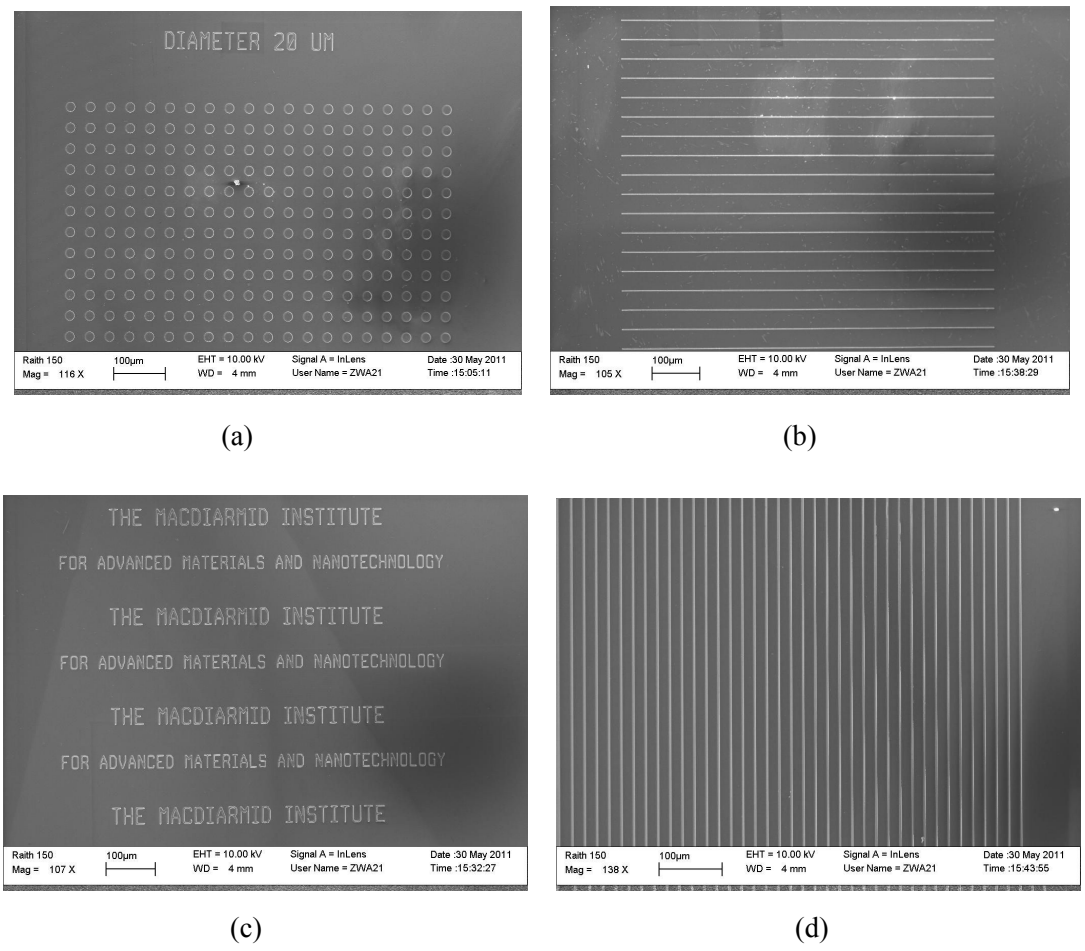

Figure 4.3 SEM images of micro-scale features on Ni stamp (a) pillar features (b) horizontal line features (c) Text features (d) vertical line features.

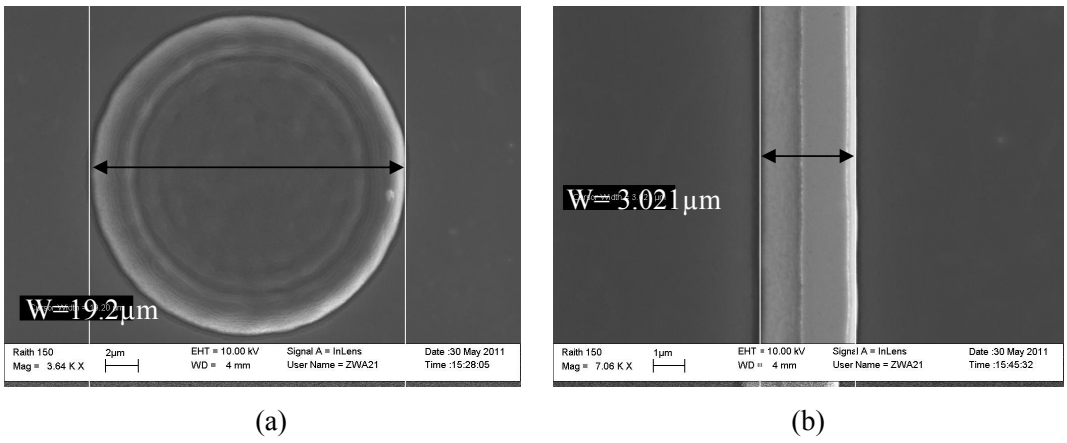

Figure 4.4 SEM measurements of replicated fine features on Ni stamp (a) diameter measurement (b) width measurement.

developed. The most common effect of underexposure is the rounded corners on the pattern. Underdevelopment can lead the same effect as underexposure, for example, the

residual photoresist in the corners or the edges. To avoid both effects, more accurate timing of exposure and develop should be applied.

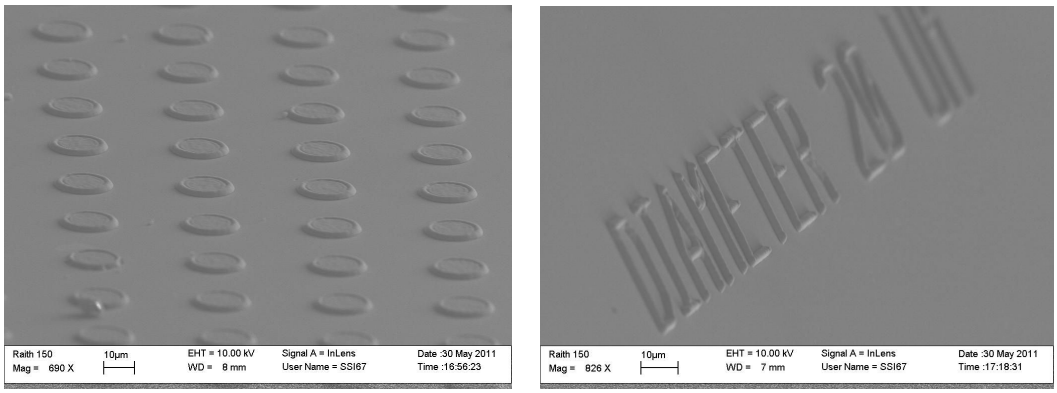

Figure 4.5 3D SEM images of Ni stamp (a) pillar features (b) text features.

4.2.2 Electron Beam Lithography

The other technique to design the stamp with fine features (nano-scale) is electron beam lithography (EBL). EBL refers to a lithographic process that uses a focused beam of electrons to form the circuit patterns needed for material deposition on the wafer. The EBL system used in nanofabrication laboratory is Raith 150 EBL tool which is an ultra-high resolution electron beam lithography system used for direct writing complex patterns onto resists at resolution of 50 nm; the system also has a scanning electron microscope to image and navigate the samples.

In comparison with the photolithography process, the advantage of using EBL is that the submicron patterns can be easily generated without the use of a mask. While the resolution of photolithography is mostly limited by the diffraction, this is not the limiting factor for EBL due to the short electron wavelength. The resolution of an EBL system is mostly constrained by the electron scattering from the substrate. However, EBL is not suitable for a large scale pattern exposure because EBL is a serial process. It this work, EBL was used to design the nano-scale features onto the stamp. The patterns can be created by L-Edit Tanner Tool or Raith 150 software itself. The EBL features developed for the Adidas campaign with the names of 1073 All Blacks was used for this work, the size of the entire feature is 191.62 μm (U) $\times$ 10928.1 μm (V), and the approximate size of each character is 3 μm (U) $\times$ 5 μm (V). Figure 4.6 shows a string of names from the designed patterns.

Single pixel line (line width = 0 μm) writing mode was employed to achieve the high resolution as well as saving the exposure time. The procedures in detail were described in Section 3.3.2; the feature after development is shown in Figure 4.7. Unlike the

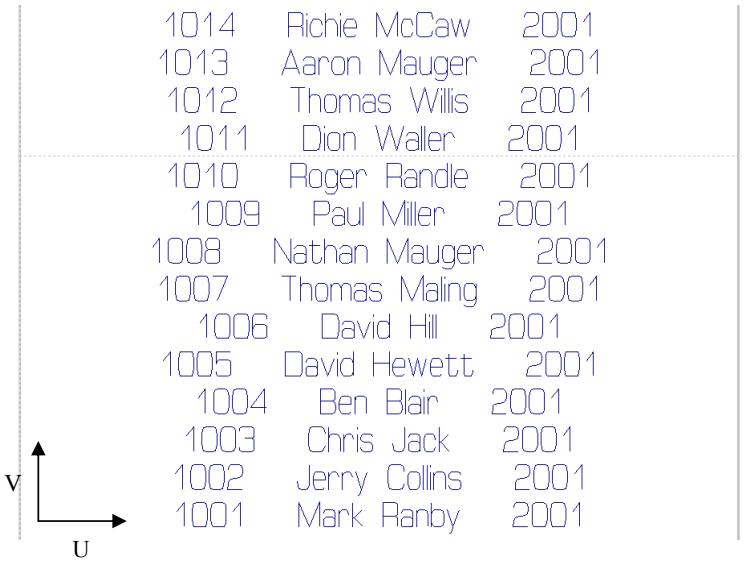

Figure 4.6 Patterns for EBL exposure.

mirror-image features developed after photolithography process, the developed features generated by maskless EBL process were exactly replicated from the designed patterns. This indicates that the stamp manufactured by the photolithography process is just the opposite in contrast with the EBL process.

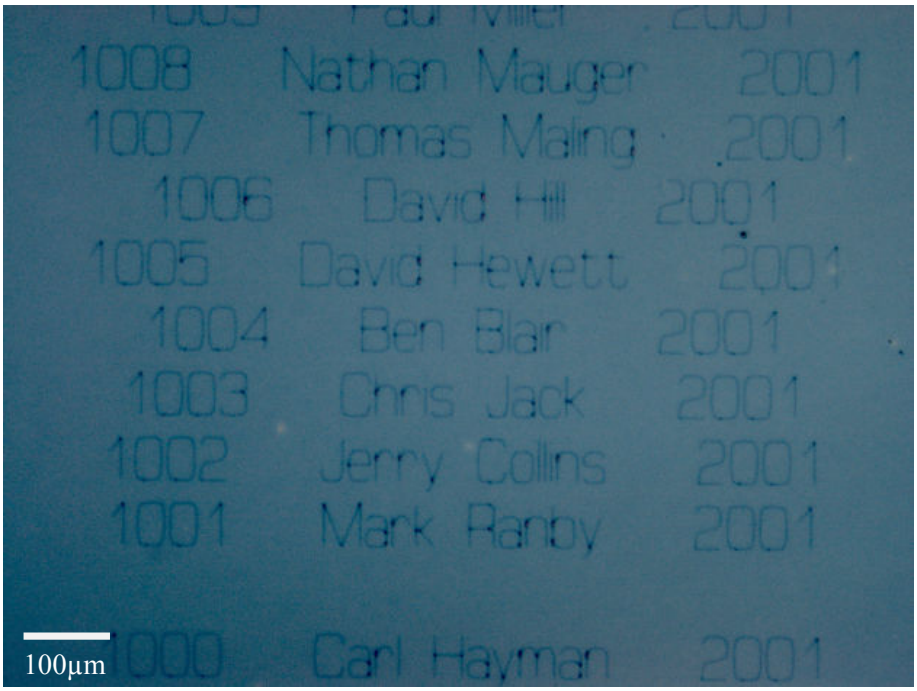

Figure 4.7 Text features generated by EBL after development.

After electrode formation and nickel electroplating, the SEM images of nano-scale features on nickel stamp are shown in Figure 4.8. The optimum line dose (1400 pAs/cm) was determined to use after the line does test which was explained in Section 3.3.2. Figure 4.8(a-c) show the SEM images of developed features on Ni stamp with various resolutions. The resultant line width of every single character was measured from the SEM image, 225.8 nm (Figure 4.8(d)) is fairly close to the corresponding line width according to Figure 3.16. If the line does is increased, the overall feature size will be enlarged, as a result, longer exposure time is required.

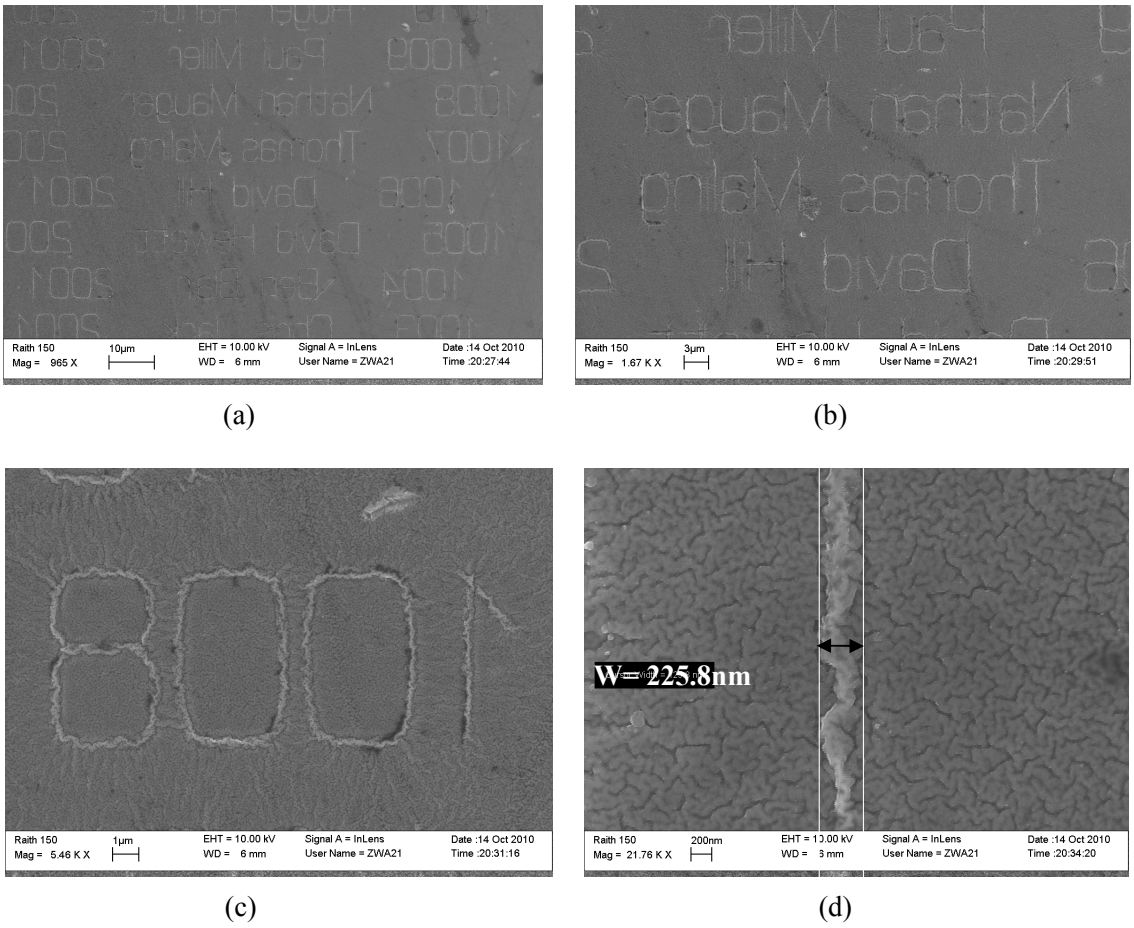

Figure 4.8 SEM images of nano-scale features on Ni stamp with various resolutions (a) 10 μm resolution (b) 3 μm resolution (c) 1 μm resolution (d) 200 nm resolution.

4.3 FIBRE GUIDE STRUCTURE

In comparison with those fine features on the nickel stamp, guide structures are produced so that fibres can be easily aligned to the guide structures during the continuous roller-imprint process. The guide structures consist of a series of parallel large grooves ($\sim$100 μm thickness) with 1 mm spacing, and micromachining is the basic idea to build up these alignment grooves. Figure 4.9 illustrates the schematic diagram of the nickel

stamp with fibre guide structure for this self-aligning process. As introduced at the beginning of this chapter, SU-8 lithography and potassium hydroxide (KOH) etching are two methods used for this work. The procedure details of both methods have been described in Section 3.2.1 and Section 3.2.2. This section begins with a brief introduction of SU-8 lithography process and the relevant work that has been performed. This includes the step by step results of manufacturing the nickel stamp, a discussion of problems that occurred for the use of SU-8 as well as the methods to resolve those issues. Section 4.3.2 demonstrates the process developed for creating KOH etched Si grooves, and the improved results of using this process which includes the examples of fine writing on the grooves. Section 4.3.3 concentrates on the edge beads effects for the fine writing on the grooves.

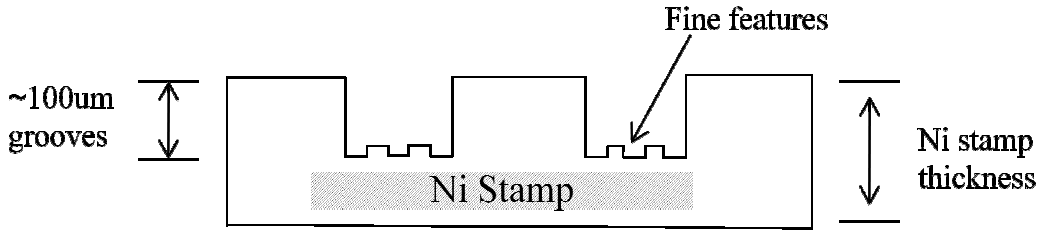

Figure 4.9 Schematic diagram of nickel stamp with guide structures.

4.3.1 SU-8 Grooves

The negative, epoxy-based photoresist SU-8 has been widely used as a resin for making high aspect ratio, functional MEMS device structures and packaging parts [Conradie and Moore 2002, Zhang et al 2001]. Due to its bio-compatibility and chemical resistance, SU-8 is also ideally suited to the fabrication of micro- channels for micro-fluidic and bioMEMS devices [Chuang et al 2003, Gadre et al 2001]. In this work, SU-8 is used as the alignment grooves for the fibre imprinting process.

The details of making the SU-8 grooves are described in Section 3.2.1, the next procedure is the fine features writing on those grooves. A new mask with some alignment marks was made which contains the same patterns used for the fine feature stamp (see Figure 4.1). To make sure that the patterns are exposed at the right positions on those SU-8 grooves, mask alignment must be done quite precisely during the exposure, otherwise misalignment is very likely to happen. Positive photoresist AZ1518 is again used for the fine features writing, the process of photolithography is presented in Section 4.2.1. Figure 4.10 shows the measured thickness of exposed fine features on top of SU-8 grooves.

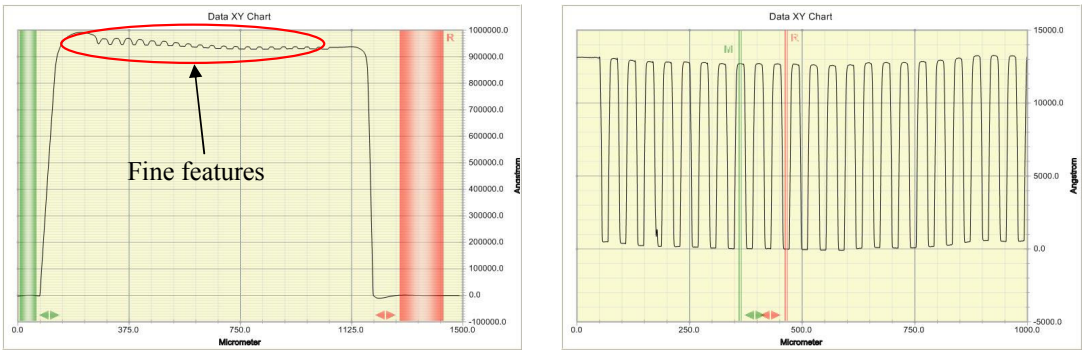

(a) (b)

Figure 4.10 (a) Thickness of fine features in comparison with SU-8 grooves (b) thickness of fine features.

Figure 4.10(a) shows the thickness comparison between the SU-8 groove (∼95 μm) and the fine features on top. The average thickness of those fine features (Figure 4.10(b)) is also measured by profilometry which is around 1.3 μm. In fact, the uniformity of spin-coated AZ1518 photoresist layer is influenced by the edge beads effects due to the large groove structures, which will be explained in Section 4.3.3. Figure 4.11(a) shows the fine features on top of SU-8 grooves after development, where the resolution is seriously affected by the transparent SU-8 structures. Bottom antireflective coating (BARC) AZ-BARLi-II is applied to solve this problem; before spinning-coat AZ1518 photoresist, a thin layer of BARC is firstly coated onto the SU-8 structures to reduce the reflection from the silicon substrate. Figure 4.11(b) shows the improved resolution by introducing the BARC layer.

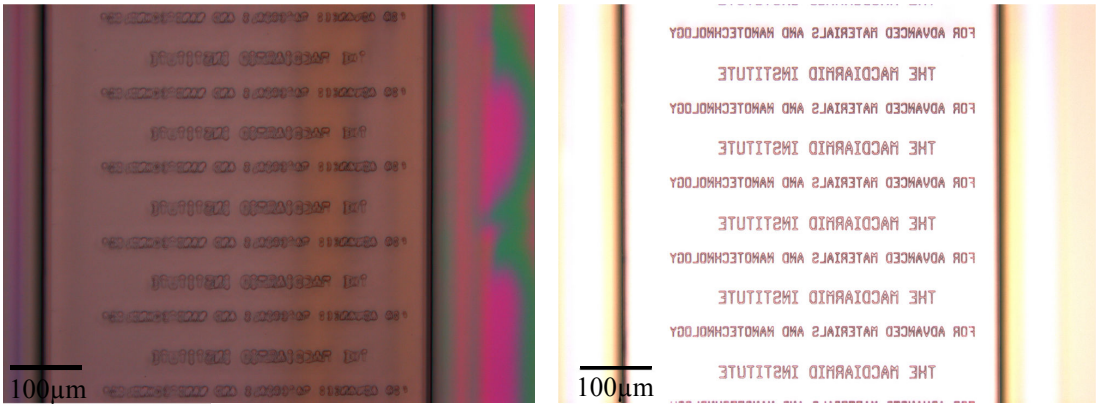

(a) (b)

Figure 4.11 Fine features on top of SU-8 grooves after development (a) without using BARC (b) using BARC.

As discussed in Section 3.4, there comes another problem while the seed layer is deposited on the SU-8 grooves. The vertical sidewalls of SU-8 grooves are not metalized due to the directional deposition of e-beam evaporation. As a result, there is no continuous electrical connection over the SU-8 surface which leads the loss of SU-8 grooves on the fabricated stamp as lack of nickel is electroplated on the sidewall. Figure 4.12 shows a failed stamp without metalized sidewalls of SU-8 grooves after nickel electroplating.

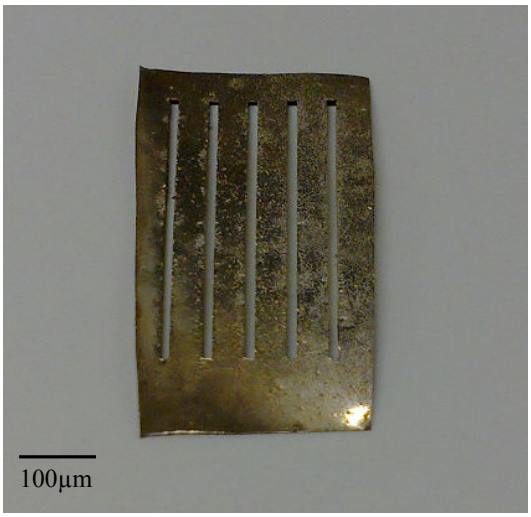

Figure 4.12 Failed stamp after nickel electroplating (loss of SU-8 grooves).

The method to resolve the problem of SU-8 sidewall coverage is by creating an angle (>45°) between the sample and the wafer holder during the e-beam evaporation. In this work, a plastic form cut into the trapezoid shape is used to produce the angle (Figure 4.13), make sure the sample is positioned right above the e-beam crucible. In addition, the depositing thickness of the seed layer was increased to at least 50 nm to ensure uniformity. To check the sidewall coverage after e-beam evaporation process, a multimeter is used to measure the resistance between the top and the base of the SU-8 grooves. The biggest issue of using SU-8 lithography to manufacture the stamp is that the SU-8 grooves tend to come off from the substrate while peeling off the stamp after nickel electroplating, which indicates that SU-8 structures can only be used as the one-off mask. A hypothesis of cause may be the stress generated from the electroplating, leads to the breakdown of the adhesion between SU-8 structures and Si substrate when delamination procedure is taken place. The resultant problem of this is the time consuming because of the relative long process of producing the SU-8 grooves. There is no other way to resolve this issue unless applying KOH-etched grooves which will be discussed in the next section.

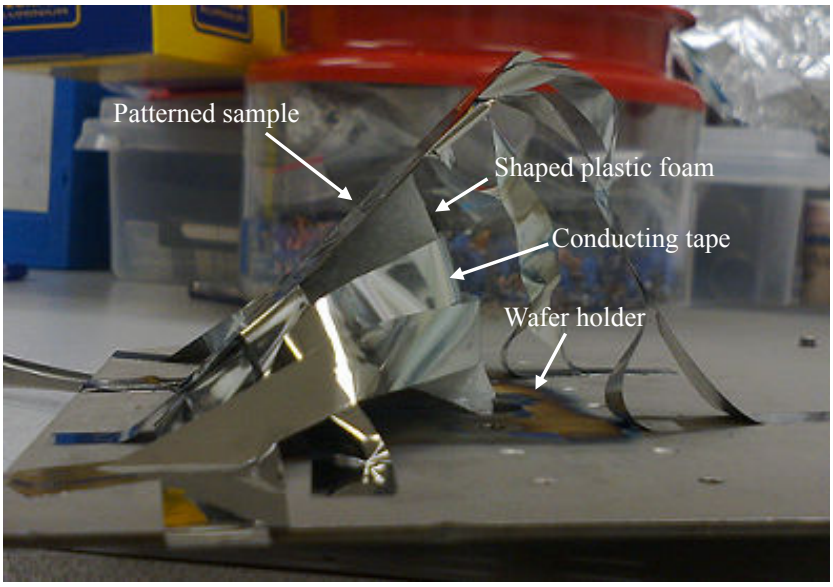

Figure 4.13 Shaped plastic foam between the sample and the wafer holder.

4.3.2 KOH-etched Si Grooves

As explained in the previous section, there are a few drawbacks of using SU-8 grooves as the guide structures, therefore the alternative method of using KOH-etched Si grooves is replaced. KOH is one of the most commonly used silicon etch technique for micro-machining silicon wafers; concentrated KOH solutions will etch along the (100) crystal plane several hundred times faster than long the (111) plane [Bean 1978].

The KOH-etched Si grooves are made followed by the process described in Section 3.2.2 (see Figure 4.14), the mask opening width (W_m) is designed at 2000 μm. The etched silicon depth (d) is measured by profilometry which is approximate 130 μm. The width of sloped sidewall (W_s) is measured from the edge of the bottom silicon substrate to the edge of top surface which is 84 μm. The resultant {111} etch-stop sidewall angle (θ) is 57° which is close to the geometry of the anisotropic KOH etching (54.74° angle from the plane). Figure 4.15 shows the cross-section diagram of KOH-etched Si structures.

The fine features writing on KOH-etched grooves is basically the same procedure which performed for SU-8 stamp manufacture. The exposure and developing time are consistent with fine features writing on SU-8 grooves. Figure 4.16 shows the developed micro-scale fine features on the ridges of KOH-etched guide structures which are exposed by photolithography. The feature resolution is improved without using BARC, however edge beads still affects the resolution especially on the fringe of the ridges.

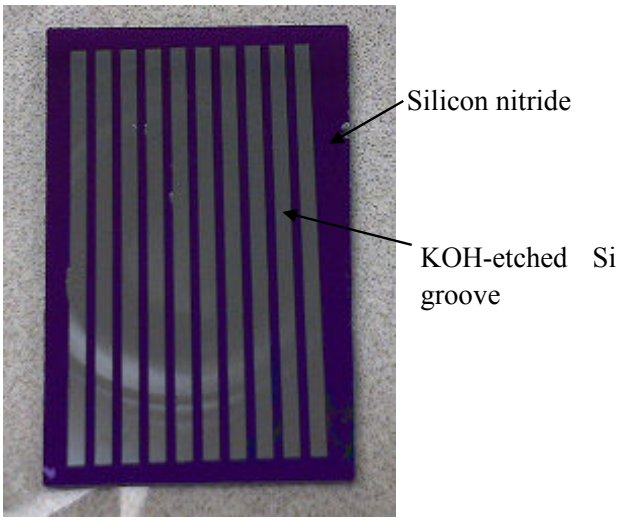

Figure 4.14 Fabricated KOH-etched Si grooves.

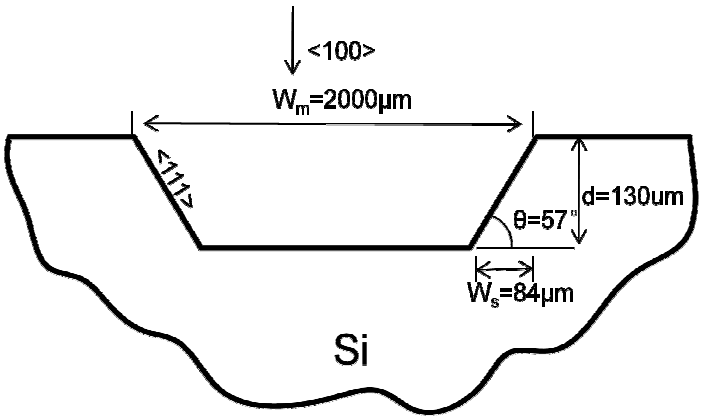

Figure 4.15 Mask opening for the etch of (100) wafers with 111 etch-stop sidewalls.

A 50 nm seed layer of nickel is then e-beam evaporated on top of KOH-etched surface; the problem of sidewall coverage for SU-8 groove no longer exists, since the sloped sidewalls etched by KOH solution allows nickel easily build-up on those areas.

The sample with KOH-etched grooves requires longer plating time as the thickness of fabricated stamp must be relatively thicker in comparison with the groove thickness (130 μm). The average plating rate is 30$\sim$40 μm/hour depending on the cathode current as well as pH of the plating solution. In general, low current ($\sim$0.17 A) is applied initially for at least half an hour in order to make the distribution of deposited nickel more uniform on the fine feature surface. High current (0.4–0.5 A) is then applied for the rest of electroplating process which leads to a high growth rate, so the nickel will build up quickly on those thick grooves. The minimum plating time required for electroplating KOH-etched groove is 5 hours; in this work the sample is electroplated

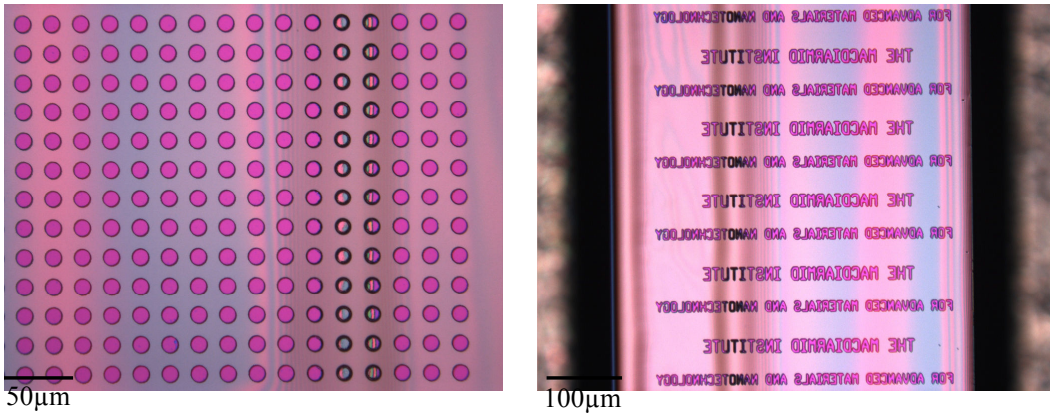

Figure 4.16 Developed fine features on the ridges (a) pillar features (b) text features.

for 7 hours to make sure the fabricated stamp is thick enough for the subsequent roller imprinting process. The stamp is easily peeled off from the mask, which indicates the plating stress has been largely reduced attributed by the sloped sidewalls. Moreover, after cleaning the mask with acetone, the KOH-etch Si mask can be reused for the next stamp manufacture; this advantage significantly reduces the time spent on the stamp fabrication process. Figure 4.17 shows the cross-sectional SEM image of fabricated nickel stamp after electroplating, the thickness of plated stamp is 220 μm ($\pm$10 μm) measured by vernier caliper.

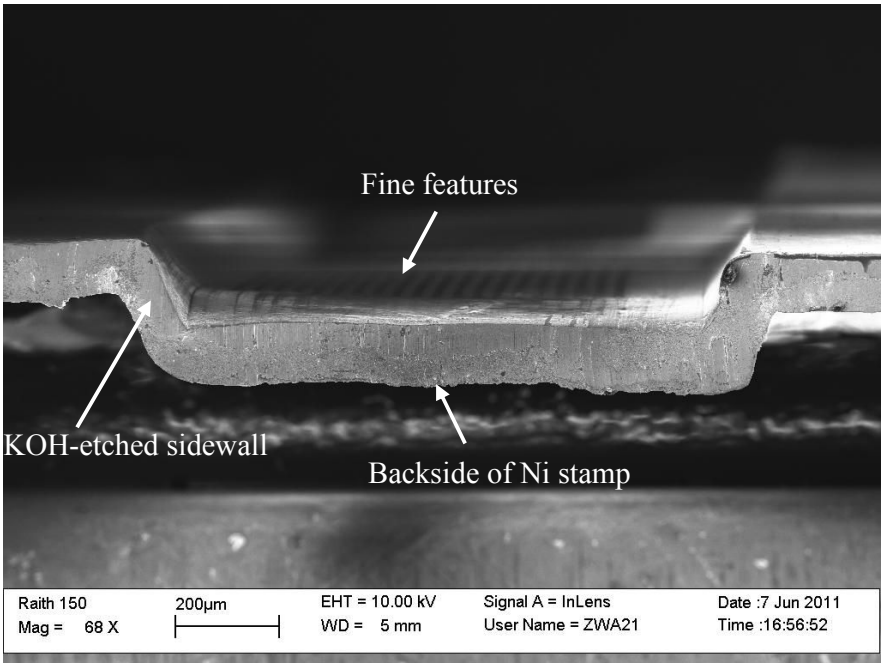

Figure 4.17 Cross-sectional SEM image of fabricated Ni stamp with KOH-etched groove.

As presented in Figure 4.17 above, the fine features are replicated on the bright side of Ni stamp with smooth surface, the surface profile of backside Ni stamp is relatively dim and rough since high current density is applied for the later electroplating stage. The KOH-etched grooves act as the guide structure on the Ni stamp with the patterned structures in between. The low resolution of fine features in this SEM image is due to the small size of fine features (∼2 μm) in comparison with the large groove structures. Figure 4.18 shows some top view SEM images of replicated micro-scale fine features on a Ni stamp.

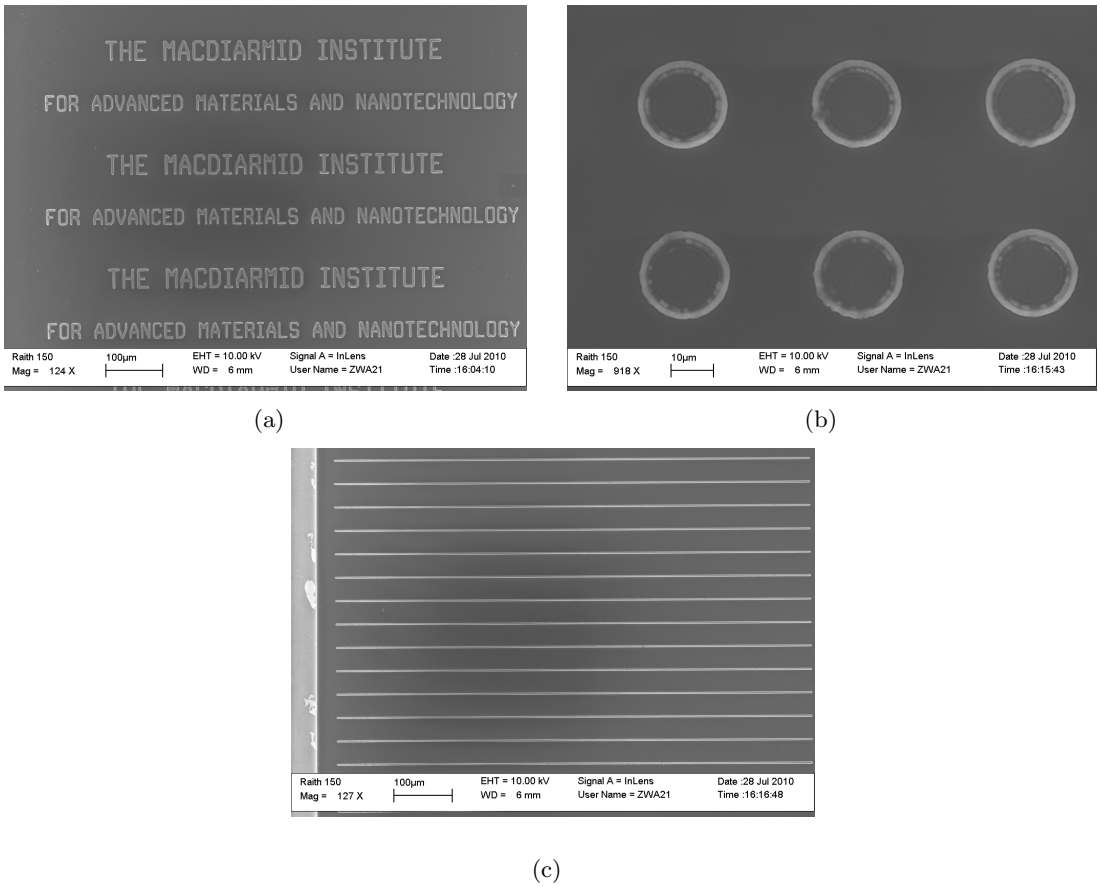

Figure 4.18 Top view SEM images of fabricated Ni stamp (a) text features (b) pillar features (c) horizontal line features.

Cross-sectional SEM and profilometry measurements are utilized to further prove the fine features on Ni stamp are well replicated from the patterned mask. Figure 4.19 shows the measured heights of replicated patterns on Ni stamp by profilometry (average height = 1.7 μm). The measured heights vary from 0.65 μm to 1.8 μm; the reason of this is the uneven surface profile of spin-coated photoresist layer. More detailed reason will be explained in Section 4.3.3.

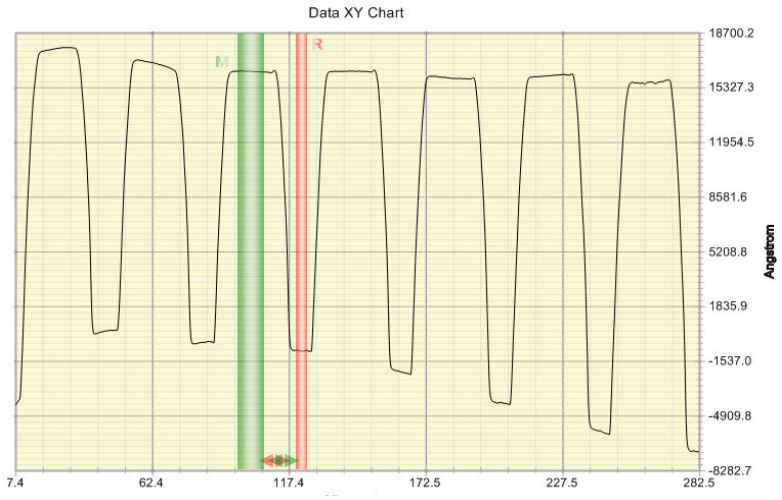

Figure 4.19 Measured heights of replicated patterns on Ni stamp by profilometry.

Figure 4.20 shows the cross-sectional SEM image of pillar structures on Ni stamp, the measured height is 1.76 μm which is close to the expected average height. The measured width of vertical line features (3.2 μm) and the diameter of pillar structures (20.4 μm) are illustrated in Figure 4.21(a) and Figure 4.21(b) respectively. The sizes replicated features are slightly larger than the designed mask (3.0 μm and 20.0 μm respectively), that is probably resulted by the over exposure of the patterns during photolithography process.

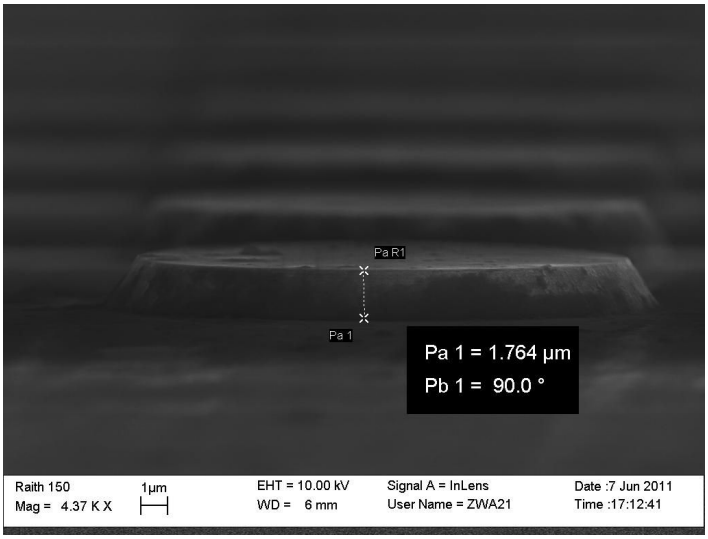

Figure 4.20 Cross-sectional SEM image of replicated pillar structure on Ni stamp.

Both profilometry and SEM measurements confirm that high-quality nickel stamp with micro features are replicated on KOH-etched Si grooves by electroplating. The

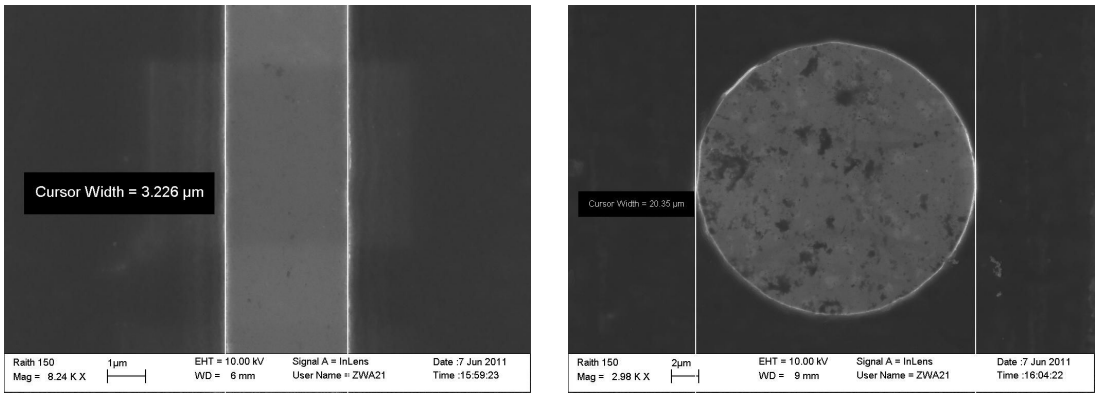

(a) (b)

Figure 4.21 SEM measurements of replicated fine features (a) vertical line width (b) diameter of pillar feature.

fabricated stamp has a high aspect ratio ridges with smooth grooves which can be used as the guide structure for later fibre imprinting process. In general, compared with SU-8 grooves, the use of KOH-etched grooves improves the resolution of fine features as well as providing the uniform nickel seed layer. Most importantly, the KOH-etched groove mask can be used for future reproduction of nickel stamps.

The Ni stamp with nano-scale fine features on KOH-etched Si grooves is also fabricated by using EBL and electroplating technique. The mask pattern has been presented in Figure 4.6, due to the sizes involved, atomic force microscopy (AFM) is used instead of profilometry to check the height of the replicated patterns after electroplating. Figure 4.22 shows Digital Instruments 3100 AFM system used for this work.

Figure 4.23(a) shows the AFM image of replicated patterns on Ni stamp over 15 μm scan size, and Figure 4.23(b) displays the measured heights of scanned features; the heights vary from approximate 20 nm to 52 nm with undesired surface roughness. The expected height of replicated features should be close to 120 nm which is the PMMA resist thickness. In fact it is not possible to coat the uniform PMMA resist layer on KOH-etched grooves, besides edge-bead effect is another issue which also causes the swing of feature heights.

4.3.3 Edge-bead Effects

As discussed earlier, for both SU-8 and KOH-etched Si grooves, the difficulty to attain uniform resist film thickness during the fine features writing because majority of the resists flow into the high aspect ratio grooves during spin-coating, only a small quantity remains on the ridges. Furthermore, edge-bead effects significantly affect the resolution of fine features writing on the ridges due to the undesired proximity-gap during exposure. As a result, the replicated features on Ni stamp have various heights as shown

Figure 4.22 Digital Instruments 3100 Atomic Force Microscope (AFM).

in the profilometry and AFM measurements in the previous sections. Figure 4.24(a) & (b) show examples of edge-bead which can be easily determined as the color change. The residual resist remains on the right-side edges of the substrate, which results a sudden increase of the resist height as illustrated in Figure 4.24(c). Build-up resists on the edge-bead areas normally lead the underexposure of the patterns, therefore the heights of replicated Ni structures which are affected by edge-bead will be much less than the others (see Figure 4.24(d)).

The conventional method applied to remove the edge beads is by dispensing the edge-bead removal (EBR) solvents, such as AZ EBR solvent, or simply wiping the edges with acetone before hard bake. However, it is not suitable for this work as the features are exposed onto the narrow regions (1 mm wide ridges), and the use of any solvents often leads the solvent spots on the resist which deteriorates the features. Basically, the edge-bead effect is inevitable for this experiment as the high aspect ratio grooves are involved as the guide structures. To minimize the impact resulted from edge-bead effects, one possible method is to apply higher spinning speeds with multiple levels of photoresist during the spin-coating procedure. Alternatively, the KOH-etched fibre guide structures could be fabricated after the fine scale lithography step, but this would require significant changes to the fabrication process.

(a)

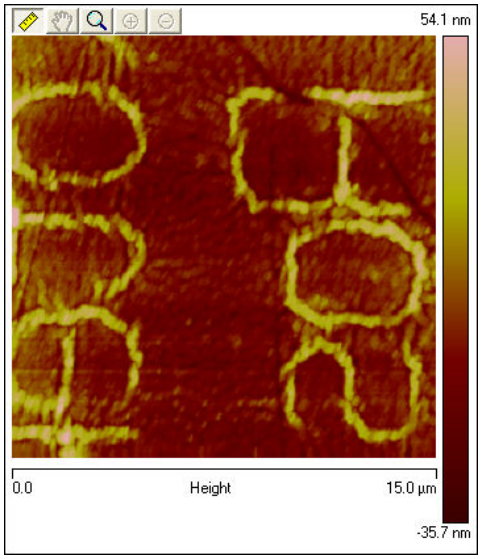

(b)

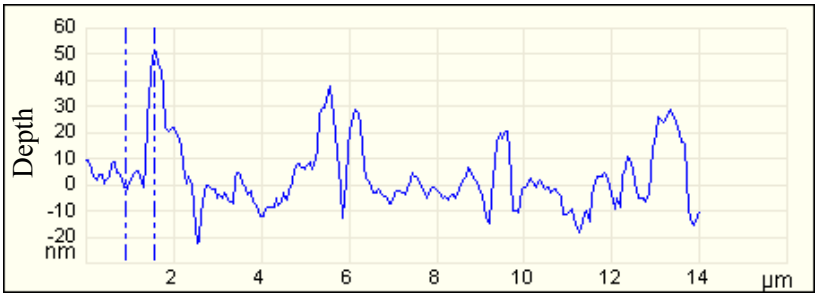

Figure 4.23 (a) AFM image of replicated features on KOH-etched Ni stamp (b) Measured heights over scanned features.

4.4 PH DECREASING IN PLATING BATH

Nickel electroplating is the last and most important process to manufacture the stamps, and a nickel sulphamate bath has been consistently used for this work. However, the difficulty in maintaining pH of the plating solution becomes a serious issue. pH decreases in the nickel sulphamate bath as electroplating carries on, Table 4.1 shows the plating time with the corresponding pH value. An electrical pH meter borrowed from chemistry laboratory in UoC is used to accurately measure the pH value every half an hour during the electroplating process. The initial pH value of the plating bath is 4.1, it then gradually drops below 2 after a three hours electroplating. The low pH leads a problem of extreme low deposition rate, sometimes even resulting in nickel seed layer coming off due to the acidic plating solution. The most troublesome aspect is that fresh plating solution has to be made up every time for electroplating which also results the money wasting of more chemical usage. In theory, pH should rise during nickel electroplating, as some hydrogen ions are removed from the plating solution at the cathode and eventually escape as hydrogen gas [Mason 2008]. If the pH falls, most

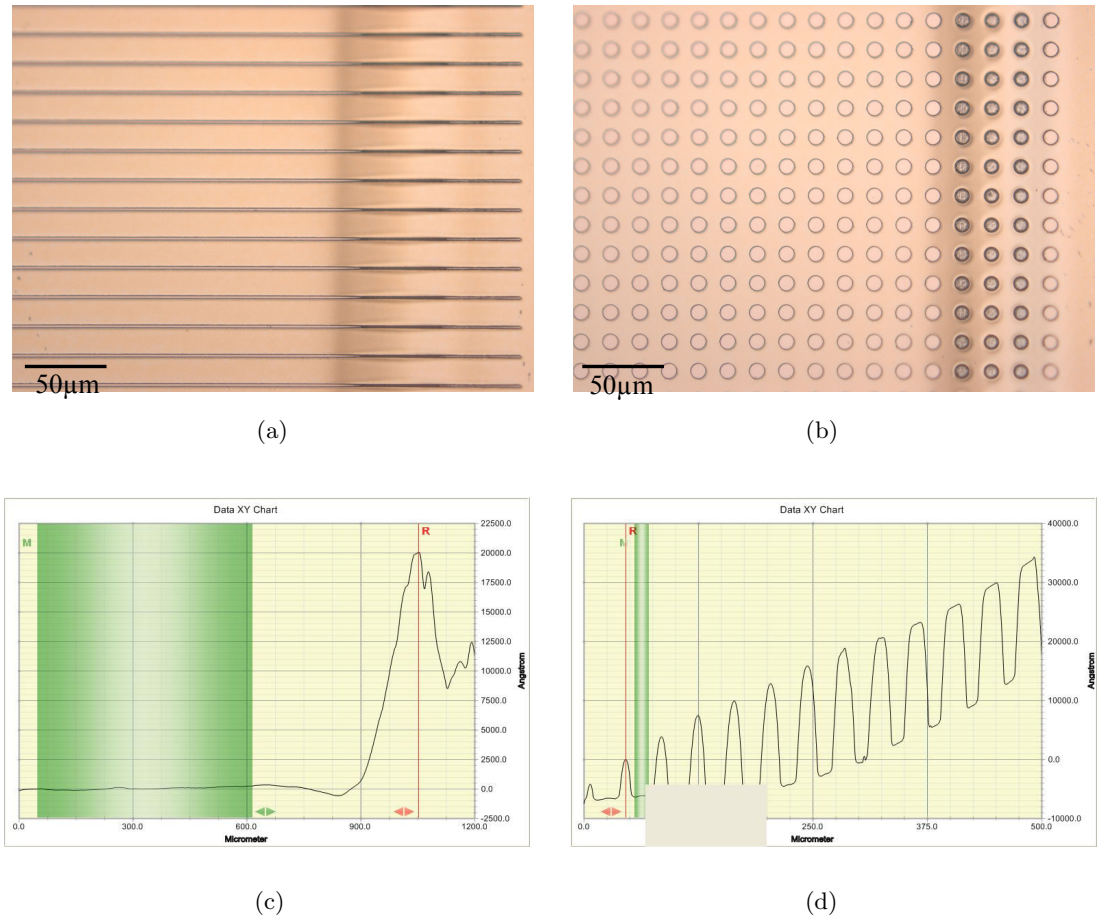

Figure 4.24 (a) Edge-bead on line features (b) Edge-bead on pillar features (c) measured step height of resist layer (d) measured heights of fabricated Ni structures.

likely the anode is not dissolving properly and hydroxyl (OH^-) ions are being discharged at the anode. The anode pellets become brown which indicates the nickel may well be passivating. The following are several other reasons that may contribute to the pH falling:

- Too much of an anode area (An anode:cathode ratio of 1:1 to 2:1 is usually recommended).
- Low boric acid content, because boric acid acts as a buffer which stabilizes the pH of the bath.
- Lack of nickel chloride.

To solve the problem of pH drop, a few suggestions could be taken into consideration. Firstly replacing the pure nickel pellet to S-round nickel [Kinghorn 2010], because pure nickel pellet in a sulphamate bath is hardly corroded, the primary reaction happened at the anode will be water hydrolysis causing pH to decrease. Nickel S-rounds are button shaped pieces of nickel, which is the most popular activated anode material

for electroplating as S-round nickel promotes anode dissolution. Nickel carbonate or sodium hydroxide can be added into the plating solution to bring up the pH, however, nickel carbonate is a potential carcinogen so is best avoided. At last, to ensure the boric acid and nickel chloride content at the correct level.

Plating time (pm)	**pH value of plating bath**
2:30	4.1
3:00	3.8
3:30	3.5
4:00	3.3
4:30	3
5:00	2.4
5:30	1.9

Table 4.1 Plating time vs. pH value of plating bath.

4.5 SUMMARY

High-quality nickel stamps with micro-scale features down to 225.8 nm are made by using photolithography/EBL process coupled with nickel sulphamate electroplating. The fabricated nickel stamp has reasonable hardness and ductility, profilometry and SEM measurements confirmed that designed structures are well replicated onto the stamp with expected resolution.

SU-8 grooves are produced as the guide structure for fibre imprinting process, however several issues occurred such as low resolution of patterned stamp, sidewalls metallization. As a result, the alternative method of KOH-etched Si grooves is developed. Improved results includes the replicated fine features on Ni stamp are shown in both optical microscope and SEM. The sloped sidewalls resolve the problem of seed layer deposition, as well as reducing the electroplated stress which makes the stamp easily to be peeled off.

Edges beads effects influence the uniformity of spin-coated photoresist, which result in the uneven heights of replicated fine features on the Ni stamp. This is an unavoidable issue as the fibre guide structures are at least 100 times larger than the size of fine features. pH drop is monitored during the electroplating procedure, and a few hypotheses are made in terms of the anode nickel and boric acid concentration. In order to resolve this problem, perhaps changing the pure nickel pellet to S-round nickel, at the meantime more control experiments should be performed to analyze the concentrations of boric acid and nickel chloride in the plating bath.

Chapter 5

IMPRINT RESULTS

5.1 INTRODUCTION

The processes of fabricating nickel stamps with fine features and fibre guide structures using different methods have been described in Chapter 4. Also, SEM and AFM measurements were applied to analyze the electroplated stamps. This chapter starts with the fibre material choice for this imprinting process. Section 5.3 demonstrates the procedures of fibre imprinting process using the roller embosser and the electroplated nickel stamp made by KOH etched silicon master. Stamp lifetime and effect of roller gap width are discussed in Section 5.4 and 5.5. Section 5.6 presents the imprinted results and issues that occurred during the imprinting process.

5.2 FIBRE MATERIAL CHOICE

Polymer fibres are firstly taken into consideration for developing this fibre-imprint technology. Polymer fibres are man-made fibres which are produced artificially from synthetic chemicals rather than growing from natural materials by purely physical process. For example, polytetrafluoroethylene (PTFE), nylon, polyvinyl chloride vinyon (PVC) and polyethylene (PE) are some typical polymer fibres which have been widely used in the industrial applications. Other fibre materials such as wool, silk and even hair will be the interesting choices for this application, however, due to the time constraint, PTFE is the only fibre material used in this work.

PTFE was firstly discovered in 1938 by Dr. Roy Plunkett at the DuPont research laboratories [ZeusInc 2005], so it is most well known by the DuPont brand name Teflon. PTFE is the polymerized form of tetrafluoroethylene; Figure 5.1 represents the structure of PTFE [ZeusInc 2005], which is composed of carbon and fluorine. Carbon-fluorine and carbon-carbon bonds are amongst the strongest bonds in organic chemistry, which accounts for many of its properties.

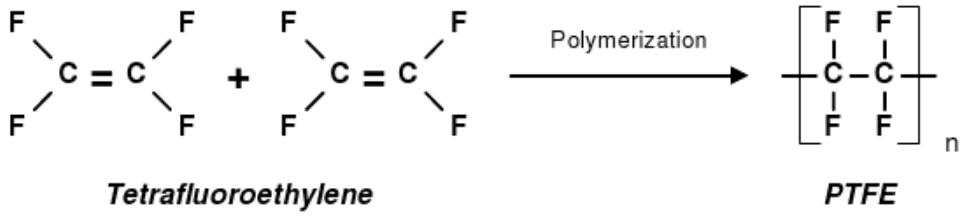

Figure 5.1 The structure of PTFE [ZeusInc 2005].

The followings are the general properties of PTFE [ZeusInc 2005]:

- Extremely low coefficient of friction
- Outstanding temperature stability
- Excellent dielectric properties
- Outstanding chemical resistance
- Outstanding sunlight and weather resistance
- Great thermal stability
- High cost

Those characteristics of PTFE make it the ideal choice in a wide range of products and applications. Probably one of the most famous uses for PTFE is as a non-stick coating found on cookware. Furthermore, PTFE is also used in the semiconductor manufacture, medical, chemical, automotive, electrical as well as cable industries. Several types of tests demonstrated that PTFE has low hardness among other plastic fibres [Nielsen and Landel 1994]; this characteristic makes PTFE suitable for this application, because this work requires the fibres to be pressed under the roller embosser. For this experiment, Teflon monofilament [ZeusInc 2011] (Zeus, Inc.) with 1 mm diameter is selected as shown in Figure 5.2, which is prepared for self-aligning imprinting process because the width of fabricated fibre-guide grooves on the Ni stamp are also 1 mm. As mentioned earlier, other plastic fibres such as nylon and polyethylene could be the alternative materials for this work, especially as polyethylene is confirmed has the lowest hardness [Nielsen and Landel 1994]. Table 5.1 shows the Vickers hardness values for a variety of polymers; for comparison the Vickers hardness of nickel is 638 MPa/mm^2 [Dennis and Such 1993] which is many thousands of times harder than any polymers. Thus, the electroplated nickel stamp will not have any deformation during the imprinting process.

Polymer	**Vickers hardness (kPa/mm^2)**
Polyvinyl chloride (PVC)	12.84
Polyethylene	1.57
PTFE	3.26
Nylon	9.2

Table 5.1 Hardness of polymers as measured by Vickers method [Nielsen and Landel 1994].

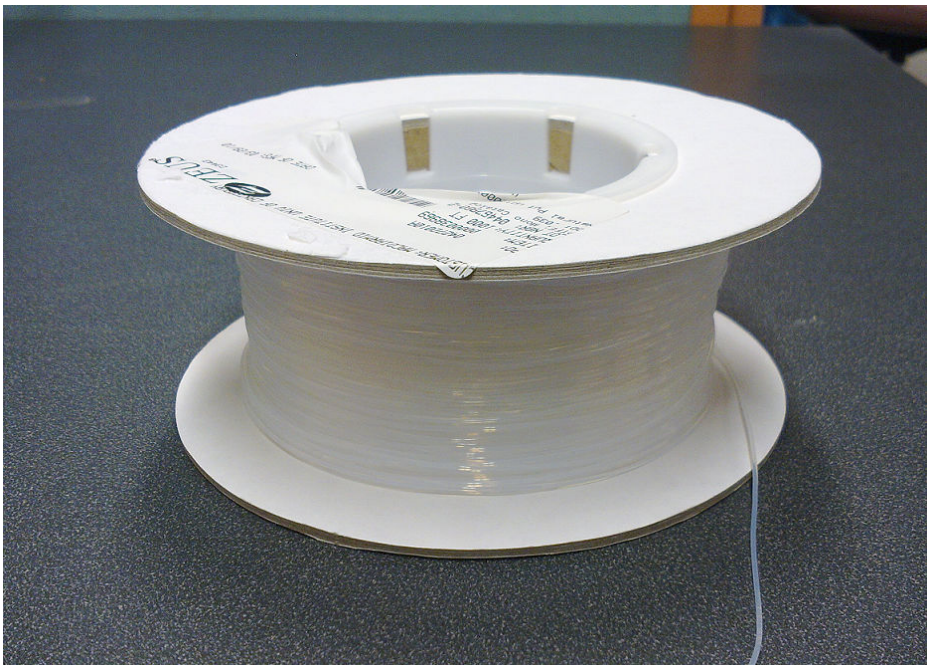

Figure 5.2 1 mm diameter PTFE monofilament [ZeusInc 2011].

5.3 EXPERIMENTAL PROCESSES OF FIBRE IMPRINTING

As the aim of this project is to develop fibre imprintinging technology by a non-thermal process and special apparatus for performing this in a controlled and repeatable fashion was required. The reel-to-reel roller embosser used for this work was made by the mechanical workshop at University of Canterbury as shown in Figure 5.3. In terms of the rolling pressure during the fibre imprinting process, the reading of two front depth gauges gives an indication of the gap width between upper and lower rollers. Each division of the gauge is 1/100 of the circle (1 mm); in other words, each division represents 10 μm, and the graduation of the small circle is 1 mm/div.

To ensure both sides of the upper roller are on the same level, calibration of two gauges is required. To perform this calibration, two pieces of paper are inserted on each side of the rollers, and the roller gap width is adjusted by slowly screwing the

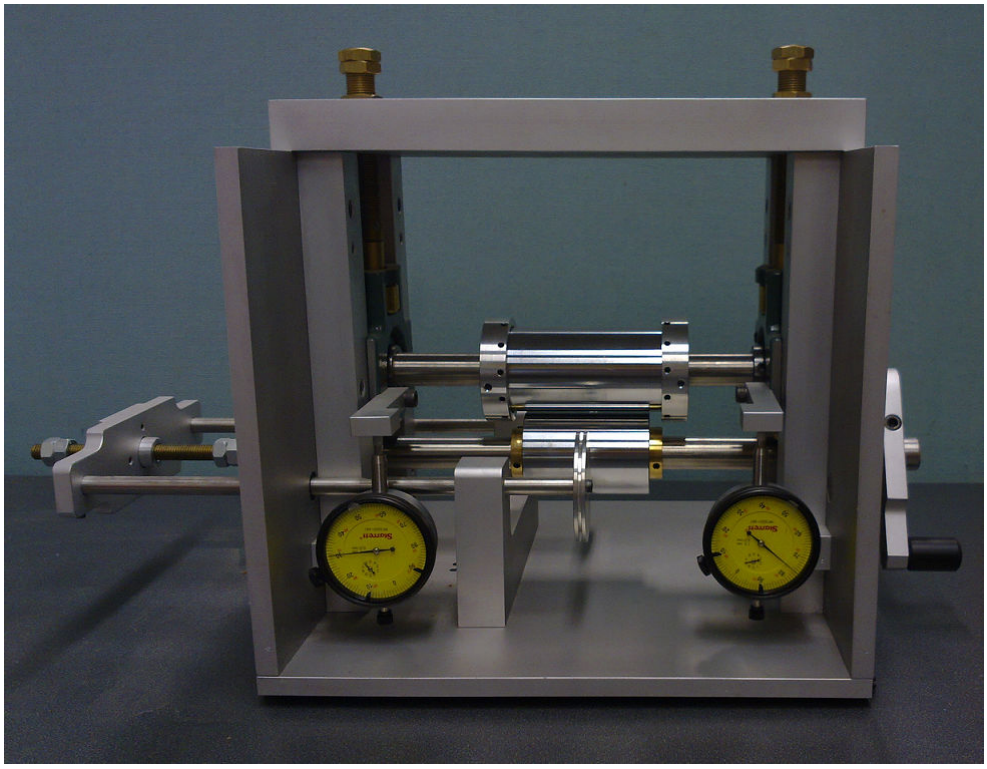

Figure 5.3 Roller Embosser.

two bolts on the top. The readings of both gauges are reset to zero once the paper is gripped from both sides. However, as the gauges fitted in this roller embosser are not digital ones, the readings from the gauges may be unprecise due to the internal torque. Instead of determining the roller gap width by those gauges, an automotive feeler gauge is a more convenient tool for the measurement. The feeler gauge set (Figure 5.4) used for this experiment has a wide range of thickness, from 51 μm to 889 μm.

To perform the fibre imprinting process, firstly the waste edges of the fabricated Ni stamp are cut out to obtain an even surface, and then the backside of Ni stamp is polished using sand paper. It is then attached to a cut piece of thin copper shim (thickness = 260 μm) by the bonding agent (Fuller Spray Bond Adhesive), so as to avoid the stamp cracking while the imprinting force is applied. Next, the roller spacing is adjusted by two top bolts while measuring the gap width with the feeler gauge, also ensuring both sides of upper roller are leveled, otherwise the pressure will be inconsistent during the imprinting process. The roller gap width is mostly determined by the thickness of electroplated Ni stamp because the thicknesses of bonded metal shim and Teflon fibre are always consistent throughout the fibre imprinting process. Once the appropriate roller gap width is determined, the roller embosser is ready for imprinting the fibres. During the fibre imprinting process, latex gloves must be worn to prevent the contamination of imprinted fibre caused by the fingerprints.

Figure 5.4 Feeler gauge.

Teflon monofilament is cut into 40 mm long piece, and then the monofilament is laid down onto the fibre-guide grooves on the Ni stamp. A small piece of cellulose tape is used in order to prevent the movement of the monofilament away from the Ni stamp. After that, slowly winding the handle on right side of the roller embosser feeds the Ni stamp along with the monofilament through the roller. The Ni stamp is de-molded from the Teflon monofilament immediately after the imprinting process is completed. Each imprint process is executed under ambient conditions.

After every imprint, the Ni stamp is cleaned with acetone for 5 min followed by a rinse in deionized water. To characterize the imprinted fibre under the optical microscope and SEM, the monofilament is glued onto a piece of silicon substrate or metal shim. The sample is then placed into the SEM sputter coater (Figure 5.5); using 40 mA plasma current (nitrogen atmosphere, 0.15 Torr) for 3 minutes will provide a 10 nm layer of gold-palladium (AuPd) so that the sample is electrically conductive for SEM images.

Figure 5.6(a) shows the original PTFE monofilament using an optical microscope, and Figure 5.6(b) shows the PTFE monofilament after the fibre imprinting process imprinted pillars. As clearly seen in Figure 5.6(c), the PTFE monofilament (1 mm diameter) is compressed into a rectangular sheet after roller imprinting, the dimension of the imprinted fibre is 1.58 mm (width) $\times$ 0.49 mm (thickness) which is measured by digital caliper. Figure 5.6(d) shows the top-view of imprinted pillar structures on PTFE monofilament.

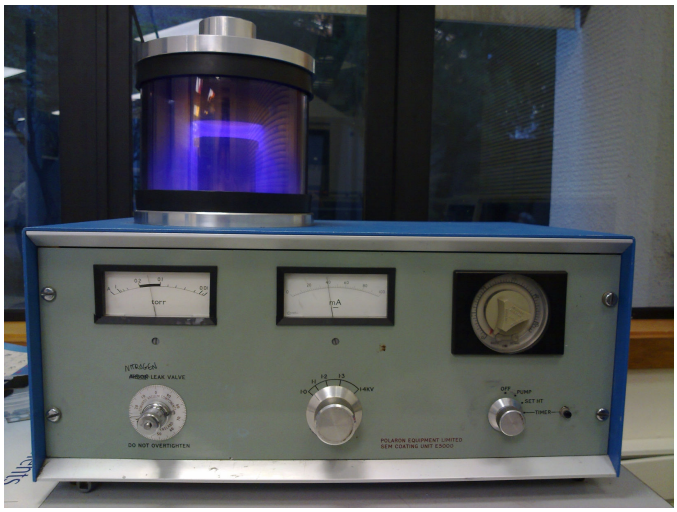

Figure 5.5 SEM sputter coater.

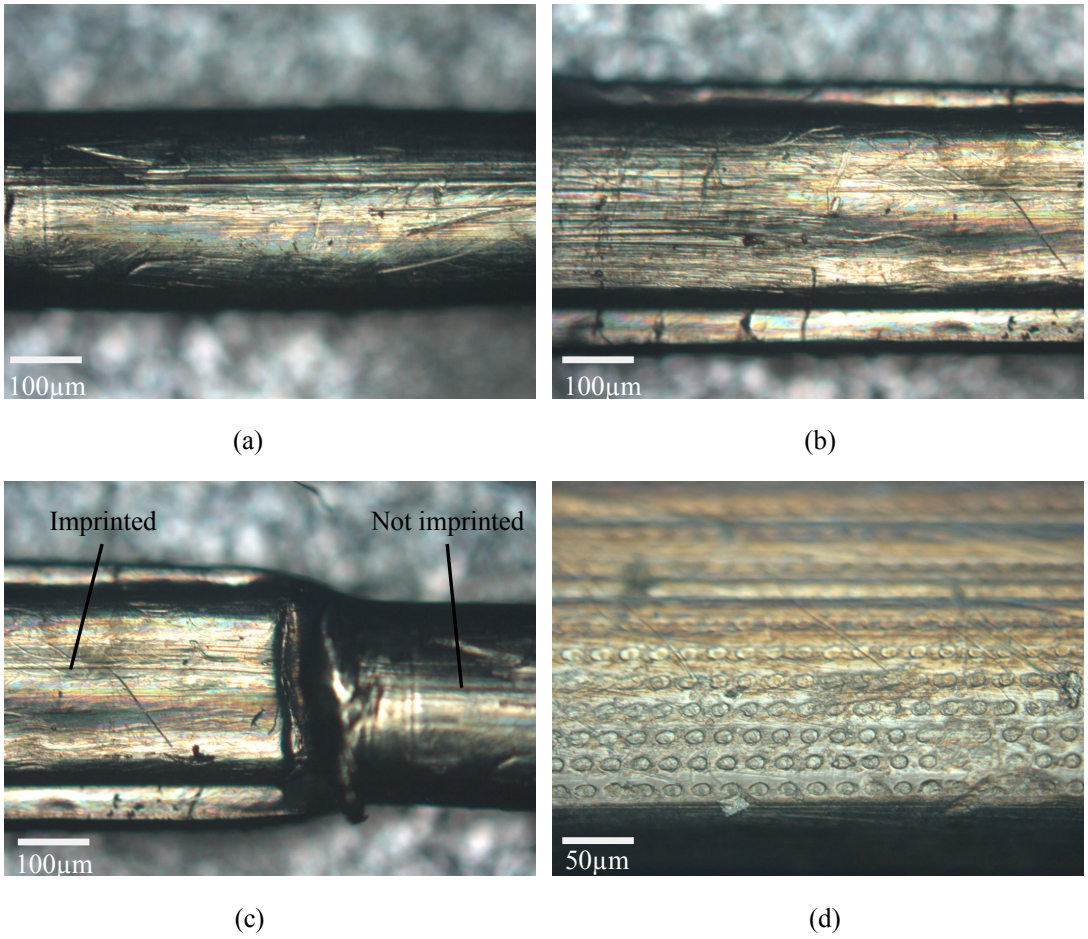

Figure 5.6 Optical microscope images of PTFE monofilament (a) before fibre imprinting prcess (b) after fibre imprinting process (c) comparison between two stages (d) imprinted pillar structures.

5.4 STAMP LIFETIME

In nanoimprint lithography (NIL), stamp lifetime was investigated by using dark field imaging in optical microscopy [Eriksson et al 2011]. Dark field imaging has been used to evaluate the stamp to identify defects resulting from the nanoimprint process. The defects in the stamp will likely be transferred to the imprinted substrates. The major sources of defects are particles and polymer residues. Similar to the defects arisen in NIL, the major defect in fibre imprinting process is PTFE monofilament residues. Defects attributed by polymer fibre residues come from the fact that the Ni stamp undergoes a mechanical rolling process during imprinting. Polymer fibre residues mainly appeared in the fibre-guide structures, because these are the areas where PTFE monofilaments have been imprinted.

The Ni stamp with fibre-guide structures has been used for more than 50 times, AFM measurement section analysis has confirmed that the height of patterned structures on Ni stamp after 50 roller imprinting is unchanged compared to the original structure height. Figure 5.7(a) presents the SEM image of the pillars structures on a Ni stamp before imprinting process; and Figure 5.7(b) shows the SEM image after 50 imprints. Clearly, no deformation was observed on the replicated pillar structures after 50 imprints; however some defects are now present. To clarify the real lifetime of the Ni stamp, more roller imprinting tests are required.

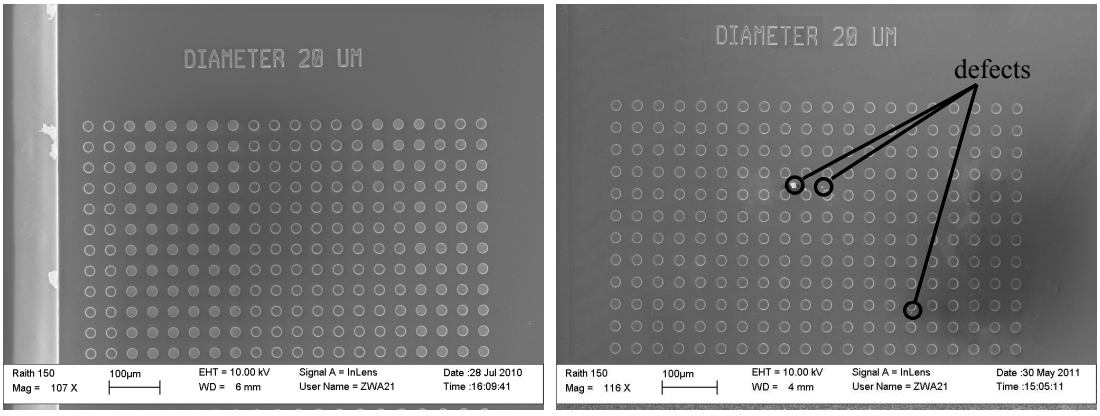

Figure 5.7 SEM images of replicated pillar structures on Ni stamp (a) before imprint (b) after 50 imprints.

5.5 EFFECT OF GAP

The roller gap is a critical factor in the fibre imprinting process, as the rolling pressure is only determined by the gap width for roller embosser. In order to obtain the optimum imprinted results, the effect of roller gap width in terms of compressed fibre thickness as

well as the imprinted pattern depths has been analyzed. A few control tests have been carried out with different gap widths by applying the feeler gauge; digital caliper and profilometry have been used to measure the compressed fibre thickness and imprinted pattern depths respectively. The Ni stamp without fibre-guide structure is used for this test; the stamp thickness is about 90 μm, and the height of nano-scale structures on Ni stamp is approximate 120 nm. Instead of using Teflon monofilament, normal Teflon tape is employed as the monofilament is particularly applied for the imprinting process with guide structures. The thickness of Teflon tape is 100 μm; a single layer of Teflon tape is initially used for the test, however the compressed single layer of Teflon tape only has a quarter of its original thickness, the imprinted patterns on the fibre are hardly distinguishable under the optical microscope because of the low contrast. To improve the contrast, bi-layers of Teflon tape were used for roller imprinting. Table 5.2 shows the effect of roller gap width in terms of compressed Teflon tape thickness and average depths of imprinted pattern. The thickness of sputtered AuPd layer is presumably 10 nm, which will be deducted from the imprinted pattern depths. The tolerance of compressed Teflon thickness is $\pm$10 μm due to the precision of digital caliper, and the tolerance of imprinted pattern depths is $\pm$5 nm due to the surface roughness of imprinted fibre.

Roller gap width (μm)	**Thickness of compressed Teflon tape (μm)$\pm$10 μm**	**Average depths of imprinted pattern (nm)$\pm$5 nm**
76	N/A	N/A
102	160	67
127	170	58
152	180	49
178	180	42
203	190	25
229	No rolling pressure	N/A

Table 5.2 Summary of roller gap widths in relation to measured Teflon tape thickness and imprinted pattern depths after roller imprinting.

As shown in Table 5.2, the minimum roller gap width allowed for 200 μm thickness of Teflon tape is 100 μm, where the imprinted pattern has reasonable depths in contrast to the height of patterned structure on Ni stamp. The Teflon tape is completely deformed during roller imprinting process with 76 μm gap width. As increasing the gap width, rolling pressure is reduced, therefore the Teflon tape undergoes less compression which results the decrease of imprinted pattern depths. Little pressure is detected at the contact area between the Teflon tape and rollers with 229 μm gap width, and no imprinted pattern can be observed under the optical microscope. The control tests demonstrated the gap width margins of fibre imprinting process with 200 μm Teflon tape, also confirmed the roller gap width is the most important factor which effects the quality of imprinted fibres. Hence, to acquire high quality of imprinted results, it

is particularly necessary to determine the optimum gap width before fibre imprinting process as utilizing different Ni stamps.

5.6 IMPRINTED RESULTS

As mentioned in the previous section, roller gap width plays an important role during the fibre imprinting process. In reality, the quality of imprinted fibres also depends on the height of patterned structures on Ni stamp as well as the rolling speed. To achieve the desired height of replicated structures on Ni stamp, simply controlling the thickness of the spin-coated photoresist during the stamp patterning is all that is required. The rolling speed actually determines the compressing duration of fibre imprinting process, which is likely to impact the depths of imprinted patterns on Teflon fibre. Similar to the control tests presented in Section 5.5, the effect of rolling speed is investigated. Instead of changing the roller gap width, different rolling speeds are applied this time. Nevertheless, the rolling speed cannot be measured for this work as the imprinting process is operated manually. The same Ni stamp and Teflon tape described in Section 5.5 are reused for this test, the roller gap width is set to 100 μm consistently throughout the test. Table 5.3 summarizes the effect of rolling speed in terms of the thickness of compressed Teflon tape and average depths of imprinted pattern. Apparently, better imprinted results are achieved with the low rolling speed. Although the contact area between Teflon tape and rollers are the same, less deformation is undergone by the Teflon tape while increasing the rolling speed.

Rolling speed	**Thickness of compressed Teflon tape (μm)$\pm$10 μm**	**Average depths of imprinted pattern (nm)$\pm$5 nm**
Low	140	72
Moderate	160	61
High	170	43

Table 5.3 Summary of rolling speed in relation to measured Teflon tape thickness and imprinted pattern depths after roller imprinting.

Teflon monofilament, 1 mm in diameter is used for fibre-guide imprinting process. The electroplated Ni stamp with KOH-etched Si grooves is fabricated as described in Section 4.3.2. The thickness of Ni stamp is approximate 130 μm, and the average height of replicated structures on the stamp is 1.7 μm. The roller gap width is set to 508 μm, which is confirmed as the optimum gap width after running control tests. The maximum allowed gap width is 813 μm, which results the least rolling pressure, and the imprinted patterns can be barely observed using optical microscope. Figure 5.8(a)&(b) present the SEM images of imprinted text structures on PTFE monofilament, Figure 5.8(c) and Figure 5.8(d) show the SEM images of imprinted pillar and vertical line structures respectively. The imprinted results confirmed that patterned structures are successfully transferred from the Ni stamp onto the PTFE monofilament.

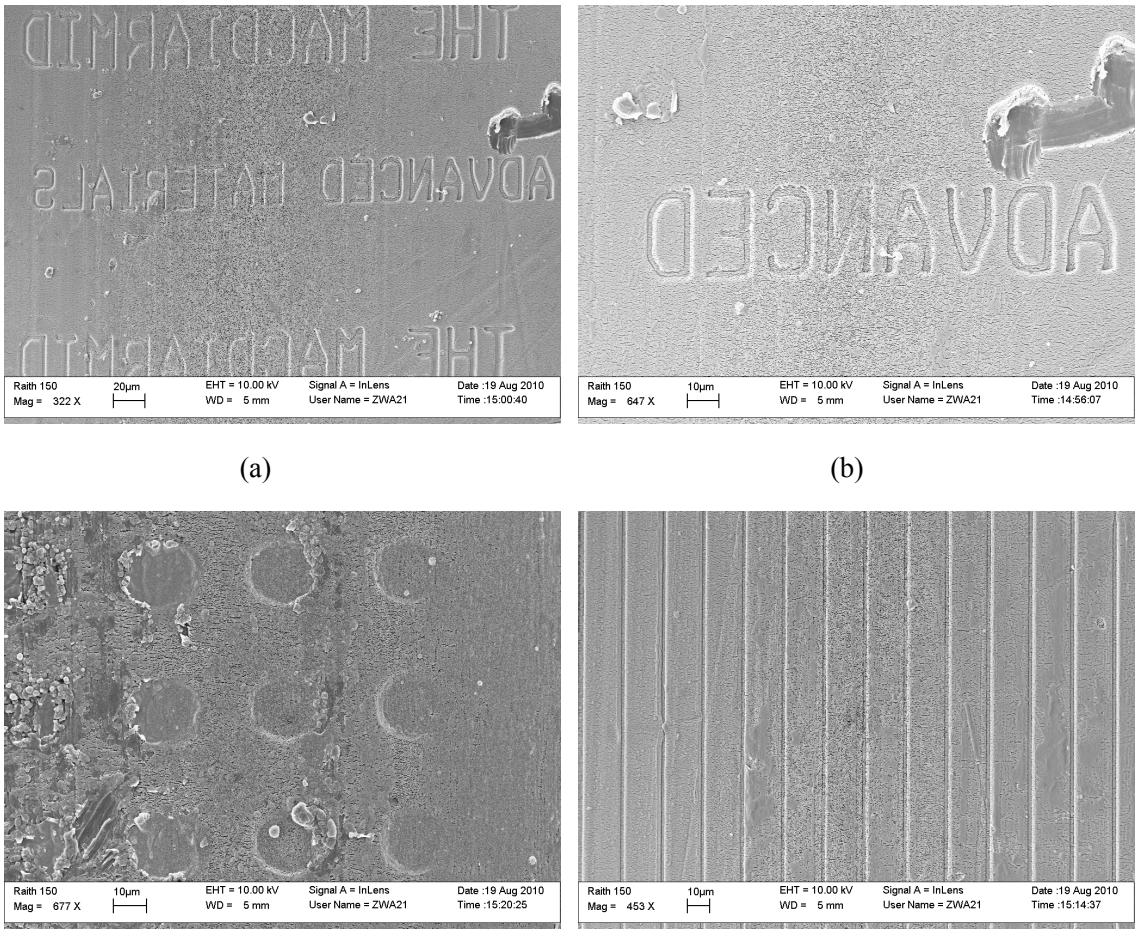

Figure 5.8 SEM images of imprinted structures on PTFE monofilament (a)&(b) text structures (c) pillar structures (d) vertical line structures.

To determine the quality of imprinted structures, SEM is utilized to measure the diameter of imprinted pillar structures as well as the width of imprinted vertical line structures. The measured diameter of pillar structures is 19.95 μm which is shown in Figure 5.9(a), and Figure 5.9(b) shows the measured width of vertical line structures which is 2.4 μm. The diameter of pillar structure is extremely close to the replicated feature size on Ni stamp (20 μm), whereas the imprinted vertical line width is slightly less than the desired value (3 μm), which is probably due to the less rolling pressure applied during the imprinting process.

AFM is utilized to obtain more accurate measurements of the imprinted pattern depths rather than profilometry, the AFM images of imprinted patterns of a letter"E" on PTFE monofilament are shown in Figure 5.10, as well as the depth measurements by using section analysis from the off-line software. The measured depth across the scanned areas vary from 0.35 μm to 1.4 μm, which is expected since the imprinted

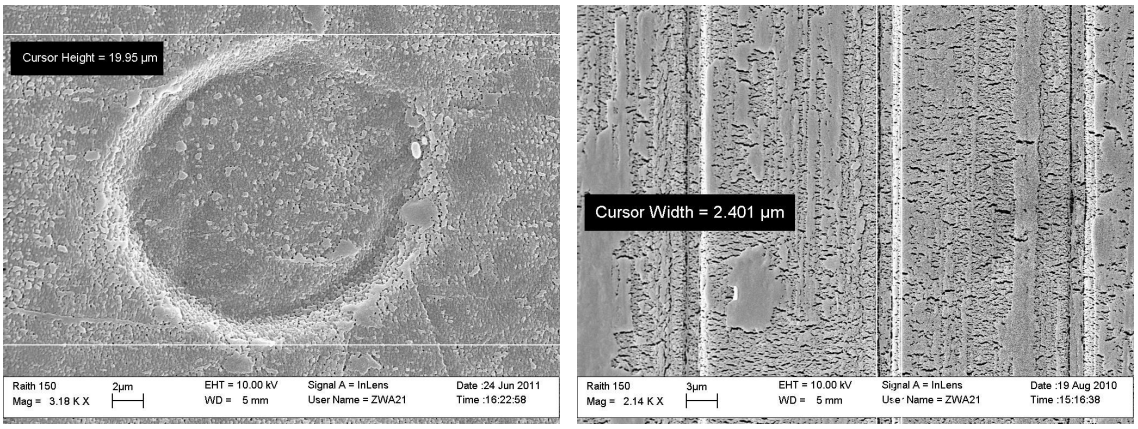

Figure 5.9 SEM measurements of imprinted structures (a) pillar structure (b) vertical line structure.

pattern depths mainly depend on the height of replicated structures in electroplated Ni stamp as the rolling pressure is fixed. As discussed in Section 4.3.2, the measured heights of replicated structures on Ni stamp varied from 0.65 μm to 1.8 μm due to the edge-bead effects. The uneven surface of imprinted fibre could be another reason which influences the measured results.

To further analyze the surface profile of imprinted patterns, high resolution 3D AFM images are captured as shown in Figure 5.11. The color difference indicates the bottom and top surfaces of imprinted patterns, and surface roughness is clearly evidenced from both images. Figure 5.11(b) illustrates the various imprinted depths over the vertical line structures.

A typical problem came across during fibre imprinting process by using roller embosser is stamp displacement during pattern imprinting, which tends to occur when high imprinting pressure is applied. As mentioned in Section 5.2, PTFE has extremely low coefficient of friction. This characteristic makes the PTFE monofilament especially difficult to compress at the fixed position. The monofilament and Ni stamp move in the opposite direction during the imprinting process, which results the phenomenon of imprinted patterns being displaced during the process. As mentioned in Section 5.3, a small piece of cellulose tape is used to minimize the monofilament movement, although this is not the optimum method to resolve this issue because the use of cellulose tape will contaminate the imprinted patterns as well as Ni stamp. Figure 5.12 shows the SEM image of imprinted pillar structures where stamp displacement has happened. The measured new 'diameter' in Figure 5.12(b) is 29.7 μm which is almost one and a half of the original diameter of pillar structures as shown in Figure 5.9(a).

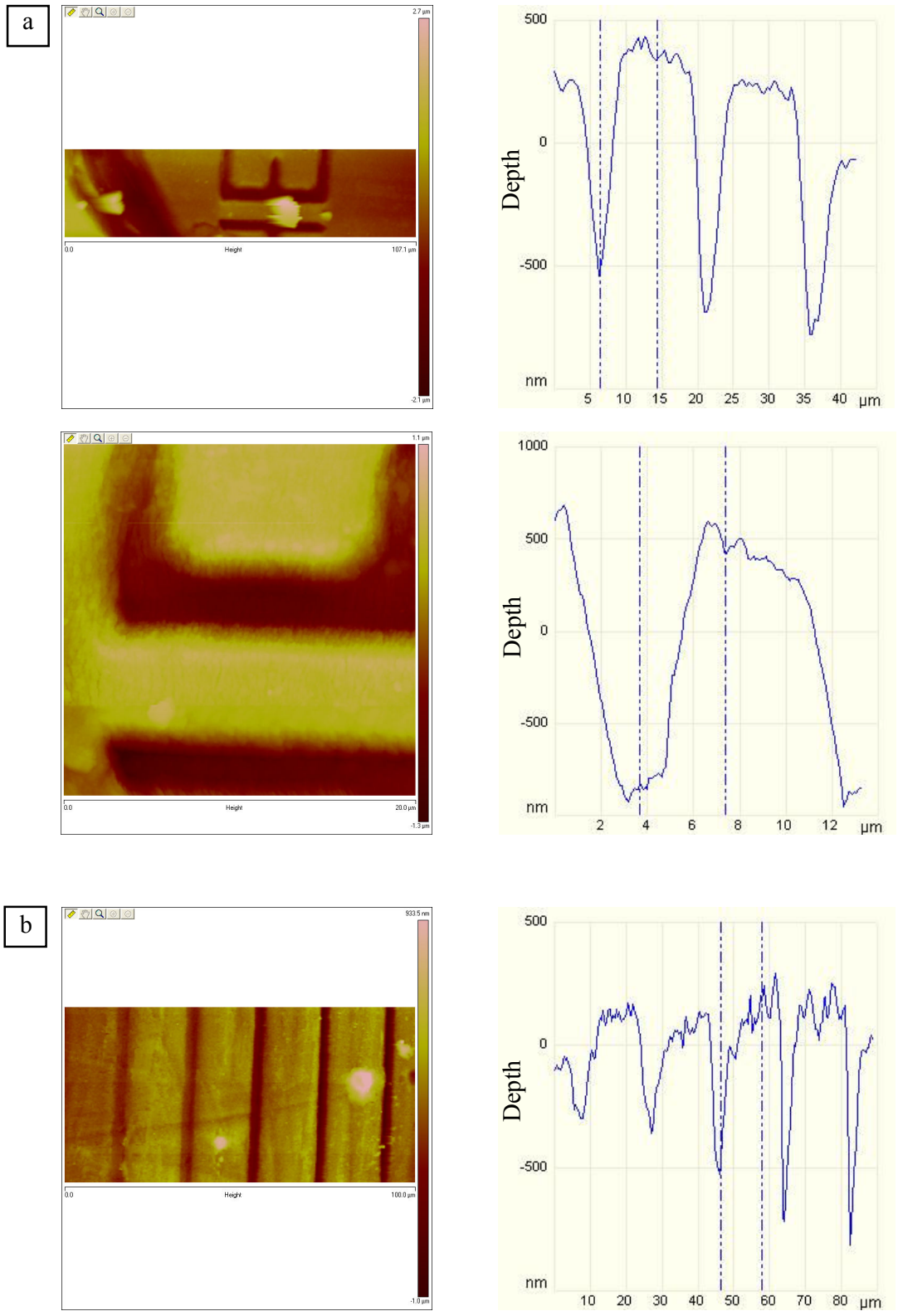

Figure 5.10 AFM cross-sectional measurements on the imprinted PTFE monofilament (a) text structure (b) vertical line structure.

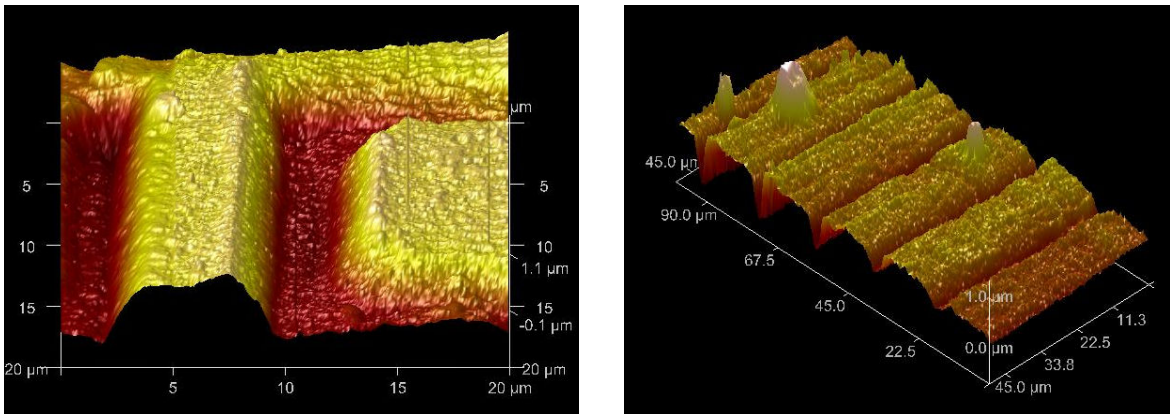

(a) (b)

Figure 5.11 3D AFM images of imprinted patterns (a) text structure (b) vertical line structure.

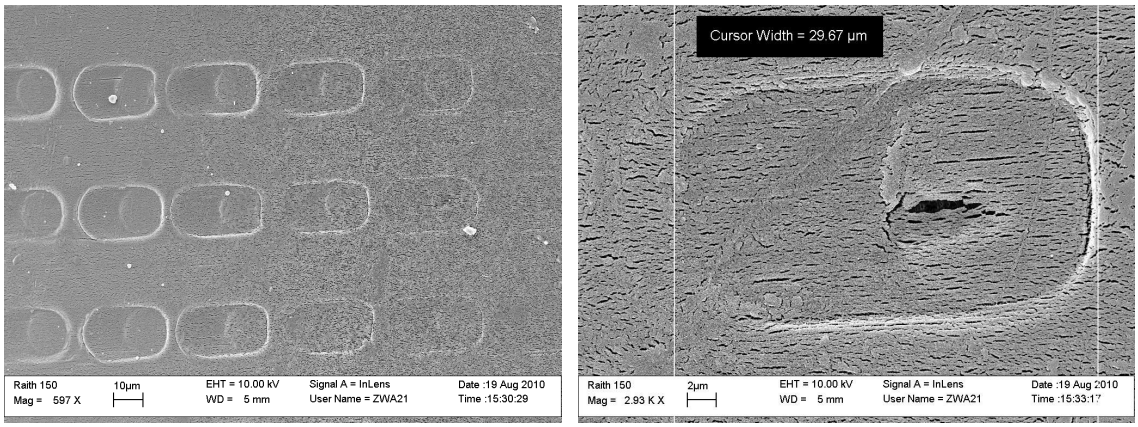

(a) (b)

Figure 5.12 SEM images of imprinted pillar structures with evidence of stamp displacement during the imprinting process.

Figure 5.13 shows the SEM image of imprinted vertical lines with stamp displacement, as a result the displaced vertical lines become wider compared with the vertical line width measured in Figure 5.9(b). To confirm this result, imprinted vertical line width is measured at two different points, which are 6.2 μm and 4.6 μm respectively.

Figure 5.14 shows the optical microscope image of imprinted text structure, where the stamp displacement significantly affects the resolution of imprinted results.

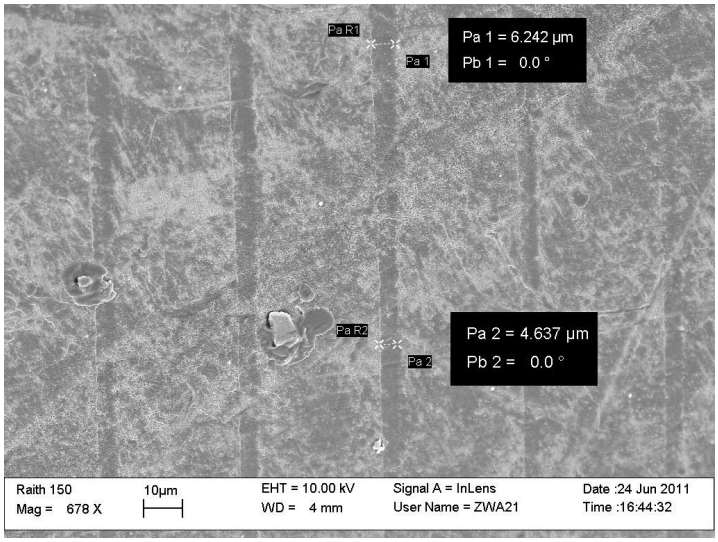

Figure 5.13 Measured vertical line width with stamp displacement.

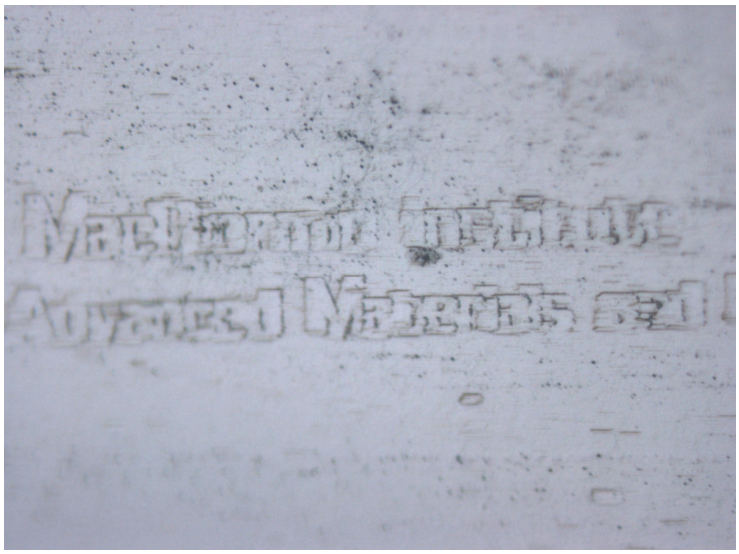

Figure 5.14 Optical microscope image of imprinted text structure with stamp displacement.

5.7 SUMMARY

The aim of the work was to perform fibre imprinting process using roller embosser, and characterize the imprinted patterns by SEM and AFM. Teflon fibre was chosen since its low hardness property, but other polymer fibres, such as nylon and polyethylene could also be considered as the alternative materials for this work. PTFE monofilament with 1 mm diameter is used for the self-aligning imprinting process, and the imprinting results confirmed that the patterned structures on Ni stamp have been successfully transferred onto the PTFE monofilament. The Ni stamps with fibre-guide structures

have been used for more than 50 times but still more imprinting tests are required to clarify the real lifetime of the stamps.

The effect of roller gap width as well as rolling speed in terms of the thickness of compressed Teflon tape and average depths of imprinted pattern were analyzed by executing control tests. The test results demonstrate that in order to achieve high quality of imprinted patterns, optimum roller gap width needs to be determined and low rolling speed should be applied. SEM and AFM measurements confirmed the imprinted patterns have reasonable dimensions as expected. Surface roughness of the imprinted fibres is observed on 3D AFM topography images, which could influence the depth measurements of imprinted patterns.

Stamp displacement of imprinted patterns was found on some occasion due to the movement of PTFE monofilament during the imprinting process. The cellulose tape is used to reduce monofilament movement with Ni stamp, and the size of displaced patterns was measured by SEM. In order to completely resolve this issue, instead of feeding PTFE monofilament along with Ni stamp through roller embosser, the Ni stamp should be bonded onto the upper roller, therefore monofilament is able to continuously feed into the roller embosser without the concern of movement. More details will be discussed in the next chapter.

Chapter 6

CONCLUSIONS AND FUTURE WORK

6.1 SUMMARY OF CONTRIBUTIONS AND ACHIEVEMENTS

The study presented in this thesis investigated the methods of developing reel-to-reel fibre imprinting processes for a range of different fibre materials. First, the method of fabricating nickel stamps was proposed and the process was experimentally demonstrated by combining microfabrication processes and electroplating technology. Second, the fibre imprinting process was experimentally demonstrated using the roller embosser. The main contributions and achievements of this work are as follows:

- The idea of using fibre guide structure was proposed in order to self-align the fibre to the features on the stamp during the imprinting process. 1 mm wide grooves with 100 μm thickness were successfully produced using two different techniques, SU-8 lithography and KOH silicon etching.

- Micro- and nano-scale fine features were written on top of the fibre-guide structures by using optical and e-beam lithography techniques. Photolithography mask was designed by L-edit Tanner Tools, and single pixel line writing mode was employed during e-beam lithography, the features sizes down to 230 nm were produced.

- The nickel stamp with fine features and fibre-guide structures were successfully fabricated using an electroplating technique. The nickel sulphamate bath was selected for this work as it produced the lowest internal stress. The plating setup was demonstrated in the nanofabrication laboratory at UoC. The nickel stamp thickness depends on the current density as well as plating time, and stamps with thickness of up to 0.5 mm were fabricated.

- Faithful reproduction of both the fibre guide structures and the fine feature patterns on the electroplated nickel stamps were verified using surface profilometry and SEM.

- The fibre imprinting process was demonstrated by using roller embosser which made by the mechnical workshop of UoC. Teflon monofilament with 1 mm diameter was primarily chosen for the self-aligning imprinting process as it has low hardness compared to other polymer fibres. The effects of roller gap width and rolling speed were analyzed in terms of compressed fibre thickness as well as the imprinted pattern depths. SEM and AFM were utilized to determine the quality and characteristics of imprinted structures. The imprinted results confirmed that the patterned structures on the Ni stamp were successfully transferred onto the teflon monofilament. The Ni stamp with fibre-guide structures have been used for more than 50 times which showed the stamp had a considerable life time.

6.2 DISCUSSION OF RESOLVED ISSUES

6.2.1 Fabrication of Fibre Guide Structures

SU-8 lithography is one of the methods to create fibre guide structures for self-aligning imprinting process. However, the use of SU-8 grooves has some issues during the process of manufacturing the stamp as summarized in Section 4.5. The first issue appeared in the process of stamp patterning, where the vertical sidewalls of SU-8 grooves cause the uneven surface of coated photoresist layer. The majority of the resist flowed into the high aspect ratio grooves during the spin-coating, and the resulting edge-beads effect significantly impacts the resolution of patterned features. In addition, the transparent SU-8 groove structures caused problems for optical lithography of the fine-scale patterns; the developed features were very likely to be destroyed due to reflection from the bottom silicon substrate. To minimize this issue, BARC was introduced. Before spin-coating the photoresist on top of SU-8 grooves, a layer of BARC was coated to reduce the reflection caused by the transparent SU-8 structures.

The high aspect ratio SU-8 grooves brought another issue while depositing the seed layer using e-beam evaporation. As described in Section 3.4, the vertical sidewalls of SU-8 grooves were not metalized due to the directional deposition of e-beam evaporation, only top and bottom regions were covered with the nickel seed layer. As a result, the electrical connection over the surface of SU-8 structures was discontinuous which resulted in the failure of electroplated stamp. To resolve this problem, a plastic form cut into trapezoid shape was inserted between the sample and the wafer holder to create an angle ($>45^{\circ}$) during e-beam evaporation to give good sidewall coating.

The main issue of using SU-8 grooves was they were likely to come off from the silicon substrate while peeling off the electroplated nickel stamp, which means the SU-8 fibre guide structures can only be treated as the one-off mask. To completely avoid those issues related to using SU-8 grooves, the method of using KOH-etched silicon grooves was developed. The sloped sidewalls of KOH-etched grooves resolved

the problem of reflection as well as the seed layer deposition. The edge-bead effect and electroplating stress were also minimized. Most importantly, the KOH-etched grooves can be reused for stamp manufacture which significantly reduced the time frame for manufacturing additional stamps.

6.2.2 Determining Roller Gap Width

During the fibre imprinting process, roller gap width becomes an issue as the reading from gauges in the roller embosser was inaccurate due to the internal torque. The roller gap width must be leveled through the imprinting process, otherwise the imprinting pressure will not be equivalent. Calibration of two gauges is necessarily required before the imprinting process. Two pieces of paper were inserted on each side of the rollers, reset the readings of both gauges to zero once the paper were gripped from both sides. The automotive feeler gauge was then used to precisely determine the roller gap width. During each imprinting process, the roller gap was adjusted by two top bolts while measuring the gap width with the feeler gauges. By doing this, both sides of rollers were leveled and the pressure would be consistent.

6.3 DISCUSSION OF REMAINING ISSUES

6.3.1 Edge-bead Effect

Edge-bead effect is one of the biggest issue which significantly affects the resolution of fine features written on the ridges. As mentioned in Section 4.3.3, high aspect ratio SU-8 grooves lead the difficulty of uniformly spin-coating the photoresist film during the stamp pateerning, because the bulk of resists flowed into the grooves during the spin-coating, and only a small quantity of resist remained on the ridges. Furthermore, the residual resist tends to remain on the edges of the ridges which resulted in a build-up on those areas. The edge-bead areas normally cause the problem of pattern underexposure. As a result, various heights of replicated Ni structures on the stamp are characterized by using profilometry in subsequent electroplating process. KOH-etched silicon grooves slightly reduced the edge-bead effect because of the sloped sidewalls, however edge-bead effect was inevitable during the microfabrication processes as the fibre guide structures were required for this work.

6.3.2 pH Drop in Plating Bath

The pH of plating bath plays a critical role during the electroplating process. The pH value must be precisely controlled thoughout the electroplating in order to minimize the internal stress of the plating bath, as well as to achieve uniform deposited thickness. The pH value should be well controlled between 3.9 - 4.5 for the sulphamate bath which

was used at this work. However, the difficulty in maintaining the pH of the plating solution is a serious issue.

As stated in Section 4.4, the pH of the plating solution decreased dramatically after a long electroplating work. The extreme low pH led the problem of low deposition rate, and even caused the nickel seed layer to peel off due to the acidic plating solution. The worst thing came up was that the fresh plating solution had to be made up every time which was not expected to happen. This requires further investigation and the development of appropriate buffer solutions to maintain the plating bath's pH in the right range.

6.3.3 Stamp Displacement During the Imprinting Process

A typical issue appeared during the fibre imprinting process using roller embosser was stamp displacement. Teflon monofilament has an extremely low coefficient of friction, thus the monofilament moved in the opposite direction with Ni stamp during the imprinting process, which resulted in the phenomenon of imprinted patterns being displaced during the process. The stamp displacement affected the resolution of imprinted results, because every single imprinted pattern was enlarged. The cellulose tape was used to prevent the monofilament movement, nevertheless the imprinted patterns and Ni stamp were contaminated. Regarding this issue, some future work could be carried out which will be described in the next section.

6.4 FUTURE WORK

The priority of the future work will be performing the imprinting process onto different fibre materials, such as nylon, polyethylene and even human hair. The proposed techniques used in this work will also be applied for other fibres, although the dimensions (width $\times$ height) of fibre guide structures may need redesigning according to the diameter of different fibre monofilaments.

In this work, the Ni stamp with nano-scale fine features on KOH-etched silicon grooves were successfully fabricated by using EBL coupled with electroplating. However, the electroplated EBL structures on the nickel stamp could not be imprinted onto the fibres by roller embosser. A hypothesis would be the heights of patterned structures on electroplated stamp were too small (<30 nm) due to the low thickness of the resist films remaining on the ridges after spin-coating. In the future, multi spin-coating with higher concentration PMMA resists could be applied in order to achieve a thicker resist layer.

As mentioned in Section 6.3.3, stamp displacement during the imprinting process was an issue as the Ni stamp moves in the opposite direction with fibre monofilaments. Instead of feeding monofilament along with Ni stamp through the roller embosser,

the Ni stamp should be fixed onto the upper roller. This could be a remaining work as fibre imprinting technique is supposed to be a high-throughput patterning process which requires continuous imprinting without manually feeding the stamp. Refitting the upper roller of roller embosser is necessary; a proposed change of roller embosser is shown in Figure 6.1 below. Positioning the Ni stamp onto the upper roller by four small screws, replacing the stamp is also convenient in case of imprinting different fibre materials using Ni stamps with various dimensions of fibre guide structures.

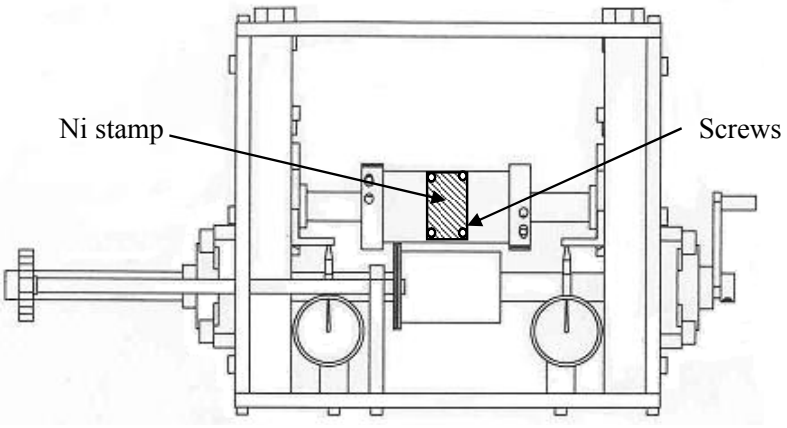

Figure 6.1 The proposed prototype of refitted roller embosser.

The last remaining work is to solve the problem of pH drop in plating bath. Some trial experiments could be performed, for example replacing the pure nickel pellet used in this work to S-round nickel, adding nickel carbonate or sodium hydroxide into the plating solution to bring up the pH value. In the meantime, make sure the boric acid and nickel chloride content are at the correct levels is an alternative approach.

6.5 SUMMARY

Two different methods of fabricating fibre guide structures were demonstrated, 1 mm wide grooves with over 100 μm thickness were created in order to self-align the fibre to the features on the stamp during the imprinting process. KOH silicon etching process is a more reliable method than SU-8 lithography process because of its sloped sidewall. Optical or e-beam lithography were used to expose micro- or nano-scale fine features, the feature size down to sub 300 nm was achieved. The stamp was successfully manufactured by combining the microfabrication processes and nickel electroplating technique. The resolution of replicated structures on the nickel stamp was confirmed by using SEM. Using the roller embosser, the fine features on the electroplated nickel stamp were imprinted onto a 1 mm-diameter Teflon monofilament. The imprinted depths depended on the height of fine features on the nickel stamp, as well as the roller gap width. The imprinted results were characterized by SEM and AFM, which confirmed the fine features on the nickel stamp were successfully transferred onto the fibre.

REFERENCES

Ahmed, N. (2010), 'Roll to roll uv embossing technology', Website. http://www.scribd.com/doc/41572855/Roll-to-Roll-UV-Embossing-Technology.

Ahn, S.H. and Guo, L.J. (2008), 'High-speed roll-to-roll nanoimprint lithography on flexible plastic substrates', *Advanced Materials*, Vol. 20.

Ahn, S.H. and Guo, L.J. (2009), 'Large-area roll-to-roll and roll-to-plate nanoimprint lithography: A step toward high-throughput application of continuous nanoimprint', *ACSNANO*, Vol. 3, No. 8.

Ansari, K., Shao, P.G., van Kan, J.A., Bettiol, A.A. and Watt, F. (2005), 'Proton beam fabrication of nickel stamps for nanoimprint lithography', *Nuclear Instruments and Methods in Physics Research B*, Vol. 231, pp. 407–412.

Bean, K.E. (1978), 'Anisotropic etching of silicon', *IEEE Trans. Electron Devices*, Vol. ED-25, Oct, pp. 1185–1193.

Bhushan, B. (2010), *Springer handbook of nanotechnology*, Springer, New York, 3rd ed.

Blaikie, R. (2008), 'Micro- and nano-scale writing onto fibres', June.

Blaikie, R. and Turner, G. (2008), 'Uc expertise getting fans closer than ever to the all blacks', Website. http://www.comsdev.canterbury.ac.nz/news/2008/080718c.shtml.

Chang, C.Y., Yang, S.Y. and Sheh, J.L. (2006), 'A roller embossing process for rapid fabrication of microlens arrays on glass substrates', *Microsystem Technologies*, Vol. 12, No. 8.

Chou, S.Y. (2004), 'Wafer-scale fabrication of nanodevices using nanoimprint lithography at all litho levels', Website. http://www.sematech.org/meetings/archives/litho/forum/20040128/presentations/34_Nano_Chou_Princeton.pdf.

Chou, S.Y. and Zhang, W. (2003), 'Fabrication of 60-nm transistors on 4-in. wafer using nanoimprint at all lithography levels', *Applied Physics Letters*, Vol. 83, No. 8.

Chou, S.Y., Krauss, P.R. and Renstrom, P.J. (1995), 'Imprint of sub 25nm vias and trenches in polymers', *Applied Physics Letters*, Vol. 67.

Chuang, Y.J., Tseng, F.G., Cheng, J.H. and Lin, W.K. (2003), 'A novel fabrication method of embedded micro-channels by using su-8 thick-film photoresists', *Sensors and Actuators A: Physical*, Vol. 103.

Conradie, E.H. and Moore, D.F. (2002), 'Su-8 thick photoresist processing as a functional material for mems applications', *Journal of Micromechanics and Microengineering*, Vol. 12, No. 4.

Dennis, J.K. and Such, T.E. (1993), *Nickel and chromium plating*, Woodhead, England, 3rd ed.

Drysdale, T.D. (2003), *Passive devices for terahertz frequencies*, PhD thesis, University of Canterbury, January.

Dutta, R.K., van Kan, J.A., Bettiol, A.A. and Watt, F. (2007), 'Polymer microlens replication by nanoimprint lithography using proton beam fabricated ni stamp', *Nuclear Instruments and Methods in Physics Research B*, Vol. 260, pp. 464–467.

Eriksson, T., Yamada, S., Krishnan, P.V., Ramasamy, S. and Heidari, B. (2011), 'High volume nanoimprint lithography on iii/v substrates: Imprint fidelity and stamp lifetime', *Microelectronic Engineering*, Vol. 88.

FaGan, M.D. (2008), *A Novel Process For Continuous Thermal Embossing Of Large-area Nanopatterns Onto Polymer Films*, Master's thesis, University of Massachusetts Amherst, September.

Fournier, J.M. (2000), *Holography: The First 50 Years*, Vol. 78, Springer Verlag, New York.

Gadre, A., Kastantin, M., Li, S. and Ghodssi, R. (2001), 'An integrated biomems fabrication technology', In *Semiconductor Device Research Symposium*, Washington, DC, USA, Dec, pp. 186–189.

Guo, L.J., Cheng, X. and Chou, C.F. (2004), 'Fabrication of size-controllable nanofluidic channels by nanoimprinting and its application for dna stretching', *Nano Letters*, Vol. 4, No. 1.

J., K., M., K., A., M., G., R., W., E. AND B., L. (2006), 'Fabrication of nanoimprint stamps for photonic crystals', *Journal of Physics: Conference Series*, Vol. 34, pp. 897–903.

KINGHORN, D. (2010), 'Battling low ph'. http://www.finishing.com/238/67.shtml.

LASER, E. (2009), 'Engraving a micro-fiber throw pillow'. http://www.epiloglaser.com/sc_pillows.htm.

LEE, R. (1992), 'Australian inventions and products'. http://www.aussiethings.biz/excel_gram.html.

MASON, M. (2008), 'ph drop in nickel sulphamate installation'. http://www.finishing.com/504/58.shtml.

MEKARU, H., KOIZUMI, O., UENO, A. AND TAKAHASHI, M. (2009), 'Guide structure with pole arrays imprinted on nylon fiber', *Microelectronic Engineering*, Vol. 87, pp. 922–926.

MICROCHEM (2011), *SU-8 2000 Permanent Epoxy Negative Photoresist Processing Guidelines For: SU-8 2100 and SU-8 2150*, Technical Report, MicroChem Corp.

NIELSEN, L.E. AND LANDEL, R.F. (1994), *Mechanical properties of polymers and composites*, M. Dekker, New York, 2nd ed.

OF ENGLAND, B. 'Banknote production'. http://www.bankofengland.co.uk/banknotes/about/production.htm.

OF NEW ZEALAND, R.B. 'Security features of new zealand's banknotes'. http://www.rbnz.govt.nz/currency/money/3258122.html.

PAI, R.S. (2001), 'Nickel electroplating sop', May. https://louisville.edu/research/cleanroom/sops/sops/nickel-electroplating-sop/nickel-electroplating-sop.html.

PLC, W.C. (1978), *The Canning handbook on electroplating*, W. Canning Limited, Birmingham, 22 ed.

SEXTON, B.A. AND MARNOCK, R.J. (2000), 'Characterization of high resolution resists and metal shims by scanning probe microscopy', *Microscopy and Microanalysis*, Vol. 6, pp. 129–136.

ZEUSINC (2005), *Technical Whitepaper, Focus on: PTFE*, Technical Report, ZeusInc.

ZEUSINC (2011), 'Ptfe monofilament'. http://www.zeusinc.com/extrusionservices/products/monofilament/standardmonofilamentsizes.aspx.

Zhang, J., Tan, K.L. and Gong, H.Q. (2001), 'Characterization of the polymerization of su-8 photoresist and its applications in micro-electro-mechanical systems (mems)', *Polymer Testing*, Vol. 20.